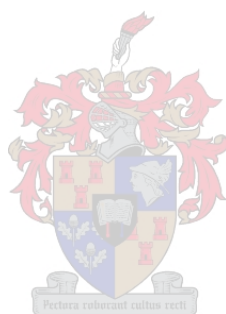


Electrochemistry and Electrophoresis of Mercury Cysteine and Dithizone Complexes

by

Lynwill Garth Martin

Thesis presented in partial fulfilment for the degree of



Master of Science (Chemistry) at Stellenbosch University

Promotor: Prof. A.M. Crouch

December 2008

Declaration

By submitting this thesis electronically, I declare that the entirety of the work contained therein is my own, original work, that I am the owner of the copyright thereof (unless to the extent explicitly otherwise stated) and that I have not previously in its entirety or in part submitted it for obtaining any qualification.

Date: 10 December 2008

Copyright © 2008 Stellenbosch University

All rights reserved

Abstract

There are various mercury species in the environment and their toxicity and availability relies on their chemical form and oxidation states. Inorganic and organic mercury is found to co-exist in water and body tissue of some organisms. Among them inorganic mercury has a lower toxicity than the organic mercury. Methyl mercury (CH_3Hg^+) is the most toxic species found in the environment because it can enter the food chain accumulating and contaminating humans.

Hence the total mercury concentration does not reflect the important information and thus the needs for the development of methods for the simultaneously separating and determination of mercury species. A study of the electrochemistry of mercury and organo mercury complexes with cysteine and dithizone indicated the formation of stable complexes, which can be utilized for the determination of the species in environmental matrices.

Cyclic voltammetry is used to determine the electrochemical properties of the complexes. A technique based on capillary electrophoresis and amperometric detection (CE-AD) has been developed for the speciation of mercury. This technique has the capability to detect mercury species that are electrochemically active. Using capillary electrophoresis in combination with electrochemical detection makes speciation of the complexes possible at lower than normal concentrations. For CE-AD the detection limits were $0.005 \mu\text{g/L}$ for Hg^{2+} and $0.4 \mu\text{g/L}$ for MeHg^+ . These detection sensitivities are attractive for environmental monitoring.

Opsomming

Daar is verskeie kwik spesies in die omgewing en hul toksisiteit hang af van die beskikbaarheid van die chemiese form en oksidasie toestand van kwik. Kwik en organiese kwik word saam gevind in riviere, die see en lewende organismes. Die anorganiese form van kwik is minder toksies as die verskillende organiese forms van kwik wat beskikbaar is. Metielkwik (CH_3Hg^+) is die gevaarlikste kwik spesie wat in die omgewing aangetref word want dit kan die voedsel ketting penetreer en verskeie gevaarlike siektes onder mense versprei wat tot hul dood kan lei. Die totale kwik konsentrasie is nie meer voldoende nie, en metodes om die verskillende kwik spesies gelyktydig te bepaal moet ontwikkel word om die tekort te oorkom.

'n Elektrochemiese studie van kwik en organokwik komplekse met sistein en ditizoon wys 'n dat 'n sterker kompleks met die twee ligande gevorm word en kan gebruik word om kwik spesies in die omgewing te bepaal.

Sikliese voltammetry (CV) is gebruik om die elektrochemiese eienskappe van die kwik komplekse te bepaal. 'n Tegniek gebaseer op kapilêre elektroforese met amperometriese deteksie is ontwikkel. Die tegniek het die vermoë om kwik spesies wat elektro aktief is, te bepaal. Kapilêre elektroforese word met elektrochemiese deteksie gekombineer en verseker dat die spesiasie van kwik komplekse plaasvind by baie laer konsentrasies. Vir CE-AD is die deteksie limiet $0.005 \mu\text{g/L}$ en $0.4 \mu\text{g/L}$ vir Hg^{2+} en MeHg^+ onderskeidelik. Die sensitiwiteit van die tegniek maak dit baie aantreklik vir toepassings in die omgewing om die konsentrasie van kwik spesies te bepaal.

GLOSSARY OF SYMBOLS

Abbreviation	Description
AD	Amperometric detection
BGE	Background electrolyte
CE	Capillary electrophoresis
CE-AD	Capillary electrophoresis with amperometric detection
CEEC	Capillary electrophoresis with electrochemical detection
CV	Cyclic voltammetry
CYS	Cysteine
CZE	Capillary zone electrophoresis
Dz	Dithizone
DzS	Dithizone sulfonate
EC	Electrochemical detection
EOF	Electro osmotic flow
EPA	Environmental Protection Agency
GC	Gas Chromatography
HPLC	High Performance Liquid Chromatography
HV	High Voltage
ICP	Inductively coupled plasma
i.d.	Internal diameter
kV	kilo Volt
L	Ligand
LOD	Limit of detection
LOQ	Limit of quantification
UV	Ultra violet
Vis	Visible
WHO	World Health Organization

ACKNOWLEDGEMENTS

The author wishes to express his appreciation to:

- Prof. Andrew M. Crouch for his support, encouragement, guidance and expertise throughout my years of study at Stellenbosch.
- The Electricity Supply Commission (ESKOM), University of Stellenbosch and the National Research Foundation (NRF) for their financial support.
- Mr. B. Botha from the Physic Workshop at Stellenbosch University for constructing the cross hair design for electrochemical detection. You are a living legend sir
- All my friends in the electrochemical section and the PGM group. The conversations in the computer room made studying at Stellenbosch worth while.
- Deidre Davids & Shafiek Mohammed for always being so helpful and just great people to have in the analytical department.
- My parents **Godfrey & Linda Martin** for supporting me from my first year of study at Stellenbosch. Thanks for your love, guidance and support. You truly are the best.
- My Ou sus **Gwyneth** thanks for everything
- To my Saviour, my Healer, my Deliver, my Friend, my Counsellor my Lord Jesus Christ who made everything possible. Without you in my life Lord all of this would have been in vane. I honour you for all the blessings and favour in my life. All honour and Glory unto You forever and ever.

CONTENTS

Abstract	i
Opsomming	ii
Glossary of symbols	iii
Acknowledgments	iv
Table of contents	v
List of figures	ix
List of tables	xi

Chapter 1

Introduction and Objectives

1.1 Introduction	1
1.2 Speciation	1
1.3 Mercury	2
1.3.2 Importance of mercury speciation	2
1.4 Statement of the problem	4
1.5 Aims and objectives	4
1.6 Significance of study	4
References	6

Chapter 2

Overview of Mercury

2.1 Introduction	8
2.1.2 Mercury species and transformation in the atmosphere	9
2.1.3 Mercury species and transformation in aquatic environment	11
2.1.4 Mercury species in soil	11
2.2 Toxicology	12
2.3 Impact of mercury on the environment	13
2.4 Sources of mercury	14
2.4.2 Natural Sources of mercury	14

2.4.3 Anthropogenic sources of mercury	14
2.5 Industrial uses of mercury	15
2.6 Environmental regulations	15
Reference	17

Chapter 3

Analytical methods for mercury detection

3.1 Introduction	18
3.2.1 Atomic absorption spectrometry	18
3.2.2 Atomic fluorescence spectrometry	19
3.2.3 Gas chromatography	19
3.2.4 Liquid chromatography	20
3.2.5 Inductively Coupled Plasma Mass Spectroscopy	21
3.2.6 Other detectors used for mercury detection	22
3.2.7 Potential of Capillary Electrophoresis for speciation of mercury	22
3.3 Electrochemical methods for studies of mercury complexes	23
3.3.2 Cyclic Voltammetry	23
3.4 Mercury speciation using capillary electrophoresis	24
3.4.2 Experimental	25
3.4.3 Influence on migration time	26
3.4.4 Capillary wall chemistry	26
3.5 Injection modes	27
3.6 Separation modes	28
3.6.2 Capillary Zone Electrophoresis	28
3.6.3 Micellar electrokinetic chromatography	29
3.6.4 Capillary Isoelectric Focusing	29
3.6.5 Capillary Electrochromatography	30
3.6.6 Separation on microchip	30
3.7 Detection in capillary electrophoresis	31
3.7.2 Absorption	31
3.7.2.1 Direct Detection	31
3.7.2.2 Indirect Detection	32
3.7.2.3 Fluorescence	32

3.8 Inductively Coupled Plasma Mass spectrometry	33
3.9 Electrochemical Detection	34
References	35

Chapter 4

Experimental procedures

4.1 Reagents and materials	39
4.2 Instrumentation	40
4.3 Preparation of standard solutions	41
Reference	43

Chapter 5

Results and Discussion I

5.1 Electrochemical studies of mercury cysteine complexes	44
5.2.1 Study of Mercury (II) and its cysteine complex	45
5.2.2 Study of Methylmercury (I) and its Cysteine Complex	49
5.2.3 Study of Ethylmercury (I) and its Cysteine Complex	52
5.2.4 Study of Phenylmercury (I) and its Cysteine Complex	55
5.3 Mercury Dithizone complexes	58
5.3.2 Study of Mercury (II) and its Dithizone Complexes	59
5.3.3 Study of Methylmercury (I) and its Dithizone Complex	60
5.3.3 Study of Ethylmercury (I) and its Dithizone Complex	61
5.3.4 Study of Phenylmercury (I) and its Dithizone Complex	62
5.4 Mercury Dithizone sulfonate complexes	63
5.4.2 Study of mercury (II) and its Dithizone sulfonate Complex	63
5.4.3 Study of methylmercury (I) and its Dithizone sulfonate Complex	64
5.4.4 Study of Ethylmercury (I) and its Dithizone sulfonate Complex	65
5.4.5 Study of Phenylmercury (I) and its Dithizone sulfonate Complex	66
Conclusion	67
References	69

Chapter 6

Results and Discussion I I

6.1 Capillary Electrophoresis with UV Detection	72
6.2 Performance	73
6.3 Separation of mercury dithizone sulfonate complexes	75
6.4 Conclusion	77
Reference	79

Chapter 7

Results and Discussion I I I

7.1 Electrochemical Detection	80
7.2 Fundamentals of Electrochemical Detection	80
7.3 Conductivity	81
7.4 Potentiometric	82
7.5 Amperometric	82
7.6 Detection modes in CEEC	84
7.6.2 End-channel detection	85
7.6.3 In-channel detection	85
7.6.4 Off-channel detection	86
7.7 Experimental	86
7.7.2 Capillary electrophoresis	86
7.7.3 Amperometric detection	87
7.8 Results and Discussion	89
7.9. Comparison of CE UV detection with CE-AD	94
7.10 Environmental mercury speciation	94
7.11 Validation of electrochemical detector for mercury detection in coal	97
7.12 Conclusion	99
References	100

Chapter 8

Overall Conclusions and Recommendations

8.1 Overall Conclusions	104
8.2 Recommendations and future work	105
8.3 Conference contributions	105

List of Figures

Chapter 1

Fig.1.1	The cycle in speciation analysis	3
---------	----------------------------------	---

Chapter 2

Fig. 2.1	Mercury cycle in the environment	9
Fig. 2.2	Mercury transformation in the environment	10
Fig. 2.3	Structure of Methylcobalmin	12

Chapter 3

Fig. 3.1	Schematic of an electrochemical cell used in Cyclic Voltammetry	24
Fig. 3.2	Schematic of CE instrument	26
Fig. 3.3	Illustration of the origin of the EOF	27

Chapter 4

Fig. 4.1	UV Absorption spectra of dithizone and dithizone sulfonate	42
----------	--	----

Chapter 5

Fig. 5.1	Cyclic Voltammogram of 0.362 mM Hg ²⁺	46
Fig. 5.2	Cyclic Voltammogram of Hg and HgL ₁ complex	47
Fig. 5.3	Cyclic Voltammogram of [HgL] complex at various ligand ratios	48
Fig. 5.4	Cyclic Voltammogram of MeHg	50
Fig. 5.5	Cyclic Voltammogram of MeHg and [MeHgL] complex	50
Fig. 5.6	Cyclic Voltammogram of [MeHgL] complex at various ligand ratios	51
Fig. 5.7	Cyclic Voltammogram of 0.376 mM EtHg	52

Fig. 5.8	Cyclic Voltammogram of EtHg and [EtHgCYS] complex	53
Fig. 5.9	Cyclic Voltammogram of [EtHgCYS] complex at various ligand ratios	54
Fig. 5.10	Cyclic Voltammogram of 0.319 mM PhHg	55
Fig. 5.11	Cyclic Voltammogram of PhHg and [PhHgCYS] complex	56
Fig. 5.12	Cyclic Voltammogram of [PhHgCYS] complex at various ligand ratios	56
Fig. 5.13	Structure of dithizone metal complex	58
Fig. 5.14	Cyclic Voltammogram of [HgDz] complex at various ligand ratios	59
Fig. 5.15	Cyclic Voltammogram of [MeHgDz] complex at various ligand ratios	60
Fig. 5.16	Cyclic Voltammogram of [EtHgDz] complex at various ligand ratios	60
Fig. 5.17	Cyclic Voltammogram of [PhHgDz] complex at various ligand ratios	62
Fig. 5.18	Structure of dithizone sulfonate	63
Fig. 5.19	Cyclic Voltammogram of [HgDzS] complex at various ligand ratios	63
Fig. 5.20	Cyclic Voltammogram of [MeHgDzS] complex at various ligand ratios	64
Fig. 5.21	Cyclic Voltammogram of [EtHgDzS] complex at various ligand ratios	65
Fig. 5.22	Cyclic Voltammogram of [PhHgDzS] complex at various ligand ratios	67

Chapter 6

Fig. 6.1	Electropherogram of mercury cysteine complex	73
Fig. 6.2	Electropherogram of mercury dithizone sulfonate	76
Fig. 6.3	Electropherogram of organomercury dithizone sulfonate complexes	76

Chapter 7

Fig. 7.1	Electrode aligning in amperometric detection	84
Fig. 7.2	Schematic representation of the CEEC cross hair design	87
Fig. 7.3	Picture of the gold micro electrode	88
Fig. 7.4	Cyclic voltamogram of a Au micro electrode	88
Fig. 7.5	Experimental set up of EC cell for mercury speciation	89
Fig. 7.6	Electropherogram of mercury cysteine complex	90
Fig. 7.7	Calibration curve of Hg^{2+} with CE-AD	91
Fig. 7.8	Electropherogram of methylmercury cysteine complex	92
Fig. 7.9	Electropherogram of methylmercury cysteine complex	92
Fig. 7.10	Calibration curve of MeHg^+ with CE-AD	93
Fig. 7.11	Electropherogram of mercury certified reference standard	95
Fig. 7.12	Electropherogram of mercury cysteine complex from coal	95

Fig. 7.13	Electropherogram of test sample C1632 complexed with cysteine	96
Fig. 7.14	Electropherogram of mercury certified reference standard (SARM 20)	97
Fig.7.15	Electropherogram of Cape Point sampling	98

List of Tables

Chapter 1

Table 1.1	Major mercury species in the environment	2
-----------	--	---

Chapter 2

Table 2.1	Analytical methods for mercury detection	16
-----------	--	----

Chapter 3

Table 3.1	Various detection modes in CE	31
-----------	-------------------------------	----

Chapter 5

Table 5.1	Ionisation state of cysteine molecules as a function of pH	45
-----------	--	----

Chapter 6

Table 6.1	LOD of mercury cysteine complexes	74
-----------	-----------------------------------	----

Table 6.2	LOD for mercury dithizone complexes	77
-----------	-------------------------------------	----

Chapter 7

Table 7.1	Electrochemical detection methods for CE	83
-----------	--	----

Table 7.2	Parameters for CE-AD	89
-----------	----------------------	----

Table 7.3	Linear regression data of mercury cysteine complex	91
-----------	--	----

Table 7.4	Linear regression data of methylmercury cysteine complex	93
-----------	--	----

Table 7.5	Experimental data of coal samples for mercury determination with CE-UV	96
-----------	--	----

Chapter 1

Introduction and objectives

1.1 Introduction

The rapid increase in the levels of environmental pollution in recent years has resulted in the increasing harm to people's health and for the global ecosystem. The need to determine different species of trace metals in the environment, air and food is becoming more important. The effects of toxicity of an element and its behaviour depends a great deal on its chemical form and concentration [1]. Originally most analytical methods only dealt with the total content of an element in an analyzed sample (such as lead, mercury or cadmium). Until recently, analytical methods allowed analyst to determine total contents only, but it was soon realized that this information was insufficient [1-2]. Trace elements have both beneficial and harmful effects depending on their concentration and chemical form in living organisms. A number of trace elements (zinc, selenium, manganese, etc.) are considered essential, with specific biological functions at relatively low levels. However, when present in excess, these elements can be harmful [3]. Toxicological investigation has shown that for living organisms, the chemical form of a specific element or oxidation state in which the element is introduced into the environment is crucial. It is therefore important to not only gain information about the total content, but necessary to determine the individual chemical and physical form of the element [1, 4].

1.2 Speciation

According to the official definition by IUPAC speciation analysis is the process leading to the identification and determination of the different chemical and physical forms of an element existing in a sample. The analytical activity involved in identifying and measuring species is hence defined as 'speciation analysis'. The determination of the concentration of specific chemical forms, such as organic mercury rather than elemental mercury is highly essential for the interpretation of their biochemical behavior or assessment of the potential danger to humans and organisms [5].

1.3. Mercury

Mercury [Hg] is a very toxic pollutant in the environment. It has serious effects on human health [6]. Mercury levels in the environment have increased in the last 10-15 years due to human activities. Mercury is a naturally occurring element that exists in several forms. The three most important chemical forms of mercury known to be present in the environment are: elemental mercury (Hg^0), which has a high vapor pressure and relatively low solubility in water, mercurous (Hg_2^{2+}) and mercuric Hg^{2+} inorganic cations which is far more soluble in water and which have a strong affinity for many inorganic and organic ligands especially those containing sulfur. Table 1 show all the major mercury species in the environment and biological samples [5-8].

Table1.1. Major mercury species in the environment

Elemental mercury		Hg^0
Inorganic mercury	Mercurous ion	Hg_2^{2+}
	Mercuric ion	Hg^{2+}
Organic mercury	Methylmercury	CH_3Hg^+
	Ethylmercury	$\text{CH}_3\text{CH}_2\text{Hg}^+$
	Phenylmercury	$\text{C}_6\text{H}_5\text{Hg}^+$
	Dimethylmercury	$(\text{CH}_3)_2\text{Hg}^+$

1.3.2. Importance of mercury speciation

The different forms in which mercury exists are commonly called species of mercury. Elemental mercury, methyl mercury and inorganic mercury are examples of different mercury species. Speciation is the term used to represent the distribution of a quantity or flux of mercury among various species. In general mercury speciation involves the following steps:

1. Sample collection/ pre-treatment storage
2. Extraction of mercury from matrix/ preconcentration
3. Identification, Separation of mercury and
4. Detection

Cases such as the Minamato incident (1950's) and the THOR Chemicals incident (1987) focused attention on the importance of speciation and the toxicity of mercury [6-8].

Mercury speciation is important to consider because of the following points.

1. It determines the way mercury is transported from sources to the local environment of humans and wildlife;
2. It determines how mercury is bound in the environment and therefore is more or less available to cause adverse effects;
3. It determines one of the most important mercury exposures of humans and wildlife: the build up of methyl mercury in fish and other aquatic foods [9-10].

The present situation worldwide as depicted in Fig.1.1.

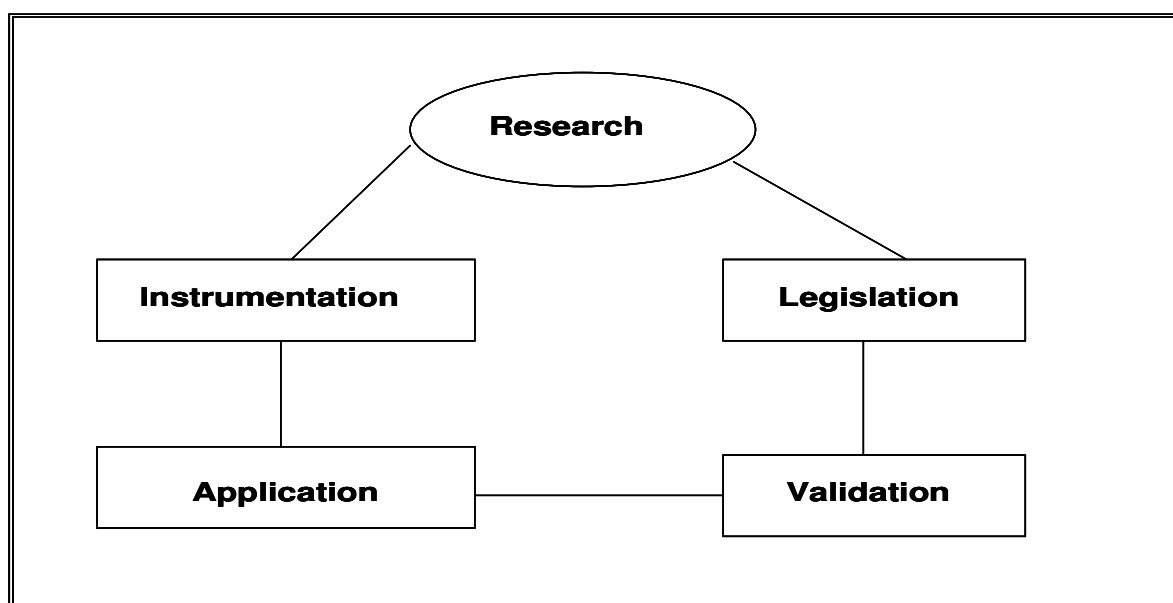


Fig.1.1 The cycle in speciation analysis

Here the progress of research fails to influence legislation. Consequently, governments continue to build almost exclusively on expressing the content of trace elements in a matrix only by the total content disregarding what chemical species there may be present in the sample. Analytical control of the legislation will provide data for total content of the trace metals only.

Consequently, there will be no need to develop simple and fast analytical methods, which could

in turn provide the more relevant speciation data. The challenge is therefore to break the cycle [11-12]. Recently, there has been an increasing interest in the separation and determination of metal species using Capillary Electrophoresis (CE) [13]. Because of its speed, resolving power, minimal sample reagent requirements and greater simplicity, it makes this analytical technique capable in a variety of areas [14-16]. We have set about studying the electrochemistry and electrophoresis of various mercury complexes with the aim of identifying different mercury species.

1.4 Statement of the problem

Mercury pollution is not just a problem in Asia or Europe but it has rather big effects in South Africa. Government has realised that certain legislation and laws need to be put into practice concerning mercury pollution in SA. The need for fast and accurate analytical techniques to detect and speciate mercury is therefore of the outmost importance. The THOR Chemical Incident is by far the biggest reported mercury pollutant episode in South Africa [6,7]. With the ongoing demand for electricity and the combustion of coal which contains a percentage of mercury (0.2-0.5 mg Hg/kg), the mercury concentration is set to rise in the near future [6-8,13].

1.5 Aims and objectives

The aim of the study is to develop a quick and inexpensive CE method by:

- Complexing mercury with suitable ligands like cysteine, dithizone and dithizone sulfonate
- Study the electrochemical properties of these complexes by Cyclic Voltammetry (CV)
- Detect and speciate these different mercury complexes with CE -UV detection
- Develop a new CE electrochemical detector (CE-ED) for mercury speciation
- Compare the detection limits of CE-UV with CE-AD

1.6 Significance of study

Currently Government has no enforced legislation on mercury levels in South Africa. Recently the South African Mercury Assessment program (SAMA) was established (April 2006). The aim of this program is to monitor and develop new analytical techniques to determine mercury in the

Chapter 1 – Introduction and objectives

environment and help government set up proper protocols for mercury determination. The Cape Town Weather Station at Cape Point is the only site in the Southern Hemisphere monitoring Hg emissions in air. Total gaseous mercury (TGM) has been monitored for the past 15 years at Cape Point. Cold vapor atomic fluorescence spectroscopy (CV-AFS) is used as the analytical tool, only giving the total mercury concentration [17].

The newly developed method will be helpful when determining mercury concentrations in analytical laboratories in South Africa from a speciation point of view.

Reference:

1. A. Gaspar, C.S. Pager, *Microchemical Journal* 73, (2002,) 53-58.
2. A. Kot, J. Namiensnik, *Trends in Anal. Chem.*, 19, (2000), 69-79.
3. L. Khotseng, PhD Thesis University of Stellenbosch, 2004
4. T.Lee, S.Jiang, *Anal. Chim. Acta* 413, (2000), 197-205.
5. A.R. Timerbaev, *Talanta* 52, (2000), 573-606.
6. P. Kuban, P.C. Hauser, V. Kuban, *Electrophoresis* 28, (2007), 58-68.
7. T.G Spiro, T.G. Stagliani, *Chemistry of the Environment*, New York, Prentice Hall, 1996.
8. A.R. Hutchison, D.A. Atwood, *Journal of Chemical Crystallography* 33, (2003), 631-645.
9. UNEP Global Mercury Assessment Revised Draft July 2002, Geneva Switzerland
10. M. Leermakers, W. Baeyens, M. Horvat, *Trends in Analytical Chemistry* 24, (2005), 353- 360.
11. T. Berg, E.H Larsen, *Fres. J. Anal. Chem.*, 363, (1999), 431-434.
12. D.R. Williams, *Coordination Chemistry Reviews* 185, (1999), 177-188.
13. J. Pycyna, E. Pacyna, F. Steenhuisen, S. Wilson, *Atmospheric Environmental* 37, (2003), 109-117.
14. A.R. Timerbaev, O.A. Shipgun, *Electrophoresis* 21, (2000), 4179-4191.
15. E. Dabek-Zlotorzynska, E.P.C. Lai, A.R. Timerbaev, *Anal. Chim. Acta* 359, (1998), 1-26.

16. I. Medina, E. Rubi, M.C. Mejuto, *Talanta* 40, (1993) 1631-1636.

17. P. Baker, E. Brunke, F. Slemr, A. Crouch, *Atmospheric Environment* 36, (2002), 2459-2464.

Chapter 2

Overview of Mercury

2.1 Introduction

Metallic mercury is a shiny, silver white metal that is a liquid at room temperature. Mercury is the familiar liquid metal used in thermometers and some electrical switches. At room temperature some of the metallic mercury will evaporate and form mercury vapours [1,2].

Mercury is mined as cinnabar (HgS) ore. The metallic form is refined from mercuric sulfide ore by heating the ore to temperature above 600°C. This vaporizes the mercury in the ore, and the vapors are then captured and cooled to form the liquid metal mercury. Most inorganic mercury compounds are white powders or crystals except HgS which is a red salt and turn red after exposure to light [3]. When mercury combines with carbon the compounds formed are called organic mercury compounds or organomercurials. There are a large number of organic mercury compounds, but by far the most common organic mercury compounds found in the environment are methylmercury and phenylmercury. In the past a number of these organic mercury compounds were used in pesticides and biocides in some paints, pharmaceuticals and cosmetics [4]. While many of the uses of mercury have decreased in the recent years, some parts of the world are still using these toxic compounds. Some examples are the use of seed dressing with mercury compounds in some countries [2], use of dimethylmercury [4] in small amounts as a reference standard for some chemicals tests and thimerosal (which contains ethyl mercury) used as a preservative in some vaccines and other medical and cosmetic products [3].

Mercury levels in the environment need to be monitored more strictly due to the fact that all mercury species can interchange in the environment [1]. The most common organic mercury form that micro organisms and natural processes generate from another is methylmercury. Methylmercury is of particular concern because it can build up in many edible freshwater and saltwater fish and marine life to levels that are many times greater than levels in surrounding water. Methylmercury can be formed in both chemical processes (abiotic) and by micro organisms (biotic) in the environment. It's believed that that its formation in nature is predominantly due to the latter. Being an element, mercury cannot be broken down or degraded

Chapter 2 – Overview of Mercury

into harmless substances. Mercury may change between different states and forms in its cycle [4].

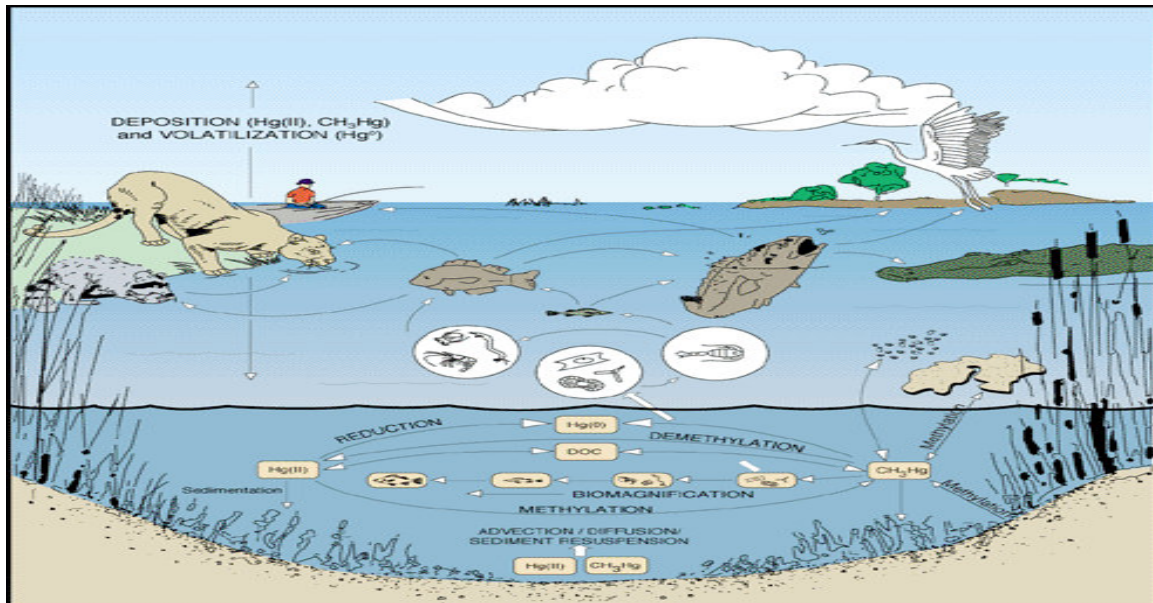


Fig. 2.1 Mercury cycle in the environment [4].

2.1.2 Mercury species and transformation in the atmosphere

The atmospheric chemistry of mercury involves several interactions:

- Gas and aqueous phases reactions (in cloud and fog droplets);
- Partitioning of elemental and oxidised mercury species between the gas and solid phase;
- Partitioning between the solid and aqueous phase in the case of insoluble particulate matter scavenged by fog or cloud droplets.

The interplay between mercury atmospheric processes and chemistry is summarised in figure 2.2 below [9].

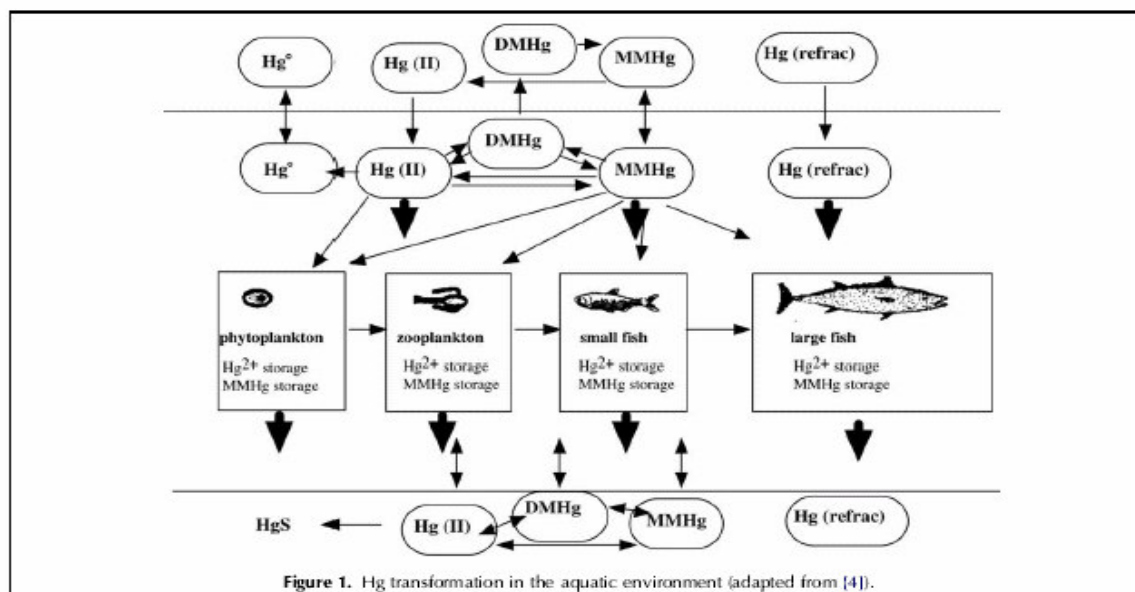


Figure 1. Hg transformation in the aquatic environment (adapted from [4]).

Fig.2.2 Mercury transformation in the environment [2].

It is estimated that between 6000 and 10800 tons of mercury resides in the atmosphere at any given time [1]. Most of the mercury enters the atmosphere as Hg^0 , a huge amount also resides there as Hg^{2+} in the atmospheric water droplets. During the atmospheric lifetime of mercury, it can travel a considerable distance, resulting in elevated mercury levels far from mercury contamination source. There has been several review papers on the atmospheric mercury chemistry over the last few years [5-7]. This chemistry is dominated by a series of only partially understood redox reactions that occur either in the gaseous phase or aqueous phase. In water droplets, Hg^0 can be oxidized to Hg^{2+} by ozone (O_3), reactive chlorine species and to a lesser extent by hydroxyl radicals. Which process dominate is not known at this time, although it is assumed that overall oxidation occurs more rapidly than reduction, since the mercury does eventually tend to return to earth as Hg^{2+} and most of the reaction are believed to occur in the aqueous phase [3]. Gaseous Hg^0 can be oxidized to Hg^{2+} by a number of molecules, including ozone and hydrogen peroxide during the day and nitrate radicals by night. It appears that sunlight increases the rate of mercury oxidation in the gas phase, although the reason for this is not known [4]. Recent studies have shown that the oxidation of elemental mercury as a result of reaction with O_3 , in fact occurs rapidly and estimations of the atmospheric lifetime of elemental mercury have had to be reduced from around a year to a matter of few months. The rate of oxidation of elemental mercury is important to atmospheric mercury chemistry because oxidised mercury

compounds (such as HgO and HgCl₂) produced are more soluble and more nonvolatile and therefore more rapidly scavenged by atmospheric particles. The most important characteristics of mercury that set it apart from other metals commonly found in the atmosphere, are its tendency to be readily re-emitted to the air once deposited. Being in the vapour phase and relatively inert to chemical attack by other air contaminants and only partially soluble in water support the concept of mercury being a global pollutant. Comparing the residence time of mercury with other metals found in the atmosphere which has an atmospheric life time of a couple of days or at most a few weeks illustrate this important effect of mercury in the atmosphere [1,2,4].

2.1.3 Mercury species and transformation in aquatic environment

Methylmercury can be produced by chemical processes (abiotic) or by micro organisms such as bacteria (biotic) in the environment. The efficiency of microbial mercury methylation generally depends on factors such as microbial activity and the concentration of bioavailable mercury. Temperature, pH, redox potential and presence of inorganic and organic complexing agents all play a role. Methylmercury is the predominant mercury species found in fish. In an updated mercury overview the United States Environmental Protection Agency (US EPA) states that in most adult fish, 90% to 100% of mercury content is methylmercury [2-4]. Fitzgerald (2007) has reviewed aspects of the mercury cycle in oceans and other waters. From open ocean studies it is clear the elemental mercury, dimethylmercury and methylmercury are common mercury species found in aquatic environment [8].

2.1.4 Mercury species in soil

In soil the formation of inorganic mercury compounds are preferred. Compounds such as HgCl₂, Hg(OH)₂ and inorganic Hg²⁺ are found in soil which can form complexes with organic anions. This complexing ability limits the mobility of mercury in soil. Much of mercury in soil is bound to bulk organic matter. For this reason mercury has a long retention time in soil and as a result, the mercury accumulated in soil may continue to be released to surface waters and other media for long periods of time [4,9].

2.2 Toxicology

The bioinorganic cofactor cobaltamin has been called nature's most beautiful cofactor but is also perhaps one of nature's most deadly. It's responsible for methyl transfer reactions, including the methylation of inorganic Hg^{2+} . Methylcobalamin (a structural analogue of vitamin B12 fig.2.3), contains a cobalt atom in an octahedral geometry with an axial methyl group. In sulphate reducing bacteria such as *Desulfovibrio desulfuricans* the methylation of mercury by methylcobalamin is enzymatically catalyzed [3,4,10]. The mechanism of this reaction is not fully understood, although it is believed to be a one step process. The methylated product is stable in water due to the more covalent nature of the mercury carbon bond. It is also soluble in lipid membranes common to living organisms. Although all forms of mercury are toxic the methylated form of mercury is considered to be by far the most toxic.

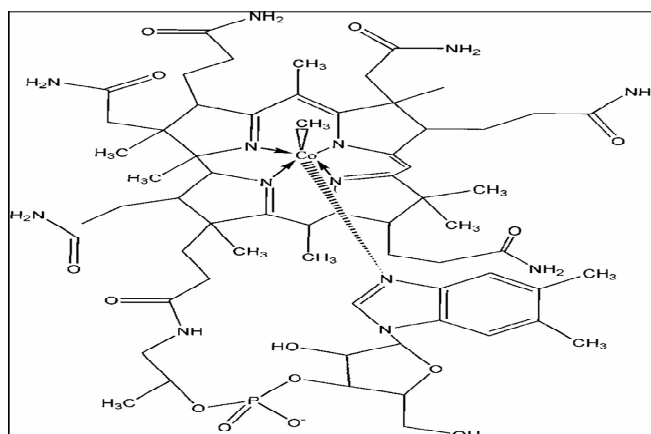
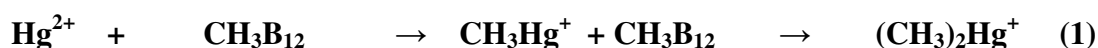


Fig. 2.3 Structure of Methylcobalamin [3].



The liver reabsorbs rather than excretes methylmercury due to a process known as enterohepatic recirculation [3]. This is why methylmercury tends to bioaccumulate in living organisms, once it is consumed, it is almost never excreted. Methylmercury also crosses the blood-brain barrier and tends to accumulate in the brain of mammals. Methylmercury is a well-known neurotoxicant. Once inside the human methylmercury attacks the nervous system by binding to key biological sulphur-containing compounds. The result is a loss of feeling in the hands and feet, constriction in vision, tremors, loss of hearing and eventually death. History records several major cases of

Chapter 2 – Overview of Mercury

methylmercury poisoning [1]. When methylmercury was first synthesized and reported in the early 1850s, two of the chemist working on the project died and a third was debilitated. In 1956 residents of the Minamata Bay, Japan area, suffered from a strange nervous disorder due to polluted waste water containing mercury. This was eventually diagnosed as mercury poisoning due to waste dumped by the Chisso Minamata Acetaldehyde Plant and the Minamata Chemical Industrial Plant. The pollution affected the people in the form of methylmercury poisoning known as “Minamata disease”. People eating large quantities of contaminated fish and shellfish from the Bay were all infected. Many people lost their lives or suffered from physical deformities [1,4,11,12].

In September 1971 due to fears of famine Iraq imported large amounts of seed wheat which have been treated with methyl mercury fungicides. Imported mercury treated seed grains arrived after the planting season and were subsequently used as grain to make into flour that was baked into bread. Unlike the long term exposure in Japan, the methyl mercury poisoning incident in Iraq was much shorter, but the magnitude of the exposure was high. The number of people admitted to the hospital with symptoms of poisoning has been estimated to be approximately 6500, with 459 fatalities reported. Currently a new epidemic of Minamata disease is building in the Amazon River region, where gold mining has resulted in widespread mercury release into the river. There the mercury is methylated and is now bio accumulating in fish. No deaths has yet been reported but many people seem to suffer from mild cases of Minamata disease [2-4,11,12].

2.3 Impact of mercury on the environment

An important factor in the impacts of mercury to the environment is its ability to build up in the organism and along the food chain. The term **bioaccumulation** refers to the net accumulation over time of metals within an organism from both biotic (other organisms) and abiotic (soil, air and water) sources. Biomagnification refers to the progressive build up of some heavy metals by successive trophic levels-meaning this relates to the concentration ratio in a tissue of a predator organisms as compared to that in its prey. Although all forms of mercury can accumulate to some degree, methyl mercury accumulates to a greater extent than other forms of mercury. Inorganic mercury can also be absorbed, but is taken up at a much slower rate with lower efficiency than methyl mercury [1-4].

2.4 Sources of mercury

The emissions of mercury to the biosphere can be grouped in the following categories:

- Emissions due to natural mobilisation
- Anthropogenic sources
- Re-emissions of previous anthropogenic releases
- Product and process releases of mercury

2.4.2 Natural Sources of mercury

Natural sources include volcanoes, evaporation from soil and water surfaces, degradation of minerals forest fires etc. Mercury can be found in all geological media in relatively small concentrations. Elemental and some oxidized mercury are permanently coming to the atmosphere due to their volatility. High temperature in the earth mantle results in high mercury mobility and mercury continuously diffuses to the surface. Today's emissions of mercury from soil and water are however not only from natural sources but are also influenced by previous deposition of mercury from other sources. This makes it very difficult to determine the actual natural mercury emissions. A number of attempts have been made to estimate the global natural emissions of mercury. It is however difficult to do so with any precision and research is still done in this field by different research groups [2-4].

2.4.3 Anthropogenic sources of mercury

Mercury is naturally present in coal and other fossil fuels as well as in minerals like lime for cement. Coal fired power production have shown to be the single largest global source of atmospheric mercury emissions. This is due to the increasing global power consumption worldwide [5]. Mining and other metallurgic activities involving the extraction and processing of recycled minerals like iron, steel, gold and zinc also contributes to mercury releases as an anthropogenic source [3].

2.5 Industrial uses of mercury

Mercury has found a number of uses throughout history. Prehistoric cave man appears to have used cinnabar (HgS) as a red pigment [3]. Mercury amalgams were also used to extract precious metals from ores. Until recently mercury was the preferred thermometric medium for thermometers because of its uniform thermal expansion. It has also been widely used in barometers and manometers for pressure measurements, leading to mercury contamination. Another important use of mercury is in the lighting industry. Most fluorescent lamp utilizes mercury vapour, along with an inert gas such as Argon, to convert electrical discharge to useful light. The tube shaped bulbs contain this mercury gas mix. The mercury is excited by a flow of electrons and radiates light in the UV region. Mercury in electrolytic cells used in the Chlor-Alkali industry is also a major use. Chlor-alkali plants produce sodium hydroxide and chlorine gas via the electrolysis of brine. The mercury serves as an anode converting the sodium cations to sodium metal, amalgamating the sodium and carrying it into a second reaction where it reacts with water to form sodium hydroxide. This process is a major source of mercury pollution. Because of this, the mercury cells are being replaced by diaphragm cells. Mercury cell batteries were also used widely for applications such as hearing aids. The standard mercury cell battery contains a mercury/zinc amalgam as the anode and a mercuric oxide/graphite cathode. Mercury is also found in zinc-silver cell batteries and traces of mercuric chloride are found in zinc-carbon batteries [1-4].

2.6 Environmental regulations

Federal state and local governments can issue fish consumption advisories about which fish are unsafe to eat or which bodies of water are unsafe to fish. Laws and regulations are used as major tools to protect the environment of mercury released through emissions from manufacturing use, or disposal activities. These regulations are often enforced by agencies such as the Environmental Protection Agency (EPA). The EPA provides specific rules and details for how to put the law into practice. The World Health Organization (WHO) has published a maximum daily human consumption limit of 0.48 μg total mercury p/kg body weight [9]. EPA has also published methods used by industrial and municipal facilities to analyze the components of wastewater, drinking water, sediment and other environmental samples. The following table includes a list of the more prominent methods used by the environmental community [2, 4].

Table 2.1 Analytical methods for mercury detection

Method Number	Description
EPA 200.8	Metals in water using ICPMS
EPA 245.1	Mercury in water using CV-AAS
EPA 1631E	Mercury in water using CV-AFS
EPA 7471A	Mercury in solids using CV-AAS
EPA 101A	Gaseous mercury using CV-AAS
ASTM D-6350	Mercury sampling in natural gas CV-AFS

Reference:

1. P. Kuban, P.C. Hauser, V. Kuban, *Electrophoresis* 28, (2007), 58-68.
2. T.G Spiro, T.G. Stagliani, *Chemistry of the Environment*, New York, Prentice Hall, 1996, 341-350.
3. A.R. Hutchison, D.A. Atwood, *Journal of Chemical Crystallography* 33, (2003), 631-645.
4. UNEP Global Mercury Assessment Revised Draft July 2002, Geneva Switzerland, 1-251.
5. J.M. Pycyna, E.G. Pacyna, F.Steenhuisen, S. Wilson, *Atmospheric Environmental* 37, (2003), 109-117.
6. P. Baker, E. Brunke, F. Slemr, A. Crouch, *Atmospheric Environment* 36, (2002), 2459-2464
7. W.H. Schroeder, J. Munthe, *Atmospheric Environment* 32, (1998), 809-820.
8. W.F. Fitzgerald, C.H. Lamborg, C.R Hamerschmidt, *Chemical Reviews* 107, (2007), 641-662.
9. M. Morita, J. Yoshinga, J. Edmonds, *Pure & Appl. Chem.*,70, 1998, 1585-1615.
10. S.C. Choi, T. Chase, R. Bartha, *Applied Environmental Microbiology* 60, (1994), 1342.
11. T.W. Clarkson, *Environmental Health Perspectives* 100, (1992), 31-38.
12. D.L. Rabenstein, *Journal of Chemical Education* 55, (1978), 292-296.

Chapter 3

Analytical methods for mercury determination

3.1 Introduction

A variety of methods exist to detect mercury sensitively and selectivity [1]. Several review papers have been published for the determination of total mercury concentration in environmental and biological samples. These methods are listed as follows: Cold vapour atomic absorption spectrometry (CVAAS) [2], atomic fluorescence spectrometry (CVAFS) [3], Inductively coupled plasma atomic emission spectrometry (ICP-AES) [4], mass spectrometry (ICP-MS) [5] and chromatography [6].

3.2.1 Atomic absorption spectrometry

The most popular method for determining mercury is cold vapour atomic absorption spectrometric measurement (CVAAS). This analytical technique is still widely used [1,7]. Mercury is unique among the heavy metals in that it has a very high vapour pressure at low temperatures and can be introduced to the spectrometer as a vapour with ease. Absorption at 253.7nm in the UV region has been measured with the use of mercury vapour lamps and also hollow cathode lamps as the light source. The way of releasing mercury from digested or aqueous samples is reduction. This process is then followed by volatilization and introduction of the mercury by aid of a gas stream. Sn^{2+} ions have been used as a reductant [6,8]. Procedures to eliminate interference have been important in the determination of mercury in different matrices. Two approaches have been used to remove interferences by organic vapour. A gold amalgamation method to purify the mercury vapour and an optical background correction method for the spectrometry. The gold amalgamation is based on the selective absorption of mercury on a gold surface. The organic vapour is purged out and mercury is released from the gold fibre trap by heating and then introduced into the spectrometer. Optical background correction is used to eliminate molecular absorption by organic vapours. Earlier work used a continuum light source and later work used the Zeeman effect. These methods are necessary for electrothermal atomization, or flameless atomic absorption spectrometry. Zeeman AAS is suitable for the direct analysis of solid samples or samples without prior acid digestion. Use of

quartz lamps and the 184.9 nm resonance line in the UV region provided increased sensitivity over the commonly used employed 253.7 nm line. Improved accuracy for CVAAS was obtained by using the 184.9 nm resonance line. Detection limits for Hg using the 184.9 nm is 30 times lower than using the 253.7 nm line [7-10].

3.2.2 Atomic fluorescence spectrometry

Several articles have appeared on the determination of Hg using CVAFS [11,12]. Most of the early work used flame atomization. This technique was later further developed by using an electrothermal atomization or cold vapour atomization [13]. This technique makes use of Hg autofluorescence, the narrow band emission of UV radiation by Hg^0 atoms during relaxation to the ground state after absorption of radiation of wavelength 253.7 nm. The result is a sensitive and selective detection of mercury in the picogram range [8,13]. Mercury is liberated by aeration or reduction and trapped on an Au filament. The Au filament is then heated to 700 °C to liberate Hg^0 which is then introduced to a flow type atomic fluorescence cell. The detection limit is 5 pg Hg with a relative standard deviation of 3%. Using an atomic fluorescence instrument that uses ICP as an atomization cell and a pulsed Hg hollow cathode lamp can lower the detection limits to 0.5 ng dm⁻³ [8,12].

3.2.3 Gas chromatography (GC)

In GC species are separated on the basis of volatility and the interaction between the analytes and the stationary phase. There are both packed and open capillary columns for GC, the latter being used the most efficient. Capillary columns are between 10 and 100 meters long, having an internal diameter (i.d) of 0.2 – 0.7 mm and the inner wall coated with a 0.2 – 0.5 µm thick film of stationary phase. The mobile phase is a gas, typically helium that transports the vaporized analytes toward the detector. The GC column is placed in an oven and heated to required temperatures [13-16]. For good performance in GC most mercury species need to be derivatised to become volatile and thermally stable. Butylation with Grignard reagent in an organic solvent is a common derivatisation method [17]. However, if the excess Grignard is not deactivated, methyl butyl mercury can be transformed to dibutyl mercury and the same transformation has also been seen for dimethyl mercury [16-18]. The presence of halogens such as iodine in a sample has shown to decompose alkyl mercury [18].

Chapter 3 – Analytical methods for mercury determination

In aqueous solution sodium tetraethyl borate NaBEt_4 , is used for derivatization of mercury species and produce volatile ethyl mercury species [19]. These species are purged out of solution with an inert gas onto a Tenax packed column. The mercury species are then desorbed from the Tenax by heating and with a gas stream the species are injected into the GC [8,15,20]. A disadvantages of using this method is that inorganic mercury, mono ethyl mercury and diethyl mercury cannot be separated when using NaBEt_4 . All these mercury species are derivatised to the same chemical form. Another drawback is that if the sample contains high concentrations of halides, methylmercury is reduced to Hg^0 during derivatization [19,20]. A major disadvantage of this method is the interactions of mercury compounds with the chromatographic support such as decomposition of mercury and adsorption onto tubing and pipes. This phenomenon can cause serious problems and influence experimental results. Studies have shown that after the injection of methylmercury chloride, substitution of the halide occurred with the formation of methylmercury iodide. The use of glass capillary columns can improve and solve these problems [1,21].

3.2.4 Liquid chromatography

The use of High performance liquid chromatography (HPLC) for mercury speciation has the advantage of simplified sample preparation [22]. In GC analysis it is necessary to form volatile thermally stable derivatives, whereas this is not necessary for HPLC. Another advantage of using HPLC is the relatively low cost of analysis. Aqueous buffers are used as mobile phase but in GC more expensive carrier gases are required. Combining HPLC with spectroscopic detection provides a simple and selective method for metal speciation [8].

There are different types of columns for separation of analytes. Most columns are packed with silica based particles and to the silica surface a stationary phase is chemically attached. The most common stationary phase in HPLC is octadecylsilane, ODS, also called C_{18} . [23]. ODS is non polar and is used in combination with polar mobile phase. For each analyte injected into the column there will be an equilibrium between the stationary phase and the mobile phase. A polar compound has a short retention time as the equilibrium is shifted toward the polar mobile phase and for a non polar analyte the equilibrium is shifted towards the stationary phase and it has a longer retention time [23,24]. For mercury speciation with HPLC mercury species are usually mixed with sulphur containing reagents to form a complex, which improves the chromatographic separation properties of the species. Cysteine [24] and dithizone [25] were successfully used as

complexing agents for mercury speciation. There is however also some disadvantages using HPLC for metal speciation. Some of these disadvantages are the poor retention reproducibility, tailing of peaks, the use of hazardous organic solvent, time consuming extractions to remove interfering compounds [38] and decomposition of diphenylmercury [8]. HPLC is less sensitive than GC and is better suited for polar species separation [26,27].

3.2.5 Inductively Coupled Plasma Mass Spectroscopy (ICP-MS)

Recently mass spectrometers (MS) have become more commonly used as detectors in analytical chemistry. In the MS the sample introduced is ionised and components are separated on a mass to charge ratio in the mass analyser. Samples are introduced as liquids into an inductively coupled plasma (ICP). The liquid passes through a nebulizer to form an aerosol. The ICP is an ion source, which operates at high temperatures (5000 K – 10000 K) and at atmospheric pressure. The argon plasma is generated in a quartz torch under the conditions of a radio frequency electromagnetic field (27– 40 MHz) [27]. The solvent evaporates and molecules are decomposed to single atomic ions in the plasma. As the ICP is operated at atmospheric pressure and high temperatures, the MS requires high vacuum and ambient temperatures. The ability to distinguish between masses is dependant on the resolution of the mass analyser. The resolution R , is usually defined as $R = m/M$. where m is the mean value of the two masses that are separated and M is the mass difference between them.

The main advantage of ICP-MS is that it can be used for detecting most elements at a low concentration. Detection limits are generally in the ng/l range or lower. By scanning the MS, signals for many different elements, or isotopes to charge ratios, can be detected within a few seconds. The ICP-MS performance is affected by introduction of solutions containing high amount of salts or organic solvents, as these will cause deposits of salt and carbon in the interface and MS. Organic solvents give rise to a high organic vapour pressure that will cause a high carbon load of the plasma. High amounts of carbon and salt in the plasma absorbs energy and therefore decreases the ionisation efficiency of the plasma leading to deterioration in sensitivity [8,27].

3.2.6 Other detectors used for mercury detection

Electron capture detector (ECD) was traditionally used in combination with GC for the speciation of mercury [8]. ECD is not selective towards mercury but instead selective towards molecules that contains electronegative functional groups, such as halides. Mercury species have to be derivatised by chlorides or iodine prior to detection [15]. Very low detection limits for mercury is achieved with microwave induced plasma atomic emission spectrometry, MIP-AES. It has been used successfully as a detector for mercury species eluting from GC [28]. The disadvantage with MIP is the low energy plasma that prevents it from being able to atomise large amounts of sample [8,28]. UV detectors have been used in the determination of mercury after HPLC separation [29]. These detectors are not selective, sensitivity is poor and mercury concentrations in environmental samples cannot be determined without pre-concentration of the sample [8].

3.2.7 Potential of Capillary Electrophoresis for speciation of mercury

Many analytical methods have been used for speciation of mercury. Among them, high performance liquid chromatography (HPLC) in its various separation modes is the premier technique [30]. When coupled to element selective detectors like inductively coupled plasma atomic emission or mass spectrometry (ICP-AES and ICP-MS) HPLC shows great resolving power [31]. However, HPLC procedures still do not satisfy all of the requirements for a routine analysis, mainly because of its complicated design process, time consumption and the need for expensive instruments. An alternative method is Capillary electrophoresis (CE), which offers certain advantages in these aspects. The use of CE for the analysis of inorganic species has been growing in the last decade [1]. Although CE is a relatively new and still developing technique, it has shown a potential for metal speciation. Rapid separation speed with high efficiency and a very small sample requirement are some its advantages. With the proper choice of background electrolyte (BGE) CE is well suited for speciation, because the existing equilibrium among the different species can be minimally influenced. Unlike in chromatographic methods, there is no interaction between the sample and the stationary phase. Thus, one of the possible errors arising from a shift in equilibrium because stationary phases favours one species over another is eliminated [31,32]. Although CE has not yet been extensively used for mercury speciation, there is growing interest as evidenced from the recent list of publications [33-37].

We have set about studying the electrochemistry and electrophoresis of various mercury complexes with the aim of identifying different mercury species.

3.3 Electrochemical methods for studies of mercury complexes

Electrochemistry is the science that unites electricity in chemistry. By using electrical principles, chemist design ways of converting electrical energy into chemical energy of desirable materials. Aluminum, nylon and bleach are everyday commodities that are produced by such electrochemical synthesis. Conversely, chemical energy may be converted into electrical energy. Batteries and fuel cells are devices that can perfume this conversion. Electrochemistry has many uses other than electrosynthesis, energy creation and corrosion inhibition. Electrochemical analysis is one of the most direct and accurate ways of measuring things as the purity of drinking water, the acidity in wine and the concentration of toxic metal in factory effluents. Electrochemistry will provide much needed information on the electrochemical properties of mercury complexes [38,39].

3.3.2 Cyclic Voltammetry

Cyclic votammetry (CV) is a versatile electroanalytical technique for the study of electroactive species [38]. CV monitors the behavior of chemical active species within a wide potential range. In CV a potential is applied to the system and the faradaic current response is measured (a faradaic current is the current due to a redox reaction). The current at the working electrode is monitored as a triangular excitation potential. The resulting voltammogram can be analyzed for fundamental information regarding the redox reaction at the electrode. It also provides information about the rate of electron transfer between the electrode and analyte and also the stability on the analyte in the oxidation states. A cyclic voltammogram is the plot of the response current at the working electrode to the applied excitation potential. The sweep rate can vary form a few mV/s up to a few hundrend V/s. At these high values CV is restricted by experimental complication such as double layer charging and large iR_u drop effects [39].

Voltammetry has the advantage of being a species sensitive method and not just an element sensitive technique. Voltammetric determinations of trace metals requires prior preconcentration for very low levels of concentrations in the same way as other instrumental methods [40]. This is where the electrochemical approach provides its greatest advantages because the preconcentration can be done electrochemically in the same cell as the final measurement

Chapter 3 – Analytical methods for mercury determination

without any additional contamination of the samples. Cyclic voltammetry is carried out in quiescent solution to ensure diffusion control. A three electrode arrangement is used. Working electrode includes mercury films, glassy carbon, platinum, gold and carbon paste.

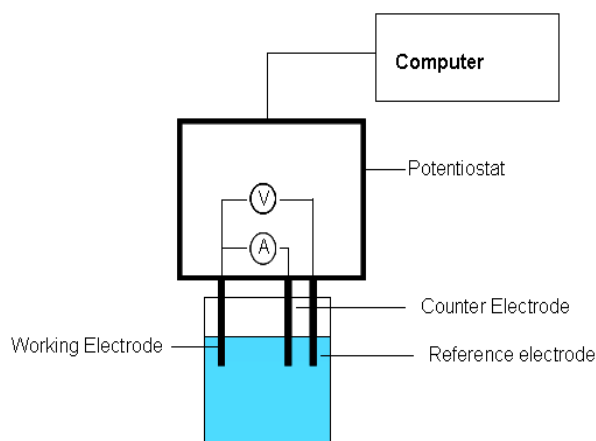


Fig. 3.1 Schematic of an electrochemical cell used in Cyclic Voltammetry

In CV the working electrode potential is swept back and forth across the formal potential of the analyte. Repeated reduction and oxidation of the analyte causes alternating cathodic and anodic current flow at the electrode. The signal of primary interest is the height of the peak. The peak height, i_p , is directly proportional to the analyte concentration, C , as described by the Randles-Sevcik equation:

$$I_p = (2.687 \times 10^5) n^{3/2} v^{1/2} D^{1/2} A C \quad (1)$$

In this equation n is the number of electrons appearing in half-reaction for the redox couple, v is the rate at which the potential is swept (V/sec), A is the electrode area (cm^2), and D is the analyte's diffusion coefficient (cm^2/sec) [38-40].

3.4 Mercury speciation using capillary electrophoresis

Capillary electrophoresis (CE) is a high resolution, fast separation technique for a variety of chemical species including anions, cations, metal-organic ligand complexes. CE has become very popular for separation of macromolecules, and is quite useful for the analysis of small ions.

Several reviews on elemental speciation and metal speciation using CE have been published recently [41-42].

This separation technique was first developed by the Swedish chemist Arne Tiselius in the early 1930s. For his studies on cerium proteins he was awarded the Nobel Prize in 1948 [41]. CE has very unique characteristics that makes this analytical technique attractive for elemental speciation. Micro sample sizes, cheap capillaries that are easily reconditioned and very fast analysis time are some of the main advantages. The mobility of an analyte in CE also called capillary zone electrophoresis (CZE) is a function of the size and charge of the analyte. Separation is on the basis of their mobility in an electric field. Resolution may be improved by adjusting the applied electric field, changing the buffer system and pH, and by using modifiers. In this chapter injection modes for sample introduction into the capillary will be discussed. [41,42].

3.4.2 Experimental

The basic components of a CE instrument are shown in Fig. 3.2. A polyimide coated fused silica capillary with an inner diameter of 25 μm -100 μm and an outer diameter of 365 μm and length 20cm to 100cm is used. High voltage (15 – 30 kV) is applied across the capillary after injection while both end of the capillary are submerged in the buffer vials. The voltage is applied to the inlet electrolyte vial using a platinum or other inert electrode and the outlet end is grounded in the same way. On capillary detection features a detection window at some distance before the electrolyte outlet reservoir with a UV-Vis or fluorescence detector. In post capillary detection such as ICP-MS the electrical connection is most commonly accomplished with a sheath conducting solution [41,42].

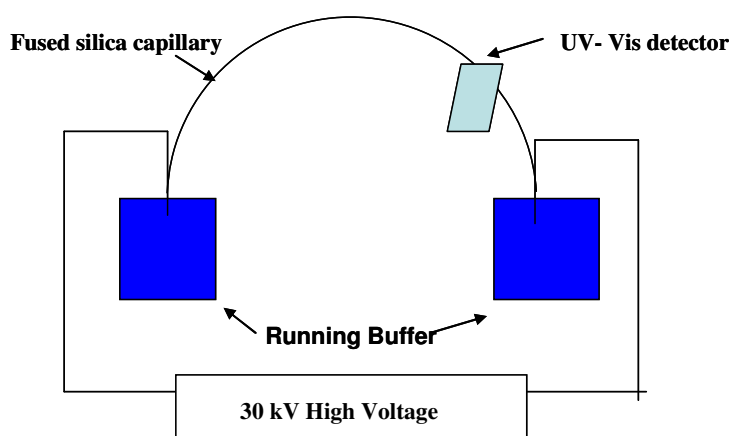


Figure 3.2 Schematic of CE instrument.

3.4.3 Influence on migration time

The applied voltage, V , produces an electric field gradient that causes positive ions to migrate toward the negatively charged end of the capillary. Negative ions migrate towards the positively charged end of the capillary. More highly charged ion tends to migrate more rapidly. Most +2 elemental ions have similar equivalent ionic conductances and therefore similar mobilities. Singly charged ions have a variety of mobilities. Larger molecular ions have mobilities that depend on their overall charge, size and shape. Bulk solution flow is due to electroosmotic flow (EOF) and laminar flow, both of which influence migration times [41-43].

3.4.4 Capillary wall chemistry

EOF is due to the ionic double layer that forms near the inner surfaces of the capillary as shown in figure 3.3. Bare fused silica has ionized silanol groups that are protonated depending on the buffer pH. Cations of the buffer solution are attracted to the silanol groups resulting in a static ionic layer of positive charges [43]. As the cations migrate towards the more negative potential end of the capillary the bulk solution is pulled along. CE has a flat flow profile in contrast to pressure driven separation techniques. The magnitude of electro osmotic flow depends on the pH of the solution [41,43].

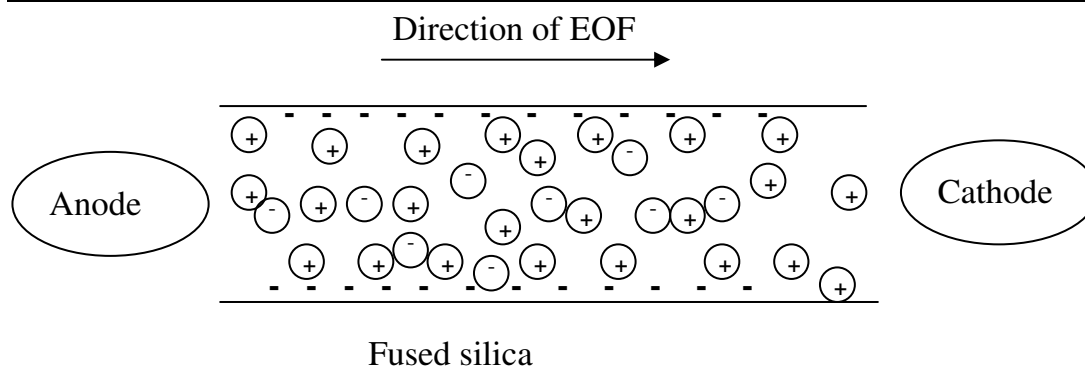


Figure 3.3 Illustration of the origin of the EOF

CE separations may be performed with EOF going either towards or away from the inlet end of the capillary. The EOF can be in the same direction as the electrophoretic migration of the analyte ions (co-electroosmotic flow mode) or in the opposite direction (counter-electroosmotic flow mode). As a result CE can provide high efficiencies and shorter analysis times than chromatographic techniques.

Positive, neutral and negative species can be separated during a single run from one injection if the EOF is optimized. The EOF can be reversed by adding cationic surfactants such as cetyltrimethylammonium bromide (CTAB) or tetradecyltrimethylammonium bromide (TTBA), are added to the buffer solution to decrease or reverse the EOF. Tetraalkylammonium salts may also be used in which case the ammonium ion covers the silanol groups on the capillary walls. Also, coated capillaries may be used to eliminate and or reverse the EOF possibly enhancing separation and increasing reproducibility [41,42].

3.5 Injection modes

Sample can be injected into the capillary by hydrostatic, hydrodynamic or electrostatic modes. Hydrodynamic injection features the sample being forced into the capillary by pressurizing the sample vessel or by applying suction to the outlet end of the capillary. Hydrostatic injection is accomplished by placing the inlet end of the capillary into a vessel containing the sample and raising the sample vessel above the outlet end of the capillary. The advantages of hydrodynamic and hydrostatic injection are predictable injection volumes and injection of an amount of sample that is independent of the analyte properties (such as charge or mobility).

Electrokinetic injection, also known as electrostatic injection, the sample moves into the capillary under the influence of an electric field. The inlet end of the capillary is placed into the sample vessel. A small voltage is applied between the sample solution and the outlet end of the capillary for a short amount of time. The voltage is then turned off and then the inlet end of the capillary is taken out of the sample vessel and placed into the running buffer vial. In this mode of injection the amount of analyte injected is dependent on the mobility of the analyte ion. If the analyte has a high mobility, a larger quantity will be injected than an analyte with a low mobility. If the charge on the analyte is neutral or opposite the charge near the capillary inlet, no analyte will be injected. The main advantages of this mode of injection is that it's possible to preconcentrate analytes improving sensitivity and detection limits [41,42].

3.6 Separation modes

CE separations can be accomplished with various modes like capillary zone electrophoresis (CZE), micellar electrokinetic capillary chromatography (MEKC), capillary isoelectric focusing (CIEF), capillary electrochromatography (CEC) as well as the newly developed microchip capillary electrophoresis (MCE).

3.6.2 Capillary Zone Electrophoresis

CZE based separation is the most widely used operation mode in speciation analysis. Its mechanism is based on the difference in the electrophoretic mobility of analytes. Analytes with different mobility will migrate in separated zones hence the name zone [41,42]. CZE was first described by Jorgenson and Lukas in 1981 [46]. They used a 75 μm i.d fused silica capillary, narrow band injection by electromigration and fluorescence detection. They were able to show fast and excellent separation with excess of 400 000 theoretical plates [42].

Analytes with the same electrophoretic mobility will co-migrate as the same zone in the capillary under the applied voltage. Under CZE conditons the migration time of the analytes in the capillary is determined by the sum of their intrinsic electrophoretic mobility (μ_{ep}) and electrophoretic mobility due to the action of EOF:

$$(\mu_{\text{obs}} = \mu_{ep} + \mu_{eo}) \quad (2)$$

where μ_{obs} represents the observed electrophoretic mobility of the complexes. In the separation process the control of the EOF plays an important role. CZE separation requires one to control and reproduce the EOF. Because of its high resolution, short analysis time and low reagent consumption CZE has received a great deal attention for metal ion speciation [41, 42, 47, 48].

3.6.3 Micellar electrokinetic chromatography (MEKC)

Neutral compounds will comigrate under CZE conditions. In MEKC mode, the surfactant added in the carrier electrolyte must be over its critical micellar concentration (CMC) to form micelles as the pseudostationary phase. There will be two phases in the running buffer. The aqueous phase and the micellar phase. Micelles are surfactant molecules into which analytes can partition based on their hydrophobicity, hydrogen bonding and ionic attraction. The most common used surfactant in MEKC is SDS. SDS is comprised of a hydrophobic tail and a negatively charged hydrophilic head. At low concentrations in water, individual surfactant molecules exist as single entities. As the SDS concentration increased, the surfactant molecules begins to interact with each other. The hydrophobic tail line up and exclude water, while the charged head groups orient towards the surface. The resulting micelles are hydrophilic on the surface but hydrophobic on the interior. [41, 42] The prominent advantage of MEKC is its ability to separate both ionic and neutral species. MEKC has also been widely used in the speciation of elements like organo metallic compounds [49].

3.6.4 Capillary Isoelectric Focusing (CIEF)

CIEF is an attractive separation technique for biologically important ampholytes, like proteins and peptides. Isoelectric focusing is characterized by high resolution and spontaneous focusing of analytes. In CIEF the ampholytes are employed to offer a pH gradient along the capillary when applying an electric field. Species with different isoelectric points (pI values) will move to and be focused on their individual pI, and then be separated from each other. The CIEF system is different than CZE. In CZE, the buffer system is homogeneous throughout the length of the capillary and through the duration of the run. In CIEF, a heterogeneous pH gradient is created inside the capillary by applying voltage across the carrier ampholytes. Using CIEF there is no need to develop a buffer system to separate solutes based on mobility. Most reported applications are for proteins [41,50,51].

3.6.5 Capillary Electrochromatography (CEC)

CEC combines the high efficiency of CZE and the high selectivity of HPLC. In CEC solvent transport is achieved by EOF instead of hydraulic flow in HPLC. The advantage of using EOF is a gain in column efficiency and the usage of much smaller particles than common in HPLC.

In CEC, separation is carried out using aqueous buffer with an organic modifier. Organic solvents like methanol or acetonitrile is commonly used. Silica base particles are packed into the fused silica based tubes of 50 m – 100 m. In such capillaries the surface charge of the particles will assist to establish an EOF. Solutes are separated by partitioning between the stationary and mobile phase while moving with the EOF through the column as in liquid chromatography. In CEC, separation will be achieved by the combined effects of electrophoresis and partitioning [41,42]. Compared with CZE and MEKC, few reports on speciation analysis have been published [52].

3.6.6 Separation on microchip

The interest in microfluidic devices has increased considerably over the past decade due to numerous advantages of working within a miniature microfabricated format. [41]. Compared with ordinary CE systems the microchip CE system has advantages as follows: highly analytical speed, low sample and reagent consumption, reduced bench space, and potential for the development of portable analytical systems. A miniaturised analytical system is also called a lab-on-a-chip or a micro Total Analysis System (μ TAS) [33]. μ TAS includes separation and detection of components present in liquid samples in a chip based device. The typical dimensions of the structures used for the various steps are in the range of a few micrometers to several millimetres in length and width. The μ TAS has been considered to become a powerful tool in analytical chemistry [33, 42].

3.7 Detection in capillary electrophoresis

A variety of detection techniques have been developed for CE. Table 1 shows the most widely used techniques [33,42].

Table 3.1 Various detection modes in CE

Detection Principle	Concentration detection limit (M)
Absorbance	10^{-7}
Indirect detection	10^{-7}
Fluorescence	10^{-12}
Amperometry	10^{-9}
Mass spectrometry	10^{-7}
ICP-MS	10^{-12} - 10^{-15}

Choosing suitable detectors will increase the selectivity of a separation if the analytes can be detected with greater sensitivity. Although the selection of detection systems is somewhat limited, UV- Vis detection is the predominant technique for metal-ion analysis

3.7.2 Absorption

For UV-Vis detection, experience from HPLC has been useful in adapting the detection to the much smaller electrophoretic separation system. Generally, detection in CE is performed on-column to cope with the nanoliter volumes encountered. This results in an extremely short path length, giving limited sensitivity for absorbance detection [37].

3.7.2.1 Direct Detection

The direct detection mode refers to an analytical signal related directly to the chemical or physical properties of the metal ion itself (e.g. the energy of emitted X-rays). Measuring the UV-Vis absorption of the analyte directly provides some specificity, when the entire spectra are obtained. The optical pathlength through the separation capillary is very small and therefore, the direct measurement of absorption is limited to compounds which have relatively high molar absorptivities [37]. Attempts have been made to increase the optical pathlength by use of a z-cell,

bubble capillary, rectangular capillary or extended light-path cell [33]. Metal ions have weak absorption peaks in the UV-Vis wavelength range. Because of this drawback a complexing ligand must be added to the background electrolyte to give adequate separation. Even with these improvements are not sufficient for sensitive direct detection and it is necessary to employ indirect methods for sensitivity [32,37,42].

3.7.2.2 Indirect Detection

Indirect detection mode refers to signals that are none specific for the metal ion and are obtained from transformed species containing the metal ion (e.g. the UV-Vis spectrum of a complexed metal ion) or from a species containing no metal ion from the sample (e.g. the signal from the background electrolyte in indirect UV-Vis detection). This method provides a means of detecting an analyte that shows little or no detector response. Indirect detection in CE holds greater potential because of its high sensitivity and broad applicability [32,34,37].

CE-UV-Vis is still the simplest and most widely used detection mode in CE. In our previous work, [honours project] airborne mercury was detected by the means of this detection mode. Although relatively good results were obtained, it was found that the limit of detection (LOD) values reported with CE-UV-VIS spectroscopy is not suitable for ultra trace analysis. In speciation analysis the choice of the detector strongly depends on the chemical form to be determined and the mode of separation used [31,33,35,].

3.7.2.3 Fluorescence

Laser induced fluorescence is a very sensitive detection technique currently available for CE [33,42]. In this form of detection, radiation from a lamp or laser source is focused onto the capillary and the resulting fluorescence is collected at right angles to the excitation beam. For compounds having a strong natural fluorescence, this mode of detection is more sensitive than UV-absorbance detection. It is much easier to detect a small signal above a “zero” background (as in the case of fluorescence) than to detect a difference between two large signals (as in the case of absorption). Although detection limits are excellent in fluorescence, the technique itself is highly selective. Few compounds naturally fluoresce and a limited number of laser

wavelengths are available for excitation. In most cases there is the need for derivatization of the sample with a fluorophore [33,41,42].

3.8 Inductively Coupled Plasma Mass spectrometry (ICP-MS)

ICP-MS has become one of the most powerful and versatile detectors for ultra trace element determination in speciation studies [41]. The unique features of ICP-MS include extreme sensitivity, great specificity, multi-elemental capacity, wide linear dynamic range, the measuring of isotopic ratios and easy modification of the sample introduction system. Different chromatographic methods were coupled with ICP-MS. Good results was obtained but lots of problems arise in following this route [53].

CE offers an alternative separation approach to chromatographies [54].

CE-ICP-MS coupling is an alternative to HPLC or GC coupling to ICP-MS. The main advantages of CE-ICP-MS is as follows:

- Complex mixtures of elemental species may be resolved using mild separation conditions to preserve species integrity;
- Derivatization stages are not needed in most cases;
- Optimum CE separation conditions can be easily accommodated to final ICP-MS detection (avoiding problems with HPLC that derived from incompatibilities between the composition of the liquid mobile phase and plasma stability);
- Elements and isotopes in any of the species present in the sample can be identified and reliably quantified on-line at the same time with great specificity and extremely high sensitivity;
- Very small sample volumes are required for a measurement.

However, the main disadvantages of CE-ICP-MS coupling is:

- Maintenance of the electrical connection at both ends of the CE capillary;
- Cost
- Preservation of the separation profile obtained from UV detection, avoiding any laminar flow affecting the inside of the capillary derived from coupling

- The highest transport efficiency of analytes from the end of the CE capillary to the plasma [54,55].

3.9 Electrochemical Detection

An alternative method is to use Electrochemical detection (EC) [33]. An alternative to conventional spectroscopic methods, this method is ideally suitable for CE. Its rapid speed, high separation efficiency, high selectivity and sensitivity and variety of configuration and materials that can be employed make this method suitable for mercury detection at ultra trace levels [35]. This technique will be discussed in more detail later.

References:

1. P. Kuban, P.C. Hauser, V. Kuban, *Electrophoresis* 28, (2007), 58-68.
2. F. Browner, T.S West, *Talanta* 16, (1969), 75-80.
3. C. B'Hymer, K. Wrobel, J.A. Caruso, *Journal of Chromatography A* 975, (2002), 245-266
4. C. Barshick, P. Britt, A. Lake, A. Vance, *International Journal of Mass Spectrometry* 178, (1998), 31-41.
5. M. Hempel , H. Hintelmann, R.D Wilken, *Analyst* 117, (1992), 669-672.
6. X. Yin, H.F Scholer, *Frensius Journal of Analytical Chemsitry* 361, (1998), 761-766.
7. J.M Ombaba, *Microchemical Journal* 53, (1996), 424-428.
8. M. Morita, J. Yoshinga, J. Edmonds, *Pure & Appl. Chem.*, Vol.70, (1998), 1585-1615.
9. H. Emeteborg, N. Hadgu, D. Baxter, *Journal of Analytical Atomic Spectrometry* 9, (1994), 297-302.
10. G. Lindest, *Analyst* 95, (1970), 264.
11. N. Bloom, *Journal of Fisheries and Aquatic Sciences* 46, (1989), 1131-1140.
12. T. J Vickers, R.M. Vaught, *Analytical Chemistry* 41, (1969), 1470-1476.
13. J.D. Wiaferder, R.A. Stab, *Analytical Chemistry* 36, (1964), 1367-1372.
14. Y. Chai, R. Jaffe, A. Alli, R. Jones, *Anal. Chim. Acta* 334, (1996), 251-256.
15. N. Demuth, K.G. Heumann, *Analytical Chemistry* 73, (2001), 4020-4027.

16. L. Lambertsson, E. Lundberg, *Journal of Analytical Atomic Spectrometry* 16, (2001), 1296-1301.
17. Q. Tu, J. Quin, W. Frech, *Journal of Analytical Atomic Spectrometry* 15, (2000), 1583-1588.
18. B.D. Quimby, J.J Sullivan, *Analytical Chemistry* 62, (1990), 1027-1034.
19. M. Jimenez, R.E Sturgeon, *Journal of Analytical Atomic Spectrometry* 12, (1997), 597-601.
20. L. Liang, M. Horvat, N. Bloom, *Talanta* 41, (1994), 371-379.
21. T.W. Clarkson, *Environmental Health Perspectives* Vol.100 (1992), 31-38.
22. S.C Hight, J. Cheng, *Anal. Chim. Acta* 567, (2006), 160-172.
23. Y.C. Wang, C.W. Wang, *Journal of Chromatography A* 628, (1993), 133-137.
24. C. Sarzanni, M. Aceto, E. Mentasti, *Journal of Chromatography A* 626, (1992), 151-157.
25. R. Eiden, R. Falter, H. Scholer, *Frensius Journal of Analytical Chemsitry* 359, (1997), 439-441.
26. L.Liang, M. Horvat, B. Gelein, S. Balogh, *Talanta* 43, (1996), 1883-1888.
27. W.Liu, K.Lee, *Journal of Chromatography A*, 796, (1998) 385-395.
28. E. Bulska, D.C. Bulksa, *Analytical Chemistry* 249, (1991), 545-555.
29. C. F. Harrington, *Trends in Analytical Chemistry* 19, (2000), 167-179
30. N. Bloom, A.Grout, E.Prestbo, *Anal. Chim. Acta* 546, (2005) 92-101.
31. Q. Pheng, L. Jin-Ming, *Electrophoresis* 26, (2002), 3333-3341.

32. E. Dabek-Zlotorzynska, E.P.C. Lai, A.R. Timerbaev, *Analytic Chimica Acta* 359, (1998), 1-26.
33. C. Vogt, G.L. Klunder, *Frensenius Journal of Analytical Chemistry* 370, (2001), 316-331.
34. I. Medina, E. Rubi, M.C Mejuto, *Talanta* 40, (1993) 1631-1636.
35. E.P. Lai, W. Zhang, S. Kennedy, E. Dabek-Zlotorzynska, *Anal. Chim. Acta* 364, (1998) 63-74.
36. Y. Liu. J. Cheng, *Electrophoresis* 24, (2003), 1993-2012.
37. A.R. Timerbaev, O.A. Shpigun, *Electrophoresis* 21, (2000) 4179-4191.
38. A.J Bard, L.R. Faulkner, *Electrochemical Methods Fundamentals and Applications* 2nd Edition, John Willy & Son, NYC, (2000).
39. D.A Skoog, D.M West, F.J Holler, *Fundamentals of Analytical Chemistry* 7th Edition, Saunders College Publishing, NYC, (1997).
40. J. Wang, *Analytical Electrochemistry* 2nd Edition, Wiley & Sons, New York, (2000).
41. R. Weinberger, *Practical Capillary Electrophoresis* 2nd Edition, Academic Press, NYC, (2000).
42. J.P. Landers, *Handbook of Capillary Electrophoresis* 2nd Ed, CRC Press, Boca Raton, Florida, (1997).
43. M. Macka, P.R. Haddad, *Electrophoresis* 18, (1997), 2482-2501.
44. V. Majidi, N.J. Miller-Ihli, *Analyst* 123, (1998), 803-808.
45. V. Majidi, N.J. Miller-Ihli, *Analyst* 123, (1998), 809-813.

46. J.W. Jorgenson, K.D. Lukacs, *Science* 222, (1983), 266-275.
47. C. Quang, M. Khaledi, *Anal. Chem.*, 65, (1993), 3354-3358.
48. Q. Lu, S. Bird, R.M. Barnes, *Anal. Chem.*, 67 (1995), 2949-2956.
49. J.P Kutter, *Trends in Analytical Chemistry*19, (2000), 352-363.
50. S. Hjerten, M. Zhu, *Journal of Chromatography* 346, (1985), 265-271.
51. J.P Quirno, S. Terabe, *Journal of Chromatography A* 856, (1999), 465-482.
52. G.H. Sanders, A. Manz, *Trends in Analytical Chemistry*19, (2000), 364-377.
53. J.Savory, M.Herman, *Annals of Clinical and Laboratory Science* Vol. 29, No. 2
54. G. Llamas, F. de Campa, A. Sanz-Medel, *Trends in Analytical Chemistry* Vol. 24, (2005), 28-36.
55. T. Stiochev, D. Amouroux, D.L. Tsalev, *Applied Spectroscopy Reviews* 41, (2006), 591-621.

Chapter 4

Experimental procedures

4.1 Reagents and materials

All reagents used were HPLC or analytical grade. Ultra pure water was obtained by means of a Milli Q system. Mercury stock solutions were obtained by dissolving the appropriate quantity of its chloride (Merck) in 0.5% HCl solution to a concentration of 0.368 mM (100 ppm). Ethylmercury and Phenylmercury chloride were obtained by dissolving the salt in the minimum volume of methanol and diluting the final volume with 0.5 % HCl to give solutions of 100 ppm. All the organo mercury solutions were stored at 4 °C when not in use. The cysteine stock solution (100 mg/25 ml) 4000 ppm was prepared by dissolving L-cysteine (Fluka) with 0.01 M HCl. The stock solution was stored in the refrigerator for a maximum of one week. All complexes formed was done with solutions that are either freshly prepared or from dilutions of the relevant stock solution. The electrodes were polished prior to use with different grades of alumina slurry, rinsed thoroughly with Milli-Q water and allowed to dry. After running the experiments the electrodes were cleaned by removing the deposits using electrochemical oxidation, holding them at a fixed positive potential value ($E = +0.5$ V versus Ag | AgCl) for a period of 15 minutes and then immersed in 6 M nitric acid to remove any mercury which might have formed as an amalgam on the electrode surface.

All chemicals and reagents were purchased commercially and used as received. Ultra pure water was prepared in a Milli-Q water purification system (Millipore, Eschbron, Germany).

CHEMICALS	MANUFACTURER AND GRADE
Boric acid	Fluka
Sodium acetate	ACS –specification, Protea Laboratory
Mercuric chloride	SAAR Chem
Methylmercury chloride	Analytical Standard, Riedel-de-Haën
Ethylmercury chloride	Sigma-Aldrich
Phenylmercury chloride	Purity 99%, Supelco
Thiourea	Sigma-Aldrich 99%

Chapter 4 – Experimental procedures

Methanol	ChromaSolv, Sigma-Aldrich
L-Cysteine	Ultra 99.5%, Fluka
Glacial acetic acid	Aldrich 99%
NaOH solution for HPCE (1M)	Hewlett Packard
Sodium Hydroxide, 20-40 mesh Beads	97%, Sigma-Aldrich

4.2 Instrumentation

All electrochemical measurements were performed with a BAS CV-50W instrument. The experiments were carried out in a three-electrode cell at room temperature under a nitrogen atmosphere. The counter electrode was a platinum wire and Ag/AgCl, (3 M KCl) was used as the reference. A gold electrode was used as the working the electrode. Cyclic Voltammetry was the technique applied to study the mercury complexes. The scans normally took place at potentials between -500 mV and 600 mV. All potentials mentioned in this manuscript was measured vs. Ag/AgCl, (3 M KCl).

CE analyses were performed on a HP^{3D} CE capillary electrophoresis system (Agilent Technologies, Waldbronn, Germany). The instrument is equipped with a diode array detection at wavelengths between 190-820 nm. Bare fused silica capillaries (Composite Metal Services Ltd., Worcester, UK) of 50 μm i.d were used. Before use, the capillaries were washed with Milli-Q triple distilled water followed by 1 M NaOH and the separation buffer. The electrolyte and samples were sonicated and filtered through a 0.45 μm membrane filter prior to use. Data analysis was carried out with ChemStation (REV 6.01) software. All experiments were performed at 25 °C. Between each injection the capillary was filled with the buffer solution by flushing the capillary for 5 min. The sample was introduced into the capillary by hydrodynamic injection.

The following parameters were used throughout:

	Cysteine	Dithizone sulfonate
Potential	25 kV	-25 kV
Injection time	5 s	5 s
Pressure	50 mbar	50 mbar
Wavelength	200 nm	275 nm

^1H NMR spectra were recorded on a Varian VNMRs 300 MHz Spectrometer. UV-vis adsorption spectra for 200 – 600 nm wavelengths were recorded at room temperature on a GBC UV/vis 920 spectrophotometer with a 1 cm quartz cuvette.

4.3 Preparation of standard solutions

Preparation of borate buffer solution, 0.025 M NaBO_3 , 0.155 g of boric acid was weighed and diluted with distilled water in a 100 ml volumetric flask. The pH was adjusted to 9.3 with NaOH.

Preparation of cysteine solution, 0.033 M cysteine, 100 mg of cysteine was weighed and diluted with 0.01 M HCl in a 25 ml volumetric flask.

Preparation of sodium acetate buffer solution, 0.01 M CH_3COONa , 0.155 g of sodium acetate was weighed and diluted with distilled water in a 100 ml volumetric flask. The pH was adjusted to 3.0 with acetic acid.

Preparation of mercury standard solutions (i.e. Hg^{2+} , MeHg^+ , EtHg^+ , PhHg^+)
100 mg of HgCl_2 was weighed and diluted with distilled water in a 100 ml volumetric flask, giving a final concentration of 3.28×10^{-4} M.
10 mg of R- HgCl was weighed and dissolved in 5ml of MeOH and diluted with distilled water in a 100 ml volumetric flask.

Preparation of dithizone solution, 0.00391 M Dtz, 100 mg of Dtz was weighed and dissolved in methanol in a 100 ml volumetric flask. The solution was filtered before use.

Preparation of dithizone sulfonate solution, 0.00968 M DzS, 100 mg of DzS was weighed and diluted with distilled water in a 25 ml volumetric flask.

Synthesis of dithizone sulfonate

Dithizone sulfonate (DzS) (f.w. 462.4 as the sodium salt) was synthesised in-house using a modified method based on that developed by Tanaka et al. 1 g 4-hydrazinobezenesulfonic acid (Sigma-Aldrich) was dissolved in 6.5 ml Milli-Q water containing 0.22 g sodium hydroxide. This solution was refluxed with 10 ml ethanol and 0.5 ml CS_2 for 3 h. Upon cooling, 40 ml ethanol was

Chapter 4 – Experimental procedures

added resulting in the intermediate product. The solid was filtered and 1g dissolved in 5ml Milli-Q water, mixed with 25 ml ethanolic sodium hydroxide (0.25 g). 320 ml of n-Butanol (Fluka) was added using an ice bath, the DzS collected by vacuum filtration was washed with dried ether [1,2]. 0.418 g of the product was synthesized giving a yield of 78% : mp 162-164 °C; ^1H NMR (deuterium oxide D_2O , 300 MHz) δ 8.306 (2H, m, Ar-H), 7.845 (2H, m, Ar-H), 7.717 (2H, m, Ar-H), 6.874 (2H, m, Ar-H), 9.153 (1H, s, S-H), 12.012 (1H, s, N-H).

The spectral properties of dithizone sulfonate is shown below and are similar to those of dithizone. From the UV-vis spectra the absorption maxima for the $\pi \rightarrow \pi^*$ transition is found at 253 nm for Dtz and 275 nm DzS. The absorption maxima for $\text{n} \rightarrow \sigma^*$ transition for both compounds is found as 475 nm. For DzS, there is a red shift for the first absorption peak and an increase in intensity for both adsorption peaks. The shift and the increase in intensity is an indication of the effect of the bulky sulfonate group. The data is in good agreement with work done by Tanaka et al. and confirms the structure of DzS [1].

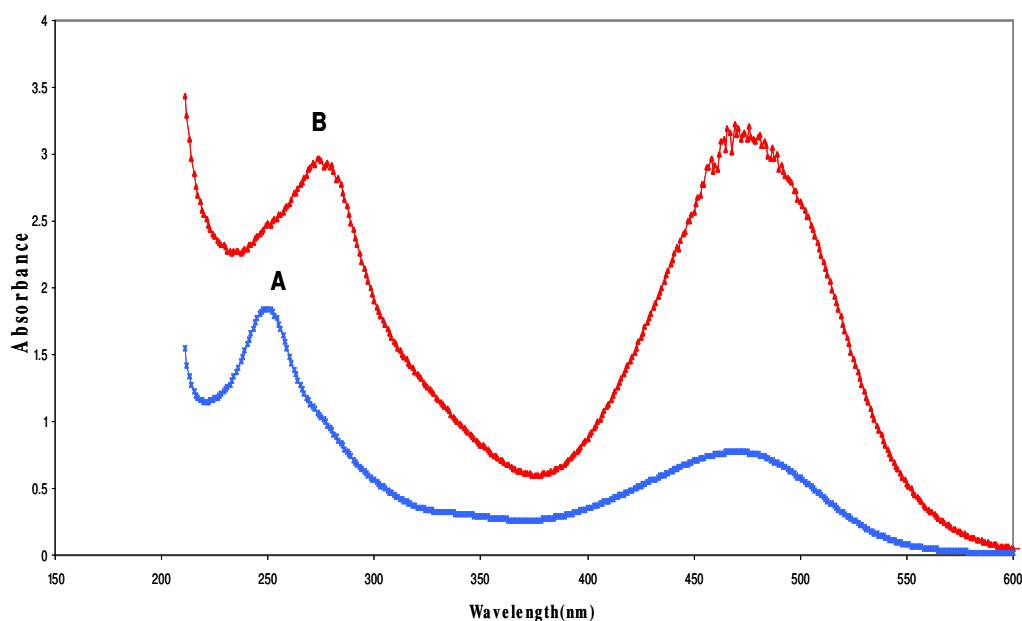


Fig 4.1 UV Absorption spectra of (a) dithizone and (b) dithizone sulfonate.

Reference:

1. H. Tanaka, M. Chimuma, A. Harada, T. Ude, S. Yube, *Talanata* 23, (1976), 489-491.
2. M.J. Shaw, P. Jones, P.R. Haddad, *The Analyst* 128, (2003), 1209-1212.

Chapter 5

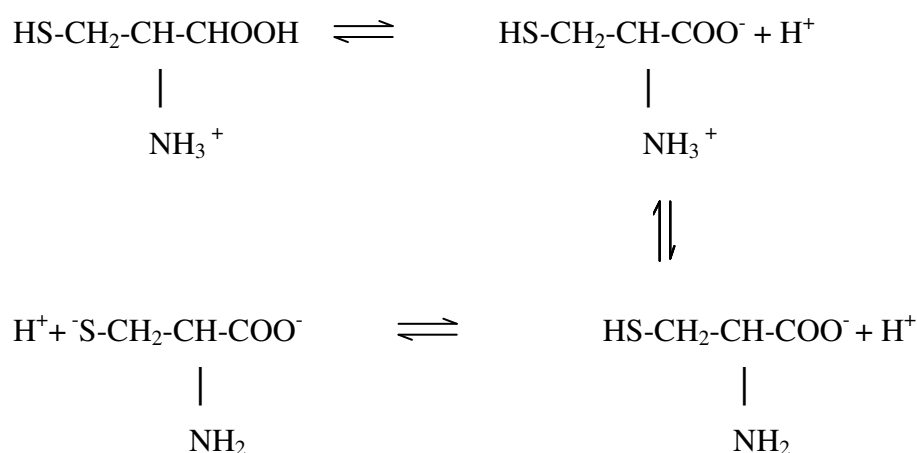
Results and Discussion I

5.1 Electrochemical studies of mercury cysteine complexes

It has long been known that mercury forms stable bonds with sulphur containing ligands e.g. (cysteine, penicillamine, dithizone). Therefore, mercury has long been used as specific reagent for sulphurhydryl groups in biological materials [1,2].

Published literature on the oxidation and reduction of the cysteine-cystine system at different electrodes is limited [3-6]. There are reports on the study of complex species formed between metals and different amino acids, among which are copper, nickel and cadmium complexed with cysteine [7-9]. There are however few reports of voltammetric studies of these complexes with mercury. In most cases only inorganic mercury (Hg^{2+}) was studied by means of stripping Voltammetry [10], Nuclear Magnetic Resonance [11] and recently by means of extended X-ray absorption fine structure (EXAFS) spectroscopy [12].

Cysteine is a substance which is of great biological importance. This fact combined with its electrochemical activity, has assigned it special interest among the amino acids for polarographic and voltammetric investigations. Cysteine is an amino acid with a thiol group, its isoionic point is 5.02 and its acid-base equilibria are as follows:



Chapter 5 – Results and Discussion I

Because of its sulphur, amino and oxygen binding groups, cysteine can form various complexes with metals such as mercury [10]. Cysteine has three pKa values as seen in the table below, so the pH where these experiments will be conducted will be crucial as these different species is pH dependant [13].

Table 5.1 Ionisation state of cysteine molecules as a function of pH

pH	CYSTEINE species present
< 1.71	HS-CH ₂ -CH-CHOOH NH ₃ ⁺
1.71 – 8.33	HS-CH ₂ -CH-COO ⁻ + H ⁺ NH ₃ ⁺
8.33 – 10.78	HS-CH ₂ -CH-COO ⁻ + H ⁺ NH ₂
> 10.78	H ⁺ + ⁻ S-CH ₂ -CH-COO ⁻ NH ₂

5.2.1 Study of Mercury (II) and its Cysteine Complex.

Mercury has two common cations in aqueous solution, a di-ion, Hg₂²⁺ composed of two singly charged ions, and a doubly charged Hg²⁺. Of these species, Hg(II) is the dominant form in most aqueous solutions. Diagrams of pH-potential indicate that Hg(I) is stable only within a narrow band of E^H values in acid solution [14]. The hydrolysis reaction of Hg(II) are significant at pH > 1. The pH of all the mercury standard stock solutions was 1.49. When conducting the CV experiment the pH was taken into account and the dominant mercury species would be Hg(II) Therefore, the Hg(I) species can be excluded from the solution. Also, because the working

environment is acidic there could be a species distribution of the chloro ions and the added cysteine ions which can also give rise to different chloro and cysteine complexes in solution. From the Log K values for HgCl^+ which is 7.31 ± 0.04 , and the Log K values for $\text{Hg}(\text{CYS})_2$ which is 39.4, we expect that the $\text{Hg}(\text{CYS})_2$ will be the only complex in solution, even in this chloride rich environment [13-15]. Cysteine is a triprotic acid and in solution there are a number of possible species that can exist. The CV experiments are conducted below pH 1.71, so the dominant cysteine species will be the positively charged cysteine molecule as evident from table 5.1. The reaction in the electrochemical cell between Hg and cysteine is represented by the following reaction:

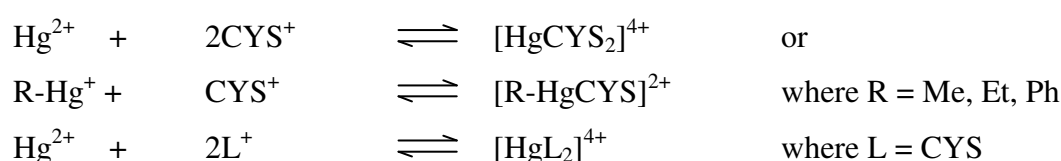


Figure 5.1 below shows a quasi-reversible cyclic voltammogram of the Hg^{2+} ion in 0.5% HCl. The CV run imposes a linear sweep in a positive direction (oxidative sweep), followed by a reverse sweep (reductive sweep) in a negative direction. During the oxidative sweep, a well-defined peak is observed at a potential of 0.135 V. This potential is the oxidation potential of mercury where $\text{Hg}^0 \rightarrow \text{Hg}^{2+} + 2e$.

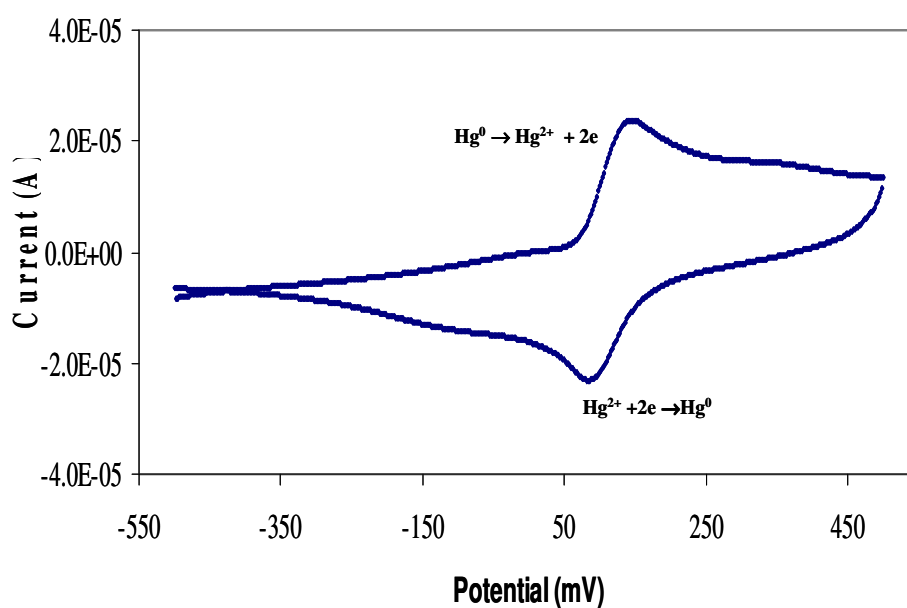


Fig. 5.1 Cyclic Voltammogram of 0.362 mM Hg^{2+} in 0.5% HCl, scan rate = 100 mV/s

The scan direction is switched to negative (reductive) sweep at 500 mV for the reverse scan. At 0.085 V on the reverse scan a peak appeared due to the reduction of $\text{Hg}^{2+} + 2\text{e} \rightarrow \text{Hg}^0$. The cycle is completed when it reaches -500 mV.

Figure 5.2 is obtained after adding aliquots of the ligand (0.033M Cysteine in 0.01M HCl) to the electrochemical cell containing the mercury ion solution. This voltammogram shows an irreversible behaviour of the complex. The mercury oxidation peak has moved from 0.135 V to 0.163 V due to the $[\text{HgL}]^{2+} \rightarrow [\text{HgL}]^{4+} + 2\text{e}$ oxidation. There is an additional peak at 0.372 V, which can be considered be due to the proposed reorganization of electrons in the metal complex.

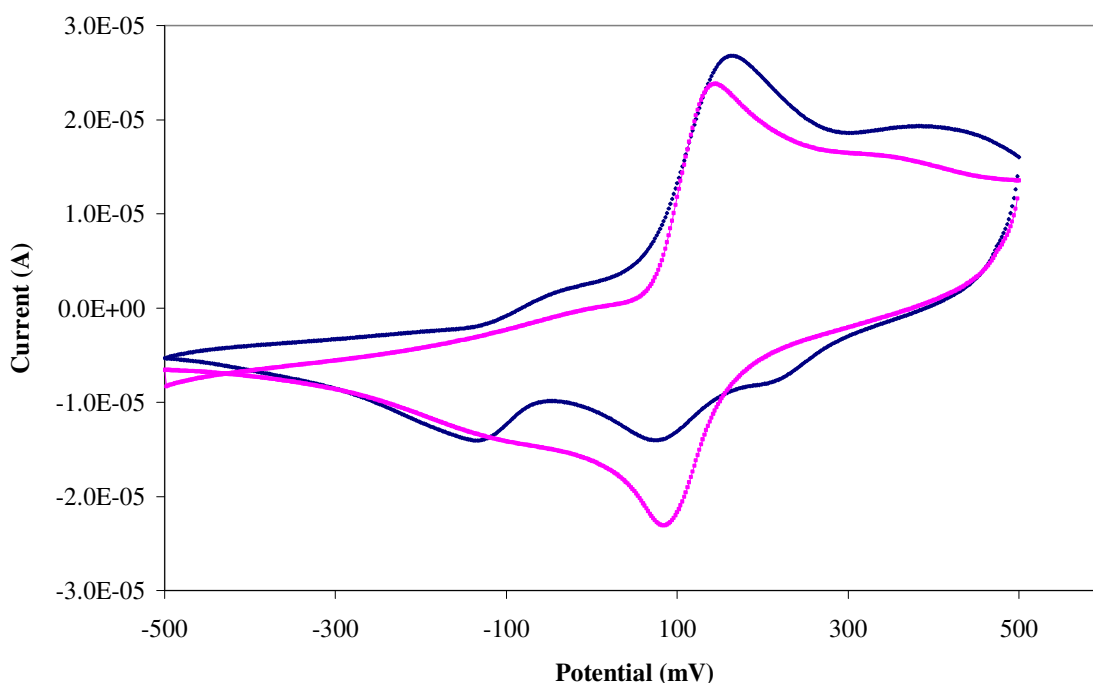


Fig 5.2 Cyclic Voltammogram of Hg and [HgL] at a 1:1 M:L ratio, 0.033M CYS in 0.01 M HCl, scan rate = 100 mV/s

The two sulphur atoms can stabilize the mercury complex due to the electron pair on both atoms. On the reverse scan the stabilized metal complexes is reduced at 0.242 V. The metal reduction peak which moved to 0.064 V, has decreased in size as a new peak appears at -0.131 V due to the complexation of mercury with the ligand and hence belongs to the metal ligand $[\text{HgL}]^{2+}$ reduction peak.

As more of the ligand was added the oxidation / reduction peak of Hg^{2+} shrinks and the peak of the metal ligand complexes increase.

Figure 5.3 shows that the oxidation peak of the $[\text{HgL}]^{2+} \rightarrow [\text{HgL}]^{4+} + 2e$ reaction decreases in size as the quantity of ligand added increase. On the reverse scan the reduction peak also decreases in size as more ligand is added. However, the new peak corresponding to the $[\text{HgL}]^{2+}$ complex increases in size as more ligand is added. The peaks also shifted to more negative potentials with added amount of ligand indicating the formation of a more stable complex. At a M:L ratio of 1:4 no peak is seen on the reverse scan for the $[\text{Hg}^{2+}\text{L}] \rightarrow [\text{Hg}^0\text{L}]$ reduction reaction. All the Hg^{2+} ions in solution reacts on the reverse scan with the ligand to form the stable $[\text{HgL}]^{2+}$ complex at -0.232 V

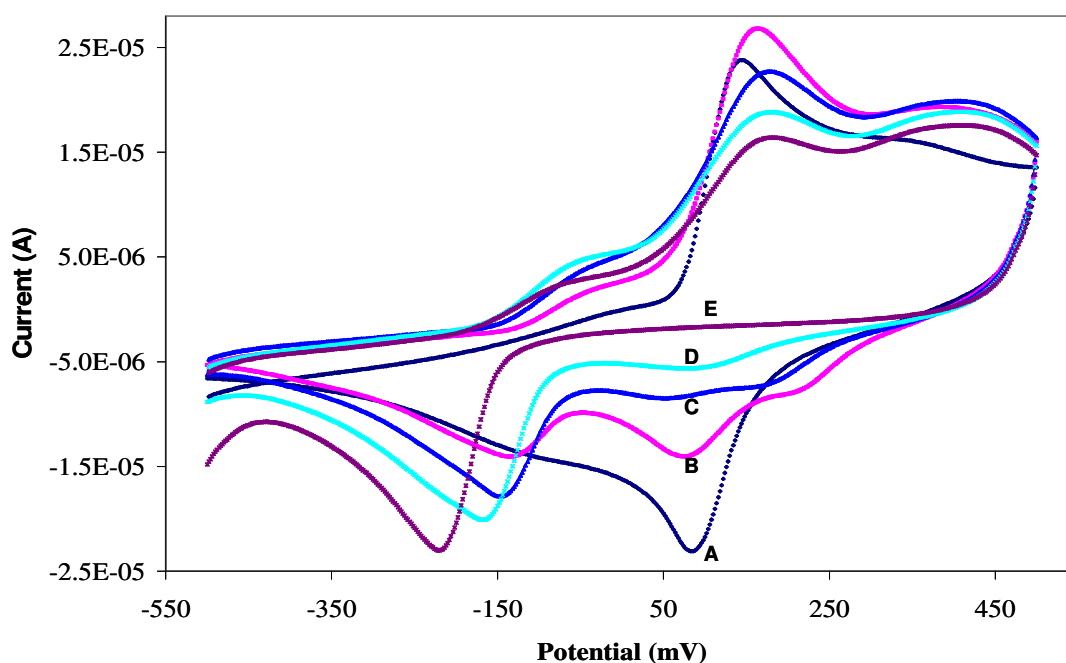
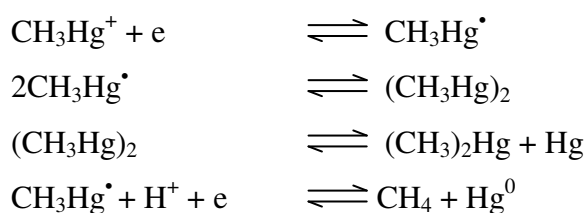


Fig 5.3 Cyclic Voltammogram of $[\text{HgL}]$ complex at various ligand ratios, 0.033 M CYS in 0.01 M HCl , scan rate = 100 mV/s . graphs, : a) Hg^{2+} , b) HgL_1 , c) HgL_2 , d) HgL_3 , e) HgL_4

5.2.2 Study of Methylmercury (I) and its Cysteine Complex.

Of all the organomercury species in the environment methylmercury is the most toxic. Because of this property, methylmercury has been studied extensively in the past. R.Agraz et al. (1995) studied organomercury species at a modified carbon paste electrode with a thiolic resin. L.M Moretto et al. (1999) studied methylmercury at a Nafion coated electrode by single and multiple pulse voltammetric techniques. Methylmercury was also studied by anodic stripping voltammetry on a gold electrode in a non-complexing environment [18]. Recently F. Ribero et al (2006) did voltammetric studies on the electrochemical determination of methylmercury in a chloride medium at carbon microelectrodes. There are however few reports in the literature on describing the voltammetric determination of methylmercury [14], most probably because of the complexity of the particular electrochemical reduction process, not alone methylmercury cysteine complexes.

Figure 5.4 illustrates the oxidation of methylmercury at -0.018 V where $\text{MeHg}^0 \rightarrow \text{MeHg}^+ + e$. A corresponding reduction peak is found at -0.070 V. As the electrode becomes a sufficiently strong oxidant dimerization reactions starts to take place. At 0.258 V Me_2Hg_2 formed which is then oxidized at 0.338 V to dimethylmercury. On the reverse scan the corresponding peak for Me_2Hg is found at 0.163 V. These voltammetric data corroborate with the following mechanism proposed by Heaton and Laitinen [20] for the reduction of methylmercury at a DME, in acidic solution:



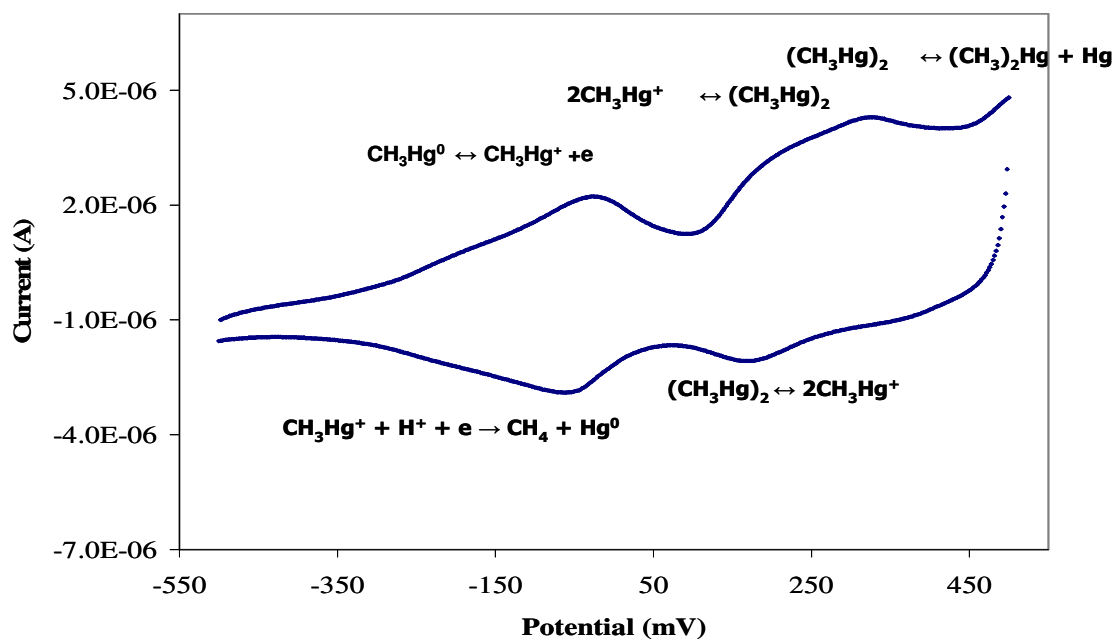


Figure 5.4 Cyclic Voltammogram of MeHg in 0.5% HCl, scan rate = 100mV/s.

Fig 5.5 is obtained after adding aliquots of the ligand to the methylmercury solution.

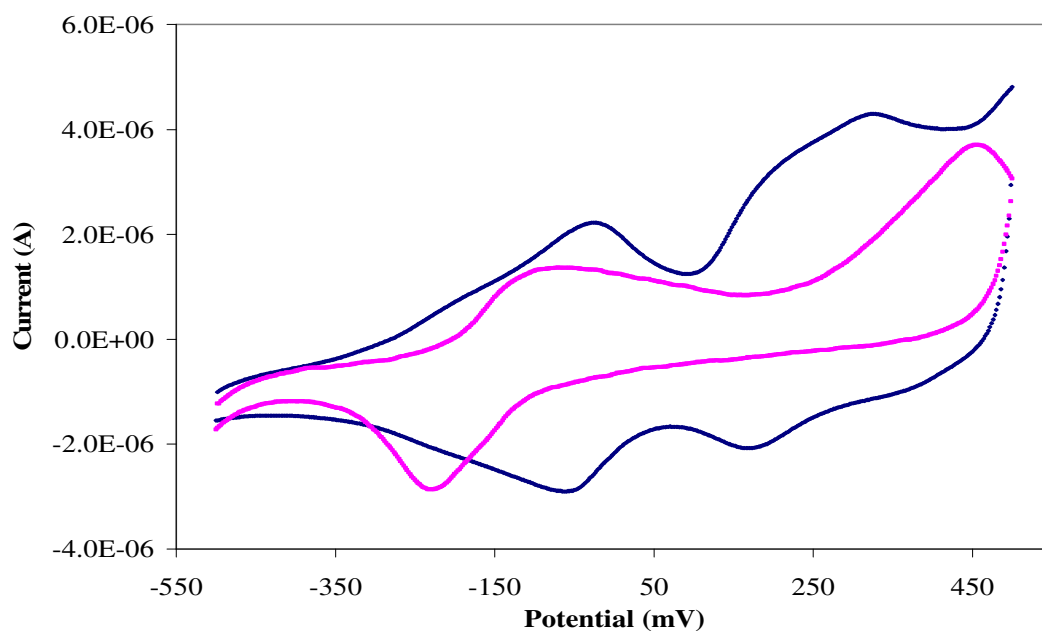


Fig 5.5 Cyclic Voltammogram of MeHg and [MeHgL] at a 1:1 M:L ratio complex, 0.033 M CYS in 0.01 M HCl, scan rate = 100 mV/s.

This voltammogram shows a non-reversible reaction. Both the oxidation peaks decrease in size and moved to more negative potentials. On the reverse scan the reduction peak of the dimer disappears as the ligand is added. The stable complex peak is found at -0.23 V on the reverse scan. As the ligand quantity is increased, two peaks are found on the forward scan, which correspond to the oxidation of mercury and a chemical reaction which take place when dimethylmercury is formed. On the reverse scan only one peak is found corresponding to the metal ligand reduction of the $[\text{MeHgL}]^{2+}$ complex. This is a classical example of an EC mechanism where the stable chemical compound, which follows the initial oxidation, is then reduced as a complex.

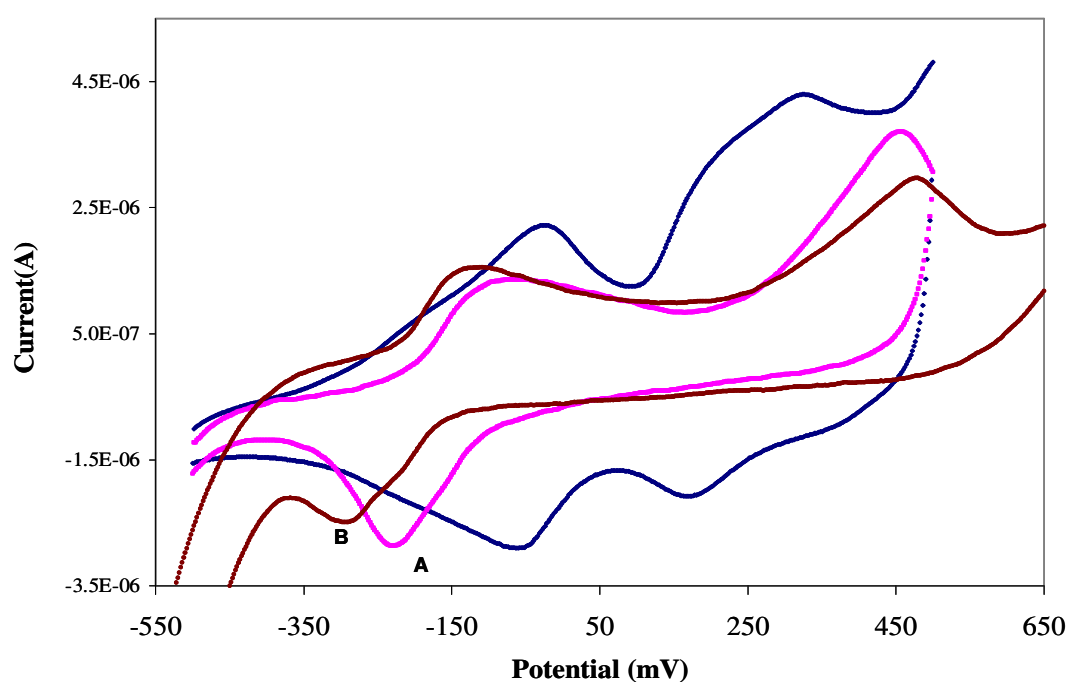


Fig 5.6 Cyclic Voltammogram of MeHg and $[\text{MeHgL}]$ complex at various ligand ratios, 0.033 M CYS in 0.01 M HCl, scan rate = 100 mV/s, graphs: a) HgL_3 , b) HgL_6

5.2.3 Study of Ethylmercury (I) and its Cysteine Complex.

Fig. 5.7 illustrates the oxidation of ethylmercury at 0.01 V where $\text{EtHg}^0 \rightarrow \text{EtHg}^+ + e$. A corresponding reduction peak appears at -0.151 V on the reverse scan. At more positive potentials two more peaks are found at 0.39 V and 0.51 V respectively with corresponding reduction peaks at 0.43 V and 0.2 V. These peaks can be attributed to the dimerization of ethylmercury as the potential becomes more positive.

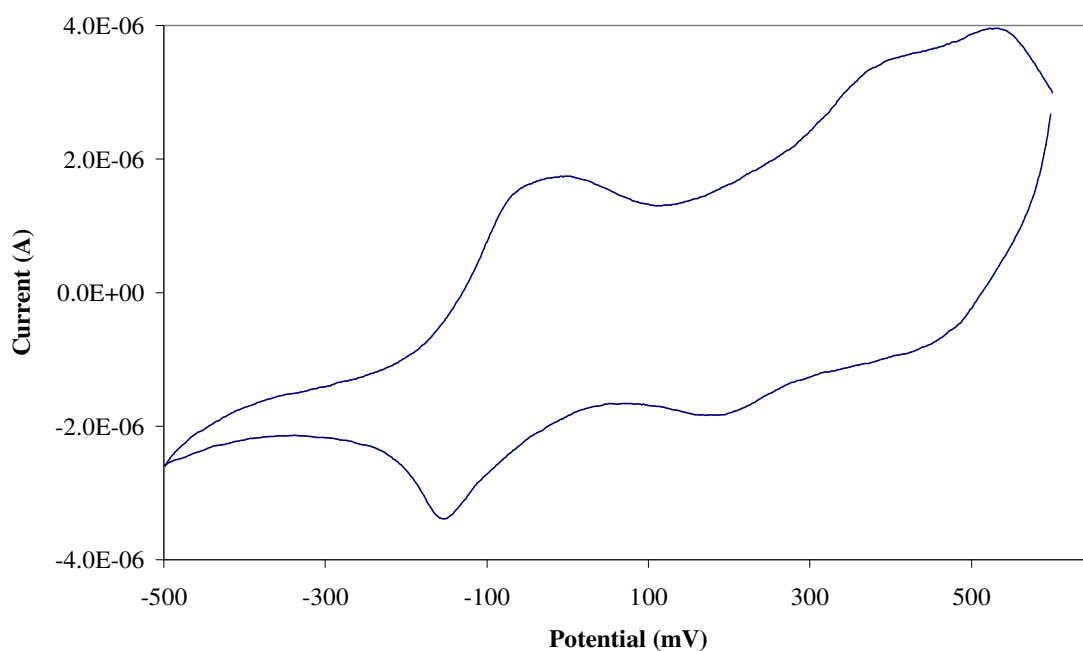


Fig. 5.7 Cyclic Voltammogram of 0.376 mM EtHg^+ in 0.5% HCl, scan rate = 100 mV/s

On the addition of cysteine, the $[\text{EtHgL}]$ complex is formed (Fig. 5.8). Both oxidation peaks have decreased in size and moved to lower potentials. The reduction peak at 0.2 V on the reverse scan has disappeared and the corresponding peak of the first electron transfer at -0.15 V has also decreased dramatically in size.

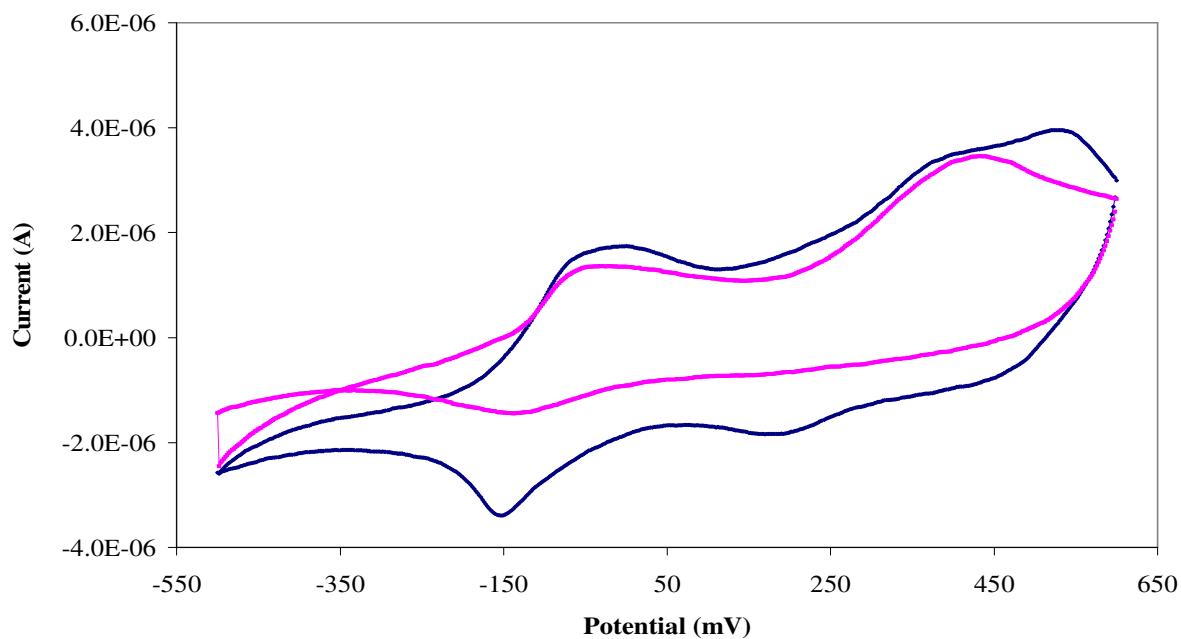


Fig. 5.8 Cyclic Voltammogram of EtHg and [EtHgL] complex at a 1:1 M:L ratio, 0.033 M CYS in 0.01 M HCl, scan rate = 100 mV/s.

As more aliquots of ligand was added, the oxidation peak of ethylmercury shifts to more positive potentials

On the reverse scan the reduction peak moved from -0.123 V to -0.203 V. This clearly shows that the chemically formed complex is stable and that its oxidation – reduction properties are quasi-reversible

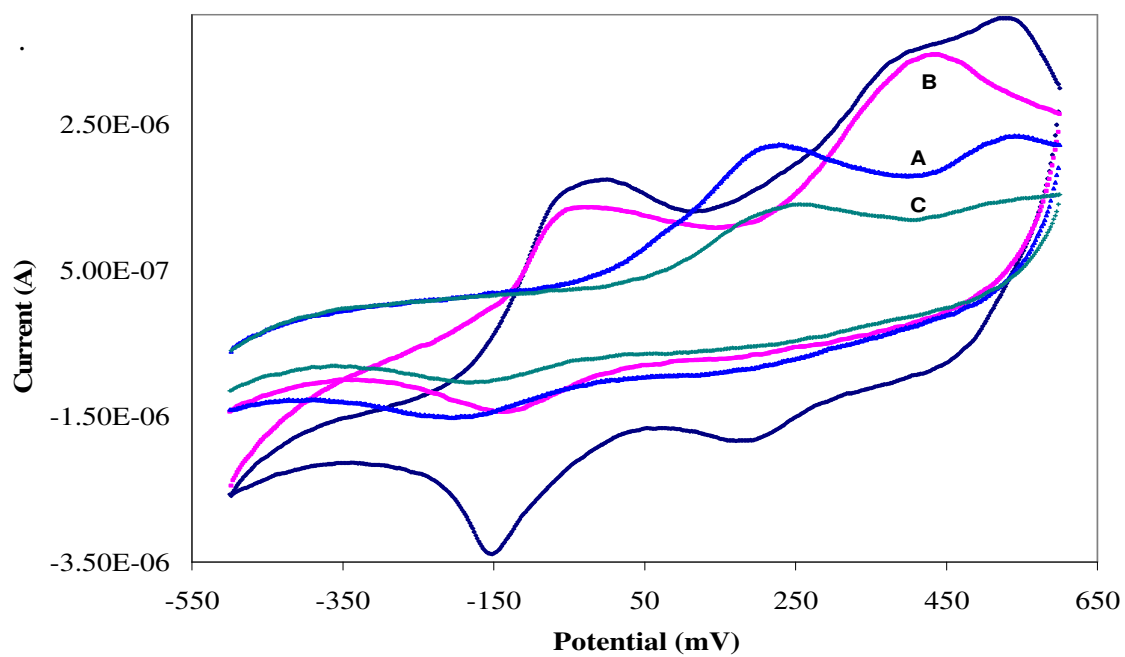


Fig. 5.9 Cyclic Voltammogram of EtHg and [EtHgL] complex at various ligand ratios, 0.033 M CYS in 0.01 M HCl, scan rate = 100 mV/s, graphs: a) ML_2 , b) ML_3 , c) ML_6

5.2.4 Study of Phenylmercury (I) and its Cysteine Complex.

All the organomercury ions showed the same mechanism, where a radical species is generated after the first oxidation step. Figure 5.10 shows the oxidation of phenylmercury at 0.05 V where $\text{PhHg}^0 \rightarrow \text{PhHg}^+ + e$ with a reduction peak on the reverse scan at -0.11 V. The second peak at 0.20 V is due to the formation of the phenylmercury dimer with a corresponding reduction peak at 0.11 V. A third peak is seen at 0.47 V with no reduction peak on the reverse scan. This peak can be attributed to the reorganization of electrons of phenylmercury to form diphenylmercury. The phenyl group donates electrons to the metal ion, thus stabilizing the molecule in the process.

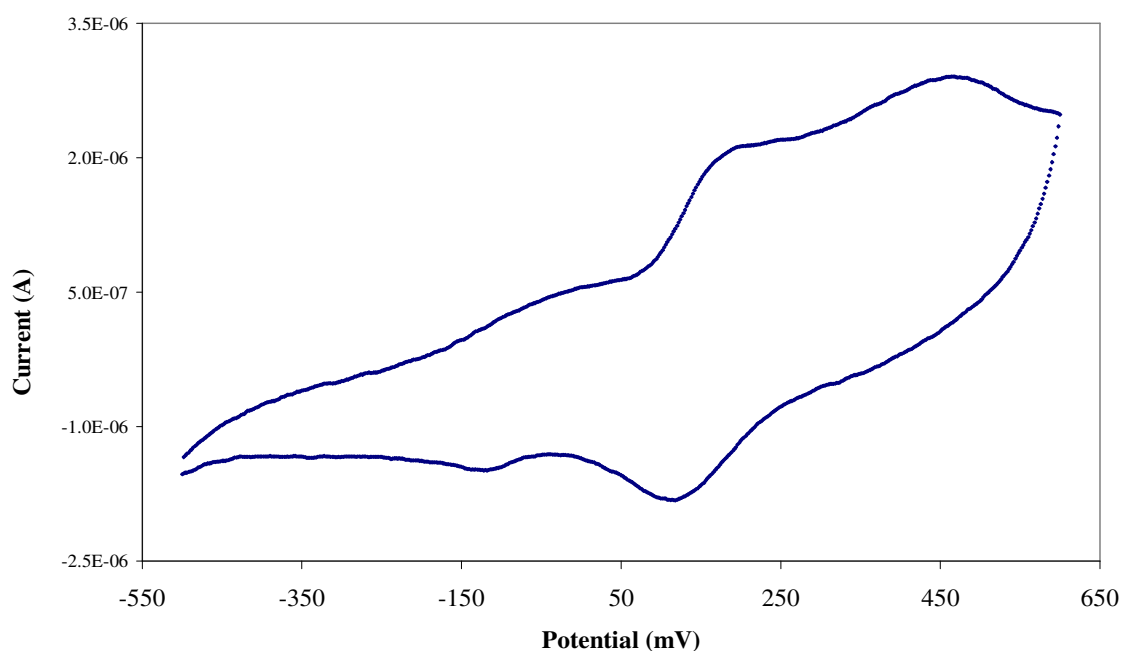


Fig. 5.10 Cyclic Voltammogram of 0.319 mM PhHg^+ in 0.5% HCl, scan rate =100 mV/s

After adding different aliquots of ligand (Fig. 5.11) one peak corresponding to the metal oxidation of the complex was found at 0.25 V and the second peak at 0.51 V can be assigned to the oxidation of the dimer to form diphenylmercury. Both peaks have decreased in size.

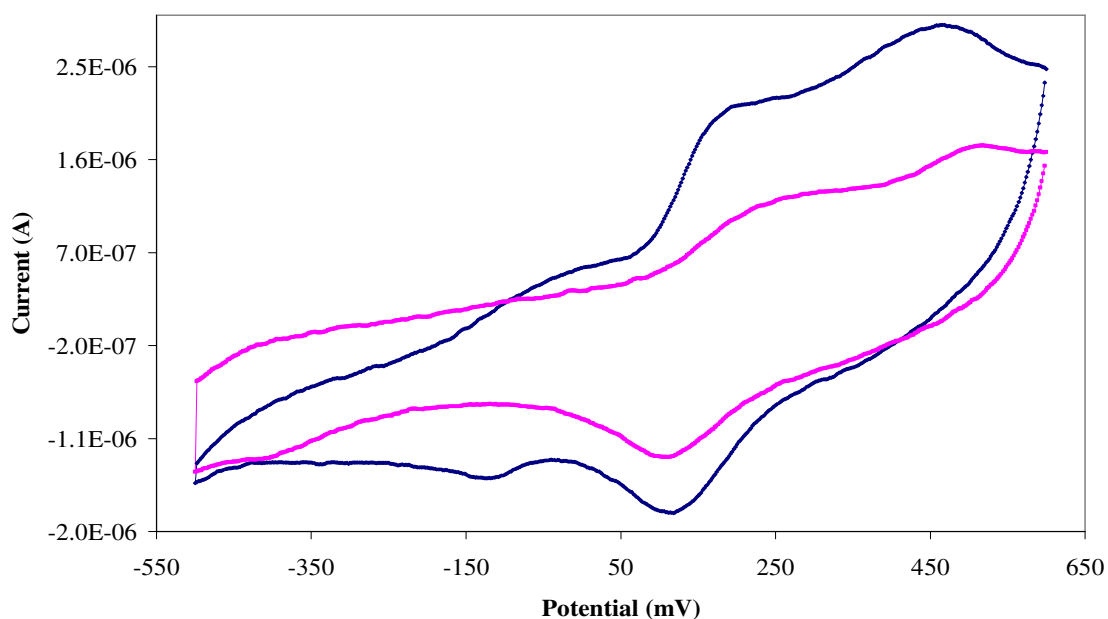


Fig. 5.11 Cyclic Voltammogram of PhHg and [PhHgL] complex at a 1:1 M:L ratio, 0.033 M CYS in 0.01 M HCl, scan rate = 100 mV/s

On the reverse scan the re-oxidation peak of mercury is at 0.1 V and a new peak appears at -0.38 V on the reverse scan due to the metal-ligand reduction of the stable phenylmercury-cysteine complex.

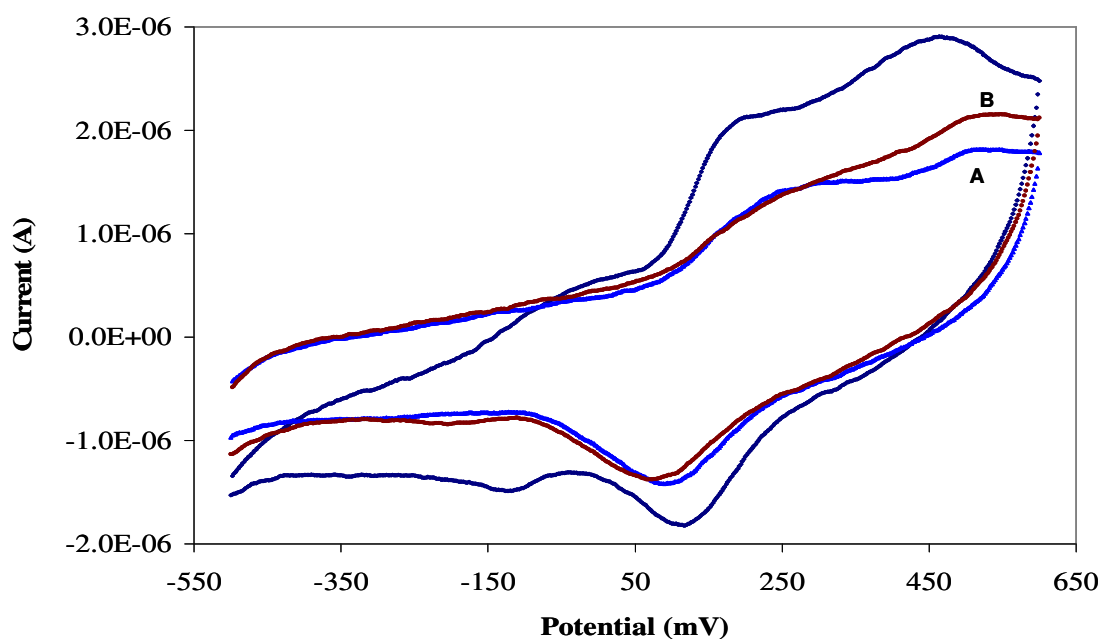


Fig. 5.12 Cyclic Voltammogram of PhHg and [PhHgL] complex at various ligand ratios, 0.033 M CYS in 0.01 M HCl, scan rate = 100 mV/s, graphs: a) PhHgL₂, b) PhHgL₆

As more ligand was added the peak at -0.38 V disappears and the peak at 0.10 V gets broader. The phenylmercury radical peak also disappears and only the diphenylmercury peak is seen. These non-reversible voltammogrammes indicates that the diphenylmercury species is stable and that the reduction peak at 0.1 V is due to the presence of elemental mercury. The formation of a gray silver layer on the electrode surface verifies this. For all the organomercury species a metal: ligand ratio of 1:1 was sufficient to form the stable mercury-cysteine complex. However, for inorganic mercury a M:L of 1:4 was needed to form the stable complex. Hg_2Cl_2 was also studied but no complex was formed with cysteine. Mercurous chloride only forms stable complexes with specific ligands [1,19].

5.3 Mercury Dithizone complexes

Diphenylthiocarbazon, best known under its common name, dithizone was introduced into analytical practice by Hellmuth Fischer just over 50 years ago [21]. By virtue of its thiol group, it can form uncharged chelate complexes with a small group of metals (Co, Ni, Zn, Pd, Pt, Au, Hg and Cd). Like the reagent itself, these are intensely colored and very sparingly soluble in water though soluble in chloroform, carbon tetrachloride and other water-immiscible solvents [21,22]. Dithizone (Dz), has been used extensively for liquid-liquid extractions procedures and the spectrophotometric determination of trace heavy metals in the environment at around the microgram level. Particular attention has been paid to the application of dithizone in preconcentration and separation techniques, in electro analytical procedures and in the design of liquid-membrane ion selective electrodes. Although a vast majority of the literature of dithizone deals with its complexation chemistry, dithizone also exhibits interesting redox chemistry resulting from the presence of its azo and sulfhydryl functionalities. Its thiol group and the formazan structure govern the electrochemical redox properties of dithizone [23-26]. Formazan can either be reduced or oxidized in a suitable medium at an appropriate redox potential, whereas the thiol group can only be oxidized. The fact that dithizone is a weak reducing agent is well known, this behaviour and the result of spectrophotometric investigations makes this compound very useful for metal ligand analysis in electrochemistry [23]. There are a few reports on electrochemical studies of mercury-dithizone complexes. Yamashita used carbon electrodes in his polarographic and voltammetric analysis of $\text{Hg}(\text{Dz})_2$ [27,28]. Studies have shown that mercury will form a stable five membered ring complexes with dithizone in a 1:2 molar ratio as shown by Fig 2.12 [29].

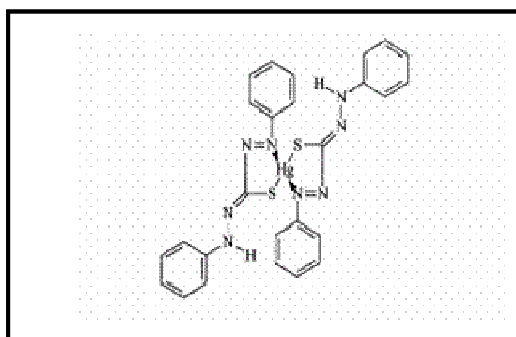


Fig 5.13 Structure of dithizone metal complex [28].

Dithizone was also extensively studied by H.M.N.H. Irving and co-workers. They studied the photo-chromism of mercury dithizone complexes and also looked at new dithizone oxidation products from redox reactions [30-33].

5.3.2 Study of Mercury (II) and its Dithizone Complexes

Figure 5.14 is obtained after adding aliquots of the ligand (3.91 mM dithizone in MeOH) to the electrochemical cell containing the mercury solution. This voltammogram shows an irreversible behavior of the complex. The metal oxidation peak has moved from 0.139 V to 0.182 V due to the $[\text{HgDz}_2]^{2-} \rightarrow [\text{HgDz}_2]^0 + 2e$ oxidation. More energy is needed for the oxidation of the metal to occur now, when only mercury was studied.

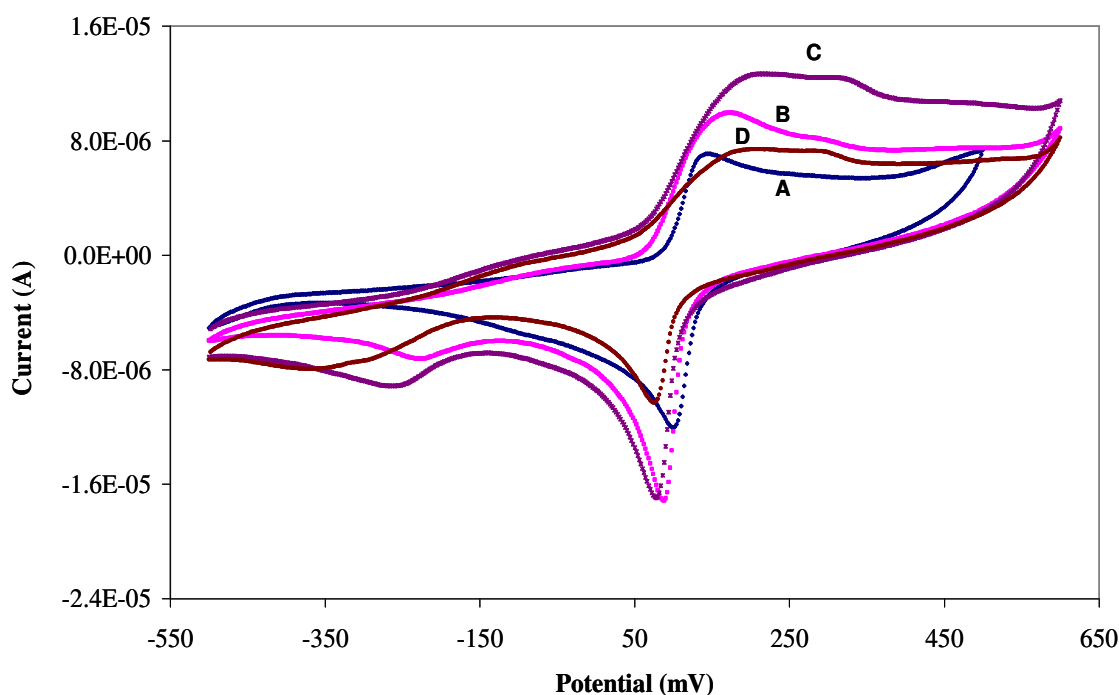


Fig. 5.14 Cyclic Voltammogram of $[\text{HgDz}]$ complex at various ligand ratios, 3.91 mM dithizone in MeOH, scan rate = 100 mV/s, graphs: a) Hg^{2+} , b) HgDz_1 , c) HgDz_4 , d) HgDz_5

There is an additional peak at 0.305 V, which can be contributed to the reorganization of electrons on the metal complex. The sulphur, nitrogen atom and the phenylring all contribute to the stabilization of the mercury complex. On the reverse scan the no peak is found for the stabilized metal complexes. The reduction peak of the metal at 0.09 V has increased in size. The increases can be contributed to a faster electron transfer rate of the complex. A new peak appears at -0.21 V due to the complexation of mercury with the ligand and belongs to the metal ligand

$[\text{Hg-Dz}_2]^{2-}$ reduction peak. As the ligand concentration increased the metal oxidation peak increased in size and moved to a higher positive potential. On the reverse scan more of the mercury ions in solution reacts with the ligand and forms a more stable complex. For an excess of dithizone the metal ligand reduction peak is found -0.352 V. The complex which is formed is very stable indicating that with added amount of dithizone the metal ligand reduction peak moves to more negative potential and forms a stronger complex.

5.3.3 Study of Methylmercury (I) and its Dithizone Complex.

Figure 5.15 is obtained after adding aliquots of the ligand. The voltammogram shows a non-reversible reaction. Both the oxidation peaks dramatically decreased in size and moved to more negative potentials.

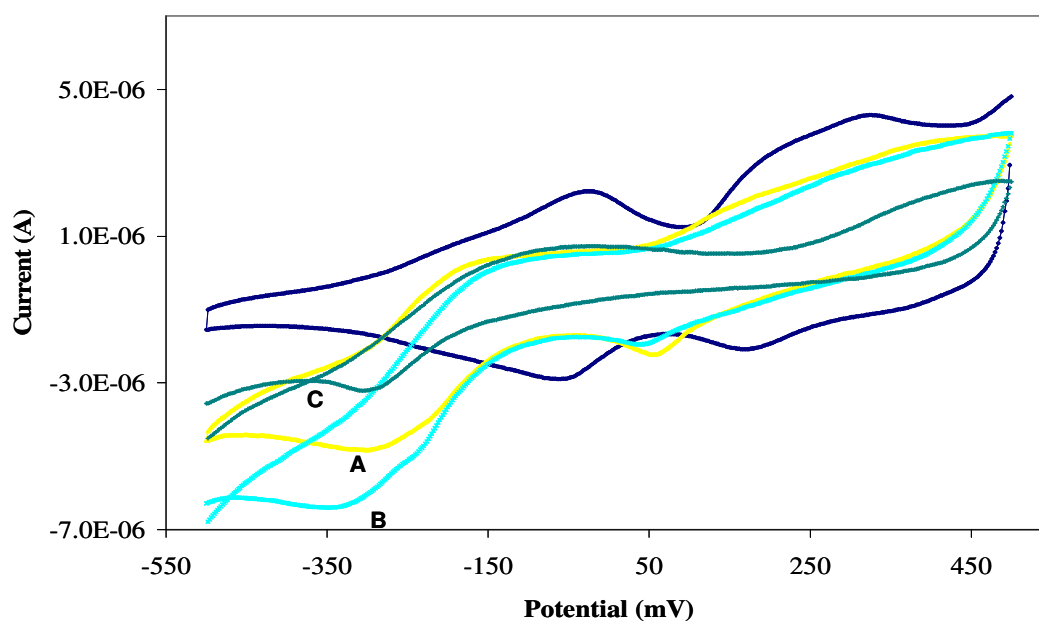


Fig. 5.15 Cyclic Voltammogram of $[\text{MeHgDz}]$ complex at various ligand ratios, 0.00391 M dithizone in MeOH, scan rate = 100 mV/s, graphs: a) MeHgDz_2 , b) MeHgDz_3 , c) MeHgDz_6

The broad peak at -0.28 V confirms the formation of the stable $[\text{MeHgDz}]^-$ complex. Adding the dithizone decreased the electron transfer rate and no clear oxidation peak can be seen. When dithizone is in excess only one peak is visible on the reverse scan and it's due to the reduction of the metal ligand complex. The complex peak becomes broader and moves to more negative potentials, indicating the formation of a stronger complex.

5.3.3 Study of Ethylmercury (I) and its Dithizone Complex.

Figure 5.16 is obtained after adding aliquots of dithizone to ethylmercury. The electron transfer rapidly decreased when the ligand was added. On the forward scan both the oxidation peaks decreased in sized and moved slightly to lower potentials. At 0.65 V a new peak appears due to oxidation of the new formed complex. On the reverse scan the two reduction peaks decreased in size. The metal ligand reduction peak is found at -0.40 V indicating the formation of the $[\text{EtHg-Dz}]^-$ complex.

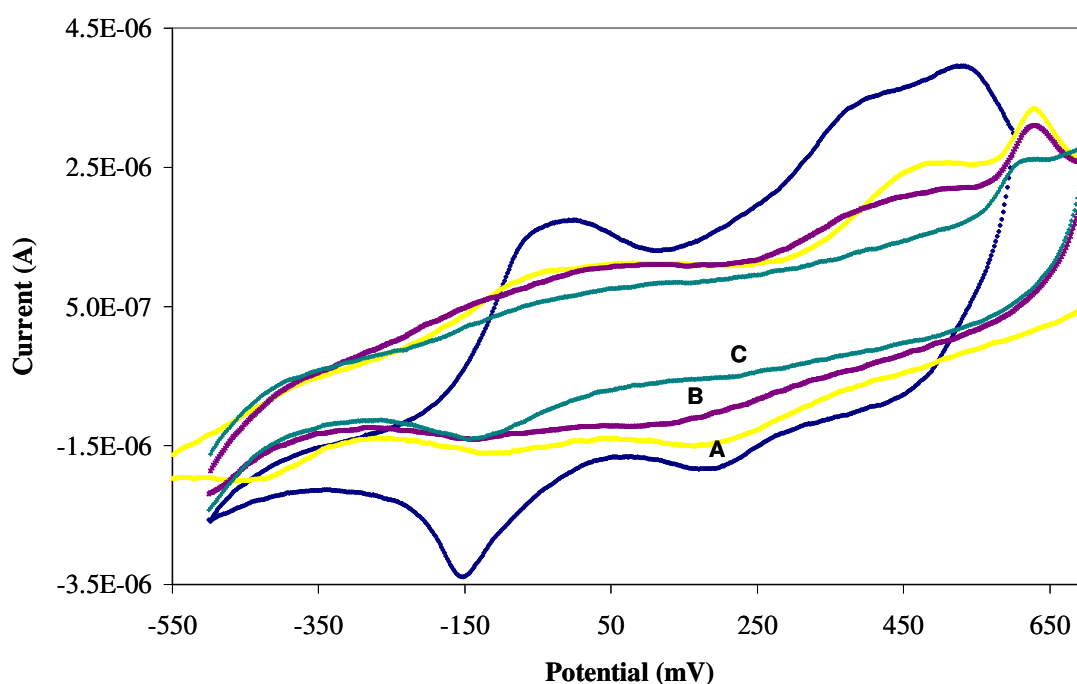


Fig. 5.16 Cyclic Voltammogram of $[\text{EtHgDz}]$ complex at various ligand ratios, 3.91 mM dithizone in MeOH, scan rate = 100 mV/s, graphs: a) EtHgDz_2 , b) EtHgDz_4 , c) EtHgDz_6

At a certain molar ratio (1:3), the oxidation peak shows no change in size. More mercury ions complexes with dithizone and the reduction peaks become therefore less visible on the reverse scan as the molar ratio increases. The complex reduction peak shifts to more negative potentials.

5.3.4 Study of Phenylmercury (I) and its Dithizone Complex.

On the addition of dithizone to the mercury solution the complex forms. Fig 5.17 illustrates a fast electron transfer reaction. During the forward scan two peaks are clearly visible. Mercury is oxidized at 0.15 V and at 0.42 V the dimer is oxidized. On the reductive sweep a sharp peak appears which can be assigned to the presence of elemental mercury. The metal ligand reduction peak is found at -0.305 V. As more dithizone was added the metal reduction peak decrease until no peak can be found. The metal ligand reduction peak becomes broader and shifts slightly to lower potentials.

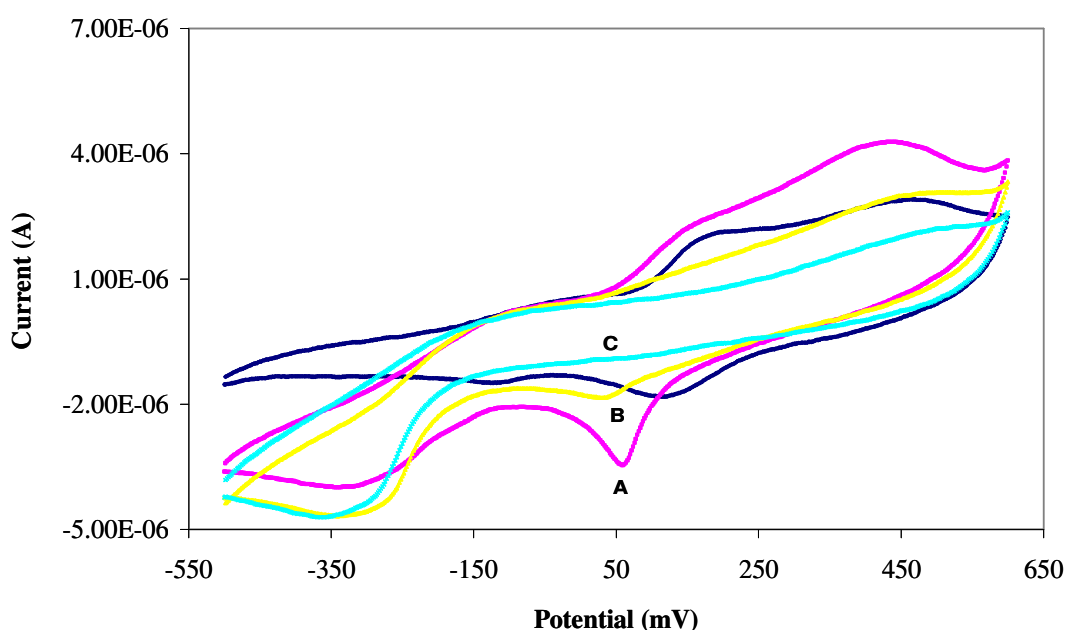


Fig. 5.17 Cyclic Voltammogram of [PhHgDz] complex at various ligand ratios, 0.00391 M dithizone in MeOH, scan rate = 100 mV/s, graphs: a) PhHgDz₁, b) PhHgDz₂, c) PhHgDz₃

5.4 Mercury Dithizone sulfonate complexes

Dithizone sulfonate (DzS), is one of the few water soluble derivatives of dithizone. To the best of the authors knowledge no electrochemical work on mercury dithizone sulfonate complexes has been reported.

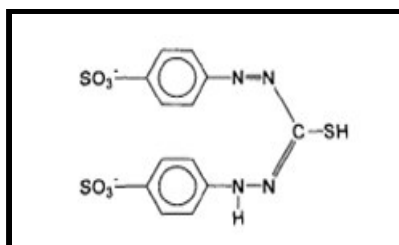


Fig. 5.18 Structure of dithizone sulfonate [24].

5.4.2 Study of mercury (II) and its Dithizone sulfonate Complex.

Figure 5.19 is obtained after adding aliquots of the ligand, 9.68 mM dithizone sulfonate (4000 ppm) to the electrochemical cell. This voltammogram shows an irreversible behavior of the complex.

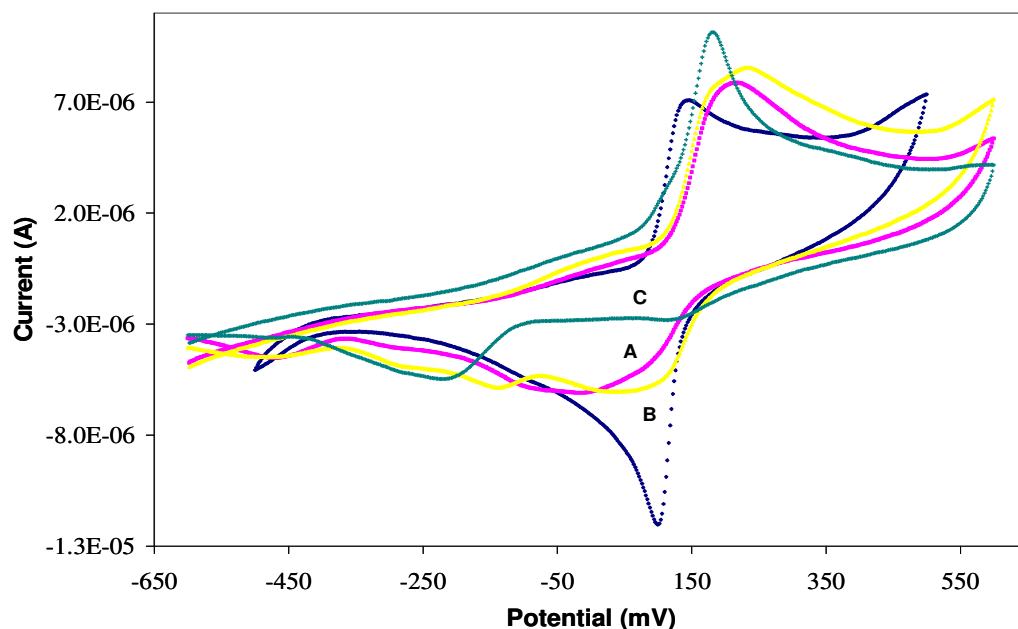


Fig. 5.19 Cyclic Voltammogram of [HgDzS] complex at various ligand ratios, 9.68 mM dithizone sulfonate in water, scan rate = 100 mV/s, a) HgDzS₁, b) HgDzS₂, c) HgDzS₆

The metal oxidation peak has moved from 0.139 V to 0.222 V due to the $[\text{HgDzS}_2]^{4-} \rightarrow [\text{HgDzS}_2]^{2-} + 2e$ oxidation. The current also increases slightly indicating a faster electron transfer when the ligand is added. On the reverse scan a very broad metal reduction peak is found at 0.08 V till -0.10 V. The metal reduction peak decreased in size drastically. The decreases in size gives an indication that the complex has formed. Because of the very broad metal reduction peak, no clear metal ligand peak can be found on the reverse scan. As more aliquots of ligand were added the anodic current increases on the forward scan. Indicating a faster electron transfer as more ligand was added. On the reverse scan the metal reduction peak decreased with added amounts of ligand. The metal reduction peak shifted to more negative potentials indicating the formation of a stronger complex. For the 1:6 M:L the metal ligand reduction peak is found at -0.238 V.

5.4.3 Study of methylmercury (I) and its Dithizone sulfonate Complex.

Figure 5.20 is obtained after adding aliquots of the ligand to the methylmercury ion solution.

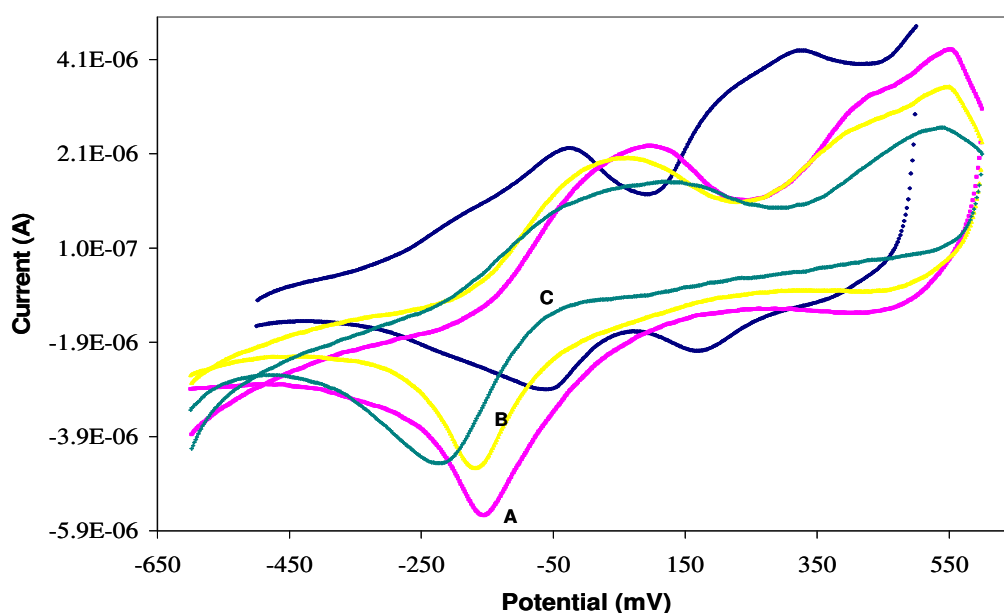


Fig. 5.20 Cyclic Voltammogram of $[\text{MeHgDzS}]$ complex at various ligand ratios 0.00968 M dithizone sulfonate in water, scan rate = 100 mV/s.

This voltammogram shows a non-reversible reaction. Both the oxidation peaks decreased in size and moved to more positive potentials.

The first oxidation peak moved from -0.03 V to 0.10 V and the second oxidation peak moved from 0.324 V to 0.562 V. On the reverse scan no metal reduction peak is found. The metal ligand reduction peak at -0.168 V confirms the formation of the stable $[\text{MeHgDz}]^{2-}$ complex.

After doubling the ligand quantity the first oxidation peak on the forward scan becomes broader and shifts to a lower positive potential. Adding the dithizone sulfonate in effect decreased the electron transfer rate. As more ligand was added the metal ligand reduction peak decreased in size and also shifted to more negative potentials.

5.4.4 Study of Ethylmercury (I) and its Dithizone sulfonate Complex.

Figure 5.21 is obtained after adding aliquots of dithizone sulfonate to the ethylmercury solution. This voltammograms shows an irreversible reaction.

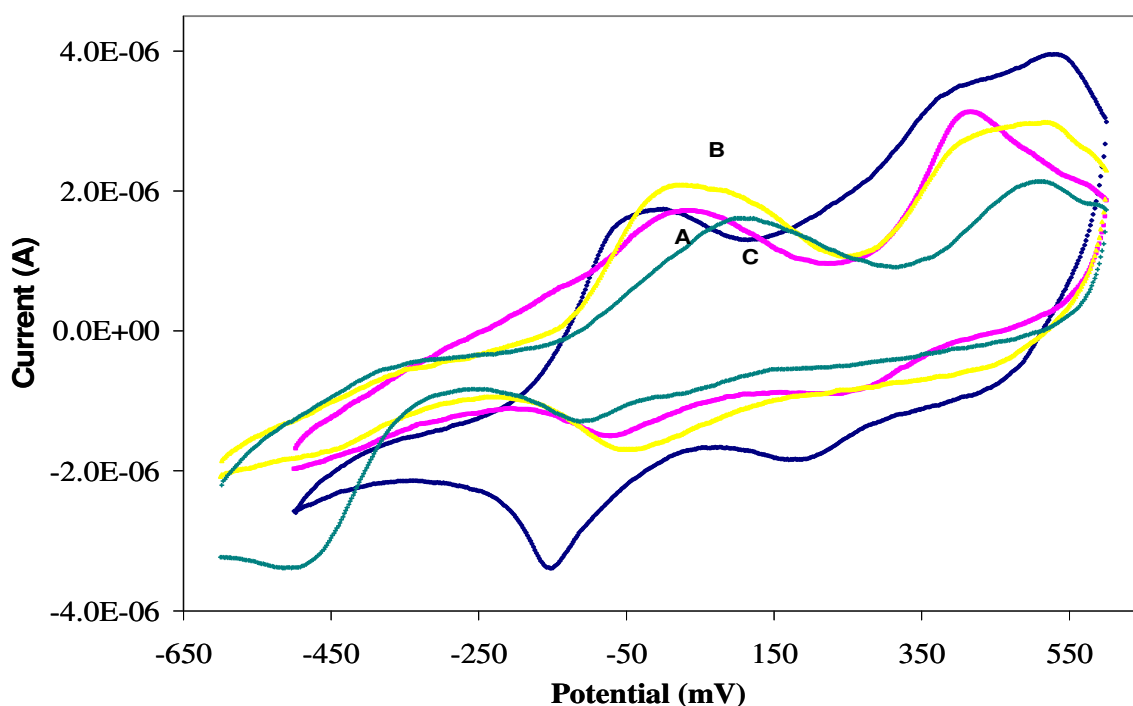


Fig. 5.21 Cyclic Voltammogram of $[\text{EtHgDzS}]$ complex at various ligand ratios, 9.68 mM dithizone sulfonate, scan rate = 100 mV/s, graphs: a) EtHgDzS_1 , b) EtHgDzS_2 , c) EtHgDzS_6

The electron transfer rapidly decreased when the ligand was added. On the forward scan both the oxidation peaks decreased in size and moved slightly to lower potentials. At 0.415 V a new peak appears due to oxidation of the new formed complex.

During the reductive sweep the two reduction peaks also decreased in size. The metal reduction peak is moved from 0.201 V to -0.072 V. The metal ligand reduction peak is found at -0.375 V indicating the formation of the $[\text{EtHgDzS}]^{2-}$ complex. Increasing the amount of Dithizone sulfonate the oxidation peak as well as the electron transfer rate decreases. The metal ligand oxidation peak moved from 0.415 V to 0.521 V indicating the formation of a more stable complex for the 1:2 M:L ratio. The metal ligand reduction peak is found at -0.42 V. As more ligand was added to the solution the metal ligand oxidation peak decreased in size. At a certain molar ratio the potential of the metal oxidation peaks shows no change. On the reverse scan the metal ligand reduction peak moves to more negative potential indicating the formation of an even stronger complex as more ligand is added to the solution.

5.4.5 Study of Phenylmercury (I) and its Dithizone sulfonate Complex.

After adding aliquots of the ligand one peak corresponding to the metal oxidation of the complex was found at 0.066 V and the second peak at 0.562 V can be assigned to the oxidation of the metal ligand complex. On the reverse scan the reduction peak of mercury has disappeared and a new peak appears at -0.223 V due to the metal-ligand reduction of the stable $[\text{PhHgDzS}]^{2-}$ complex. As more of the ligand was added the metal oxidation peak decreases in size and a slower electron transfer was also seen. On the reverse scan the metal ligand reduction peak becomes broader and moves to more negative potentials forming a stronger complex.

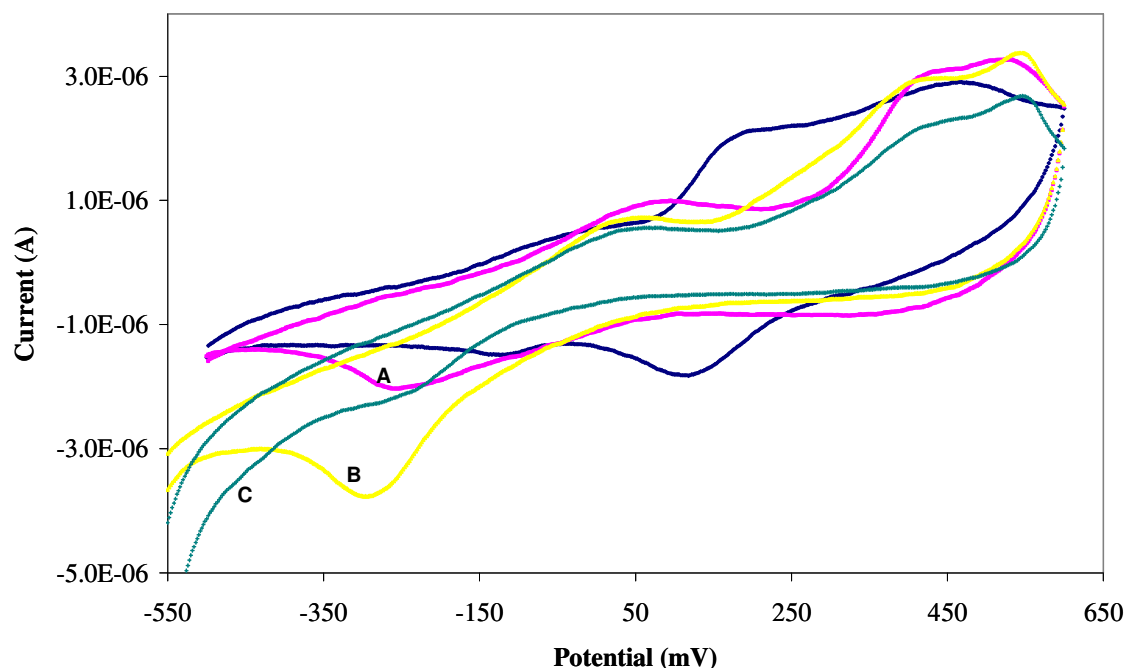


Fig. 5.22 Cyclic Voltammogram of [PhHgDzS] complex at various ligand ratios, 0.00968 M dithizone sulfonate in water, scan rate = 100 mV/s.

5.5 Conclusion

CV is used to study the electrochemical properties of four mercury species complexed with ligands such as cysteine, dithizone and dithizone sulfonate. For inorganic mercury as the ligand is added, the reduction peak of Hg^{2+} decreases and a new peak forms at a more negative potential indicating the formation of the metal ligand complex. This is characteristic of ML complexation electrochemistry. As the ligand quantity increases this newly formed peak shifts to a more negative potential as the complex becomes more stable. At a M:L ratio of 1:4, the cysteine is in excess and no change is seen in the reduction peak for more added cysteine. All the organic mercury species showed the same mechanism where a radical species (R-Hg^\bullet) is formed on the oxidation sweep and is a classical example of an EC mechanism where the stable chemical compound, which follows the initial oxidation, is then reduced as a complex. Of the three ligands used in this electrochemical study, it was found that dithizone sulfonate forms more stable complexes with the all mercury species used in this study, as is evident from the potential shifts in the cyclic voltammograms. It is concluded that when the mercury complexes are studied with CE-UV, lower detection limits will be achieved with dithizone sulfonate as the complexing agent, rather than with cysteine. For all the dithizone sulfonate complexes, a molar ration of 1:1

Chapter 5 – Results and Discussion I

was sufficient to form complexes with all the mercury species. All the metal ligand reduction peaks of the different mercury complexes were found in the range of -0.11 V to -0.395 V. For electrochemical detection in CE an applied voltage of 0.4 V or higher will be sufficient to detect the mercury complexes.

References:

1. E.O Bobo, B. Bessone, J.M Bisang, *Journal of Applied Electrochemistry* 28, (1998), 803-809.
2. H.Zejli, P. Sharrock, *Talanta* 68, (2005), 79-85.
3. S. Fei, J. Chen, S. Yao, G. Deng, *Analytical Biochemistry* 339, (2005), 29-35.
4. M. Heyrovsky, S. Vavricka, *Biochemistry and Bioenergetics* 48, (1999), 43-51.
5. T. Ralph, M. Hitchman, F. Walsh, *Journal of Electroanalytical Chemistry* 587, (2006), 31-41.
6. S. Shahrokhian, M. Karimi, *Electrochimica Acta* 50, (2004), 77-84.
7. M.J. Pena, V. Lopez, I. Alarcon, *Electrochimica Acta* 35, (1990), 47-53.
8. U. Forsman, *Electroanalytical Chemistry*, 122, (1981), 215-231.
9. H. Szalai, T. Paal, *Talanta*, 48, (1999), 393-402.
10. W.Stricks, I.Kolthoff, *J. Am. Chem. Soc.*, 75, (1953), 5673-5677.
11. B.V Cheesman, D.L Rabenstein, *J. Am. Chem. Soc.*, 110, (1988), 6359-6364.
12. F. Jalillehvand, B. Leung, E. Damain, *Inorganic Chemistry* 45, (2006), 66-73.
13. B. Onterroso-Marco, B. Lo´pez-Ruiz, *Talanta* 61, (2003), 733- 741.
14. K.J Powell, P.L Brown, R.H Byrne, T. Gajda, H. Wanner, *Pure Appl. Chem.*, 77, (2005), 739-800.
15. H. Koszegi-Szalai, T.L Pa`l, *Talanta* 48, (1999), 393-402.

16. J.B. Matos , L.P. Pereira , S.M.L. Agostinho , O.E. Barcia ,G.G.O. Cordeiro , E. D'Elia, *Journal of Electroanalytical Chemistry* 570, (2004), 91–94.
17. R. Agraz, M. Sevilla, L. Hernandez, *Journal of Electroanalytical Chemistry* 390, (1995), 45-57.
18. L. Moretto, P.Ugo, J. Chevalet, *Journal of Electroanalytical Chemistry* 467 (1999), 193-202.
19. J. Ireland-Ripert, C. Ducauze, *Analytica Chimica Acta* 143, (1982),249-254.
20. F. Ribero, M. Neto I, Fonseca, *Analytica Chimica Acta* 579, (2006), 227-234.
21. R. Heaton, H. Laitinen, *Analytical Chemistry* 46, (1974), 547-553.
22. L. Tomcsanyi, *Analitica Chimica Acta* 70, (1974), 411-416.
23. L. Tomcsanyi, *Analitica Chimica Acta* 88, (1977), 371-376.
24. S. Hardy, P. Jones, *Journal of Chromatography A* 765, (1997), 345-352.
25. J. Pemberton, R. Buck, *J. Phys. Chem.*, 87, (1983), 3336-3343.
26. S. Hardy, P. Jones, *Journal of Chromatography A* 791, (1997), 333-338.
27. J. Pemberton, R. Buck, *J. Am. Chem. Soc.*, 104, (1982), 4076-4084.
28. J. Pemberton, R. Buck, *Journal of Electroanalytical Chemistry* 132, (1982), 291-309.
29. B. Paci, J. Nunzi, N. Sertova, I. Petkov, *Journal of Photochemistry and Photobiology A: Chemistry* 137, (2000), 141–144.
30. H.M.N.H. Irving, A.M. Kiwan, *Analitica Chimica Acta* 45, (1969), 271-277.
31. H.M.N.H. Irving, A.M. Kiwan, *Analitica Chimica Acta* 45, (1969), 255-269.

32. H.M.N.H. Irving, D.C. Rupainwar, S.S. Sahota, *Analitica Chimica Acta* 45, (1969), 249-254.

33. H.M.N.H. Irving, A.M. Kiwan, *J. Chem. Soc.*, (1963), 4288.

Chapter 6

Results and Discussion II

6.1 Capillary Electrophoresis with UV Detection

For the CZE separation of mercurical complexes ligands having a free thiol group (-S-H) were selected because the reaction between the mercury compounds and the free thiol group can be considered to be practically complete [1]. All the thiol compounds of mercuricals have good light absorption characteristics. Another important requirement for the proper agent is that the formed mercury complex should possess at least a minimal charge to create a difference in electrophoretic mobilities of the formed mercury complex and thus, they could be well separated. For the separation of inorganic and organomercury compounds by CE, a derivatization step is desirable. It provides significant improvement in the CE separation of mercury. First, when used with UV-visible detection, it greatly improves the detectability of the otherwise non-absorbing Hg species. Secondly, using negatively charged anionic reagents and creating negatively charged complexes, the problem with low or no charge is solved [1-4].

Medina et al. were the first to demonstrate the separation of four Hg species (Hg^{2+} , MeHg^+ , EtHg^+ and PhHg^+) in alkaline borate buffer (pH 8.35) with 10% methanol. The sample was derivatized with 0.1% L-cysteine hydrochloride prior to CE separation. Very low detection limits were achieved when they studied fish and mussel samples by making use of a modified Westöö extraction method [1,5]. The proposed separation and extraction was later validated and modified by Carro-Diaz et al. for the determination of methylmercury in fish [6]. Gaspar and Pagar have shown that mercury species can be complexed and separated with a number of different thiolic compounds, e.g., cysteine, mercaptoacetic acid, glutathione and 2-mercaptosuccinic acid. All of these ligands were used for the separation of mercury species in borate buffer at pH 9. Glutathione gave the best molar absorptivity of all the ligands investigated at 200nm with UV detection [1,7]

In this study, four mercury compounds were investigated using L-cysteine as the complexing agent. Different parameters such as pH, temperature, voltage, concentration etc. were investigated and the best separation condition found was to be:

60 cm Fused silica capillary (52 cm effective length), 50 μm i.d, +25 kV applied voltage, 25 mM sodium borate buffer, pH 9.35 and no organic modifier.

6.2 Performance

The pH buffer used to carry out the electropherogram was the most important operational parameter. Cysteine has an iso electronic point of 6.24, thus in an alkaline media the cysteine mercury complexes formed had a negative charge [1,5].

Using the optimum conditions as described above a solution was prepared containing 20 μl Hg^{2+} , 20 μl MeHg^+ , 20 μl EtHg^+ , 200 μl PhHg^+ and 360 μl cysteine made up to 2 ml with a water:methanol (1:1) solvent. 1 ml of this solution was placed in the sample vial and injected in the CE instrument. The final separation of the mercury standards can be seen below.

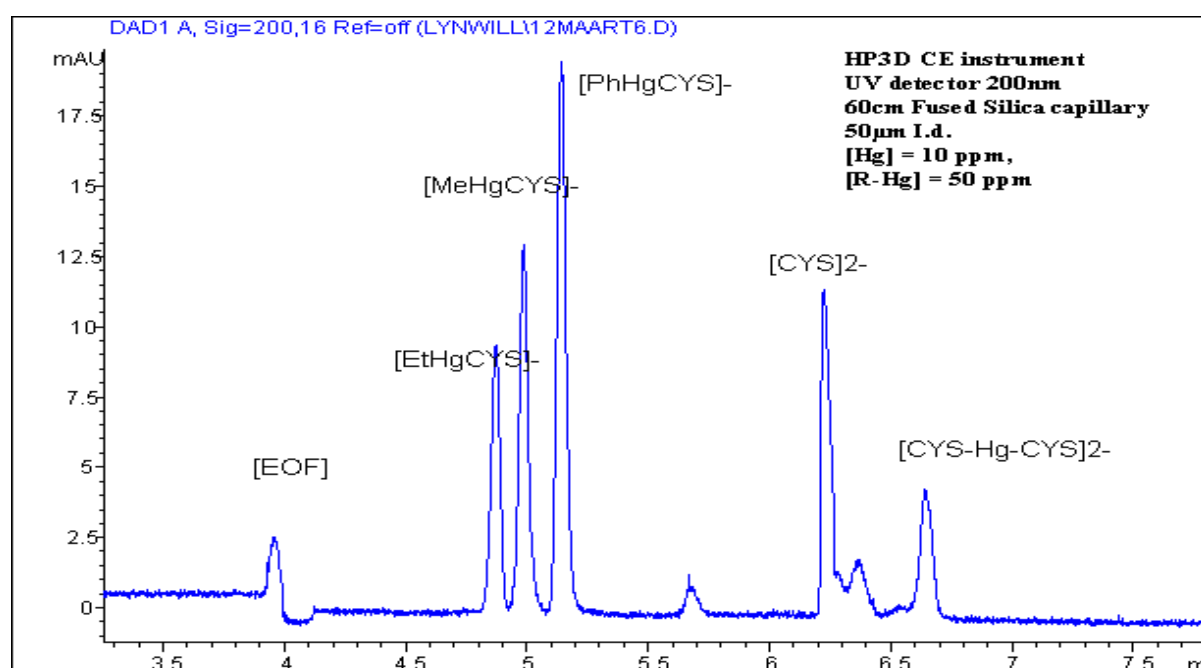


Fig. 6.1 Electropherogram of mercury cysteine complex: buffer 25 mM sodium borate, pH 9.35, Voltage = +25 kV, UV = 200 nm.

All the peaks are well resolved and can be assigned to the respected complexes. In an alkaline medium the (1:2) mercury (II) cysteine complex has two negative charges which meant that the Hg^{2+} appeared to the right of the excess cysteine peak in the electropherogram. The order of elution was EtHg^+ , MeHg^+ PhHg^+ , excess cysteine and Hg^{2+} . One would expect that MeHg

would elute before EtHg because of the molecular weight of ethylmercury. The separation of these two organomercurials is influenced by other factors. The explanation for the difference in elution time can be given by the inductive effect of the ethylgroup towards the complex. It is known that certain R-groups helps to stabilize a complex by donating electrons and thus has a stronger inductive effect making the overall charge of the complex less negative. The methyl group effect is smaller and thus the overall charge is more negative than the ethylmercury complex. Therefore, ethylmercury elutes first and then methylmercury. For phenylmercury the contribution of the aromatic ring led to a greater sensitivity as compared to the other organomercurials.

The test sample was injected 10 times under the same conditions. The limit of detection was determined with a signal to noise ratio of 3:1. Results for standard deviations (STD) and percentage relative standard deviations (%R.S.D) were calculated with Microsoft Excel. Although CE-UV-Vis is not a very sensitive detection mode for trace mercury concentration, the LOD's were found to be in the low ppm range for the mercury cysteine complexes. Table 6.1 summarizes the LOD's of the complexes.

Table 6.1 LOD's of mercury cysteine complexes

Cysteine Complex	Concentration (mg/L)	% R.S.D
EtHg ⁺	5.0 ±1.95	7.73
MeHg ⁺	2.0 ±1.03	4.83
PhHg ⁺	0.5 ±0.13	1.97
Hg ²⁺	0.25 ±0.11	2.15

6.3 Separation of mercury dithizone sulfonate complexes

Dithizone sulfonate (DzS), is one of the few water soluble derivatives of dithizone. Most dithizone complexes are uncharged and this together with their insolubility in water makes them unsuitable for CE separation. However, water soluble DzS, should be very useful for the determination of organic mercury species of the formula RHgX by CE since it forms stable

Chapter 6 – Results and Discussion II

complexes with a double negative charge of the type $[\text{RHgDzS}]^{2-}$ which should separate from the negatively charge dye. Inorganic mercury forms the negatively charge complex of the type $[\text{HgDzS}]^{4-}$ and should be well resolved from the organomercury complexes [1,8]. Mercury dithizone sulfonate complexes was first separated by Hardy and Jones. The mercury complexes were separated in under 8 minutes at 480 nm in 10 mM sodium acetate buffer at pH 4.5. Acrylamide coated capillaries were used in the separation. The high absorptivity of the ligand and the excellent detector baseline stability allowed low $\mu\text{g/L}$ LODs. This method was specifically developed for the determination of methylmercury in fish and meat extracts. The use of highly absorbing DzS reagents provides so far the most sensitive method with UV-Vis detection [8,9]. Four mercury species were studied again. In all cases the DzS metal complexes were preformed prior to CE separation. All the mercury Dzs complexes were found to be highly stable. The best separation condition for the mercury Dzs complexes were as follows:

55 cm Fused silica capillary (47cm effective length)

50 μm i.d

-25 kV applied voltage

10 mM sodium acetate buffer pH 3

25 °C

Under these conditions a good separation was achieved. The separation of methyl and ethylmercury was expected to be difficult due to the small difference in molecular weight, but separated nicely. The DzS was not pure and gave a number of small impurity peaks but did not influence the separation of the mercury complexes. The order of elution was, Hg^{2+} excess DzS, MeHg^+ , EtHg^+ and PhHg^+ . All the mercury complexes were separated under 13 minutes.

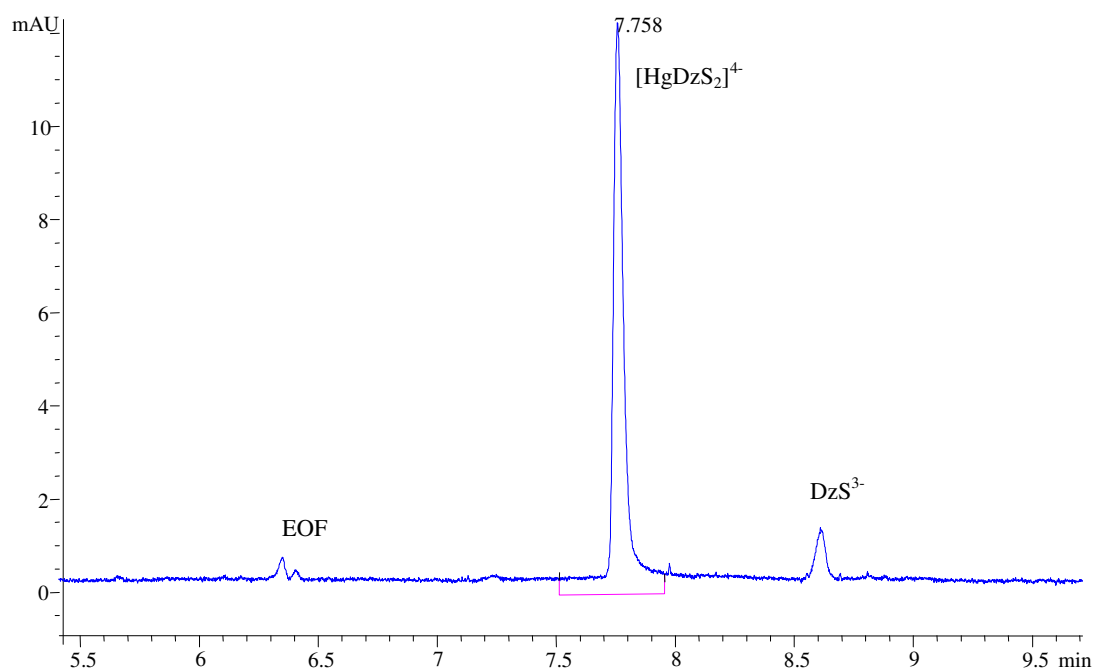


Fig. 6.2 Electropherogram of mercury dithizone sulfonate HgDzS 1 mg/L: buffer 10 mM sodium acetate, pH 3 Voltage = -25 kV, UV = 275 nm.

When all the mercury species were studied together the organomercury complexes were not detected well.

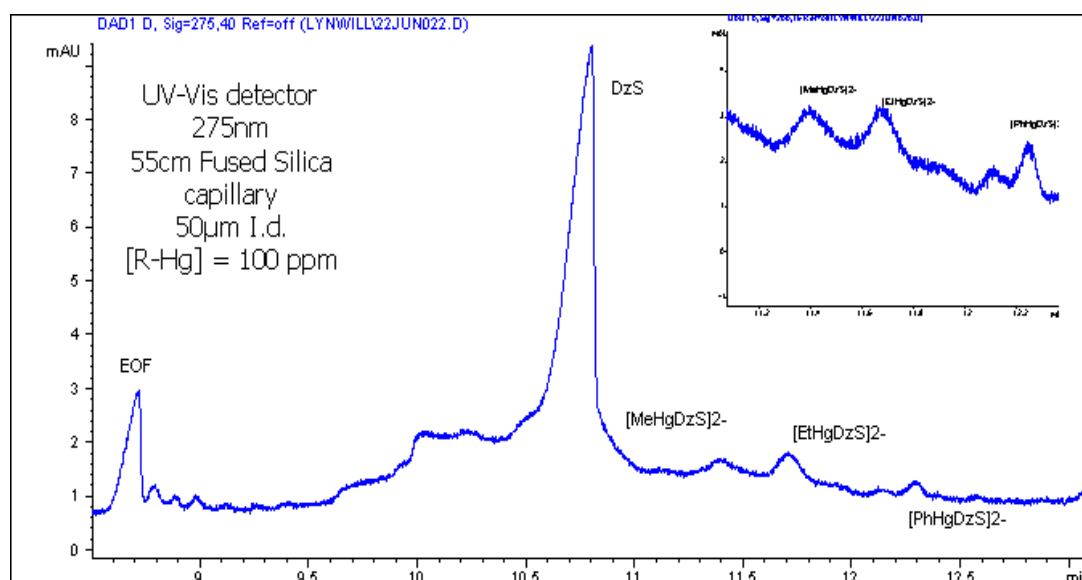


Fig. 6.3 Electropherogram of organomercury dithizone sulfonate complexes: buffer 10 mM sodium acetate, pH 3 Voltage = -25 kV, UV = 275 nm.

The complex formation of inorganic mercury with dithizone is much more favourable than the organomercury species with the ligand. When only the organomercury species were studied, all three complexes were detected and a good separation was achieved although a relative high concentration of organomercury was needed. From the electrochemical studies of the complexes, it is clear that inorganic mercury forms a stronger complex with DzS than with cysteine. So we expect lower detection limits with the mercury dithizone complexes as is evident from table 6.2.

Table 6.2 LOD for mercury dithizone complexes

DzS Complex	Concentration (mg/L)	% R.S.D
Hg ²⁺	0.05 ±0.19	3.13
MeHg ⁺	1.0 ±1.26	5.63
EtHg ⁺	1.0 ±2.32	9.31
PhHg ⁺	0.20 ±0.54	4.35

From the CE-UV results, a comparison will be made with CEEC to see if even lower detection limits can be gained for the different mercury complexes.

6.4 Conclusion

To date, capillary electrophoresis has been used to a limited extent in speciation studies of mercury. HPLC and GC still remain the two dominant techniques to detect mercury, but CE has recently shown great potential for mercury speciation [1-3]. In this study four mercury species were complexed with cysteine and dithizone sulfonate and separated under the optimum conditions described earlier. With cysteine as the complexing agent, the CE run was much shorter compared to when dithizone sulfonate was used. The run time of the cysteine complexes was in good comparison with work done by Medina and others [1]. However the detection limits with cysteine is too high and can not be adequate for mercury determination at low concentrations levels. By using dithizone sulfonate as the complexing agent better detection limits were obtained although there was an increase in the run time. The separation of the organomercury complexes was not very effective and a change of pH or buffer could overcome this problem. The use of coated capillaries could also give lower detection limits for these

species. Dithizone sulfonate has great potential as a complexing agent when mercury is detected by UV–Vis spectrometry and is the best absorbing reagent to use in speciation studies of mercury. Although in this work the separation of mercury species could be performed without difficulties, it has to be mentioned that the LOD values achievable with UV spectrophotometry are far above the concentration range of the mercury compounds found in environmental samples. This problem of detection may be solved by using more sensitive detection modes such as electrochemical detection. The presented results shows that CE could be used as a powerful tool in the separation and detection of mercury in the environment. In CE there is no need for special or sophisticated separation schemes and CE avoids the drawbacks associated with GC and HPLC. This technique is rapid and simple enough to be used on a routine basis.

Reference:

1. P. Kuban, P.C. Hauser, V. Kuban, *Electrophoresis* 28, (2007), 58-68.
2. M. Leermakers, P. Quevauviller, M. Horvat, *Trends in Analytical Chemistry* 24, (2005), 383-392.
3. E.P. Lai, W. Zhang, S. Kennedy, E. Dabek-Zlotorzynska, *Analytica Chimica Acta* 364, (1998), 63-74.
4. R. Weinberger, *Practical Capillary Electrophoresis* 2nd Edition, Academic Press, NYC, (2000).
5. I. Medina, E. Rubi, M.C Mejuto, *Talanta* 40, (1993), 1631-1636.
6. A. Carro-Diaz, A.M Ferreira, R. Torrijos, *Microchim Acta* 123, (1996), 73-86.
7. C. Pager, A. Gaspar, *Microchem. Journal* 73, (2002), 53-58.
8. S. Hardy, P. Jones, *Journal of Chromatography A* 765, (1997), 345-352.
9. S. Hardy, P. Jones, *Journal of Chromatography A* 791, (1997), 333-338.

Chapter 7

Results and Discussion III

7.1 Electrochemical Detection

An alternative method to conventional detection is to use electrochemical detection (EC) [1]. This method is ideally suitable for CE. Its rapid speed, high separation efficiency, high selectivity and sensitivity and variety of configuration and materials that can be employed make this method suitable for mercury detection at ultra trace levels [2]. Over the past years EC methods have been developed extensively for use in HPLC and have become accepted for their ability to provide low detection limits for analytes that are easily oxidized or reduced [3]. The first reported applications of electrochemical detection for CE was in 1987 from the research group of Ewing [4-6]. From these studies it was found that the sensitivity and selectivity characteristics long known for EC detection in HPLC are largely transferable into the CE domain. It turns out that, in several respects, EC techniques are even better suited for CE than for HPLC. Unlike optical detection methods, the performance of EC systems is not compromised by miniaturization as the small currents associated with the microelectrodes used are easily and accurately measured and noise generated at the electrode surface decreases with electrode area as fast or faster than does the signal. EC instrumentation is relatively inexpensive compared to laser based fluorescence or mass spectroscopy systems [7-10].

7.2 Fundamentals of Electrochemical Detection

Electrochemical detection is based on the monitoring of changes in an electrical signal due to an electrochemical reaction at an electrode surface, usually as a result of an imposed potential or current. In a solution, the equilibrium concentration of the reduced and oxidized forms of a redox couple are linked to the potential via the Nernst equation

$$E = E^0 + \frac{RT}{n} \ln (C_{\text{ox}}/C_{\text{red}}) \quad (1)$$

Where E^0 denotes the standard potential, C_{ox} and C_{red} the concentration of oxidized and reduced forms. The other symbols have their usual meaning. For each redox couple there exist a potential, known as the standard potential E^0 at which the reduced and oxidized forms are present at equal concentration. If a potential E applied with respect to the reference electrode is applied to the working electrode the redox couples present at the electrode respond to this change and thus adjust their concentration ratios according to Equation 1. In this process electrons have to be transferred from the electrode to the lowest unoccupied energy level of a species in the solution. The movement of electrons in or out of the electrode can be measured as an oxidation or reduction current. This technique is referred to as amperometry [11-15].

By an appropriate choice of the applied potential, it is possible to discriminate between different redox couples. The range of potentials that can be applied in EC detection is limited by redox processes involving the solvent. The choice of the working electrode material is an important factor in EC detection. This stems from the required electron transfer between the electrode and the analyte. There are three electrochemical detection systems suitable for sensitive detection of metal ions, i.e., potentiometric, conductometric and amperometric detection [13]. Electrochemical detection modes are relatively inexpensive and easy to adapt. Miniaturization of the electrodes and measuring chambers is no longer a problem and measurement of small currents at microelectrodes can be achieved easily and accurately. However, problems arise from the need to isolate the small detection potential from the CE voltage and current and requirements for precise alignment of the capillary and electrodes. New developments in electrochemical detection is indicative of a promising future [15].

7.3 Conductivity

Conductivity detection relies on measurement of the difference between the conductivities of the solute and the separation electrolyte, this provide a direct relationship between migration time and response factor. This is considered to be a universal detection method because the analyte is detected in the absence of a chromophore, fluorophore, or electroactive functional group [12,13]. In end column conductivity configuration in CE, one of the electrodes is placed directly outside of the channel outlet with the second electrode slightly distanced away in the outlet reservoir. For CE, this technique requires drilling two holes through the capillary wall. Two metal wire electrodes are then placed within these holes and sealed into place. This process is time consuming and hard to replicate, and the system is not robust. Critical conditions for this detection mode are the material and dimensions of the sensor electrodes, shielding from high

high-voltage interference (noise) and avoiding charge transfer reactions. Difficulties in the positioning of the electrodes are a drawback for this approach [14-15]. Despite these drawback, contactless conductivity detection has gained significant importance since its introduction in 1998 [16-18]. Besides the determination of inorganic ions in the low ppb range it is possible to apply conductivity detection for the detection of organic compounds also [17]. The *TraceDec*® contactless conductivity detector in combination with capillary electrophoresis represents a sensitive detection scheme for a variety analytes. The *TraceDec*® system offers the advantage of avoiding detection dead volumes which is of specific importance for miniaturized CE systems [16-20].

7.4 Potentiometric

Potentiometric detection is in principle the most straightforward method as no excitation signal is required and it is simply the potential developed at a sensing electrode which is measured. The potentiometric response is fast enough to prevent peak distortion, and therefore quantitative information about the analyte concentration is possible [11]. Yet, the disadvantages of this technique include tedious sensor preparation and handling procedures. The sensor lifetime is also limited and recalibration of the sensor is also a problem. This method is the least widely used of the three-electrochemical methods, because it is the most difficult one to implement [14,15,21].

7.5 Amperometric

Amperometric detection is certainly the most widely used of the three-electrochemical techniques [11]. With amperometry, which is mostly used in the direct mode (i.e., for electro active species) low detection limits have been achieved [1]. In most of the CEEC work reported to date the EC detection has been carried out amperometrically i.e., by controlling the potential applied to the sensing or working electrode and measuring the faradaic current flowing as a result of analyte oxidation or reduction at this potential. The applied potential is usually held at a constant value throughout the CE experiment, but in specific instances it can either be scanned continuously over a defined potential window (voltammetric detection) or jumped discontinuously from one potential to another (pulsed amperometric detection) [22-25]. Difficulties arise in decoupling the small detection potential from the CE voltage and current, in capillary electrode alignment and because optimum solution conditions for electrochemical detection often differ from those which gives the best CE separation [23]. The success of

electrochemical detectors is highly dependant on the working electrode material. Materials such as carbon, platinum, gold, copper, gold/mercury, or chemically modified electrodes have been used [26-27]. Detection is either performed in end-column or off-column mode, which means the absence and presence of a decoupler. The features of the three-electrochemical detection techniques are summarized in table 7.1 [22].

Table 7.1 Electrochemical detection methods for CE

<i>Method</i>	<i>Features</i>	<i>Detection limits</i>
Amperometry	Good detection limits Only possible for electroactive ions Different electrodes needed for different species Stability sometimes a problem	$10^{-7} - 10^{-9}$ M
Potentiometry	For lipophilic ions only Relatively difficult electrode preparation Different electrodes required for anions and cations	$10^{-5} - 10^{-7}$ M
Conductometry	Available commercially Universal, but good for small ions Detection limits not always adequate No adaptation of electrodes to sample necessary	10^{-6} M

Despite these attractive features, there are several concerns about EC detection that has prevented this approach from becoming a mainstream technique widely used by chemist. First, there is the question of how the small EC detection potentials and currents will be influenced by, and can be shielded or decoupled from the much larger CE voltage and current. Second, the issue of capillary/electrode alignment must be looked at within acceptable analytical performance that can be achieved without making the CEEC experiment an unduly burdensome operation to perform. The problem here is that the micro electrode must be placed very close to the capillary opening to ensure maximum interaction with the analyte species and maximum sensitivity. This alignment must be maintained over the course of several experiments and to be reproduced on a regular basis if CEEC is to provide useful and attractive quantitative analysis capabilities. A major drawback of EC is its inherent selectivity, which limits analysis to easily oxidizable or

reducible species. Another drawback is the fact that the detector electrode is in direct contact with the sample solution and might therefore deteriorate due to corrosion or fouling. The use of EC detection schemes requires a high degree of manipulative skill on the part of the chemist in order to align the microelectrode and capillary opening to maintain reproducibility during the CEEC operation [28-31]. Some of these difficulties have been addressed and a few publications have appeared in the recent literature [32-33].

7.6 Detection modes in CEEC

It is important to isolate the EC detector from the separation voltage when using amperometric detection. There are three different approaches which have been developed for this purpose and are depicted in Fig.7.1. These approaches are termed end-channel, in-channel and off-channel detection. These terms are used to specify the presence or absence of a decoupler [13,14].

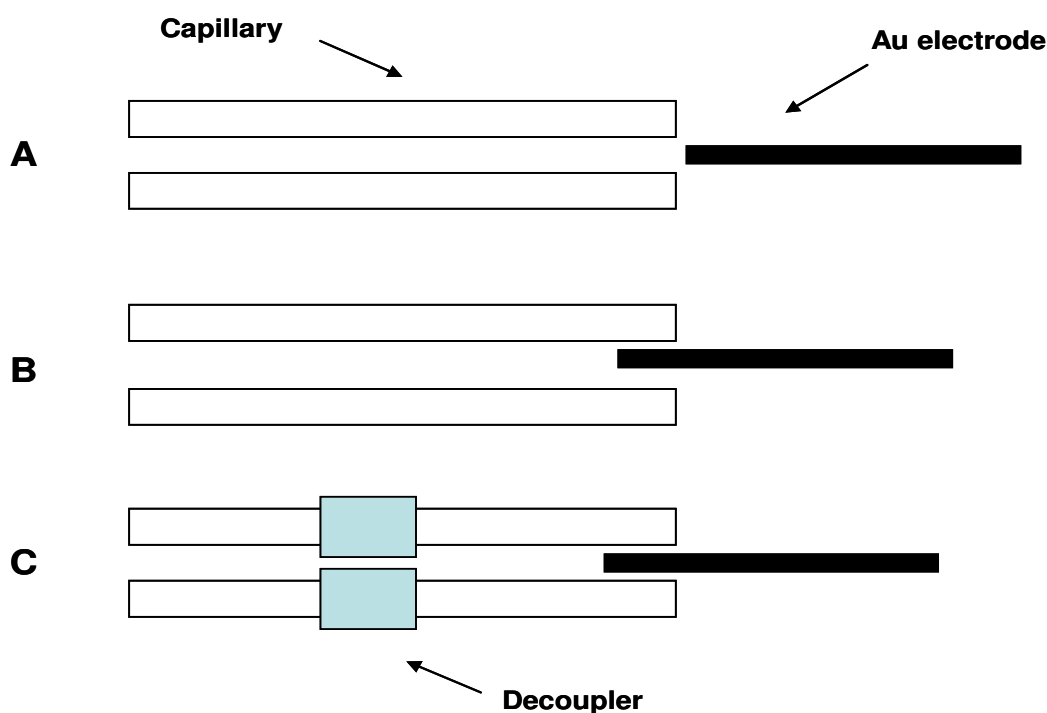


Fig 7.1 Three configurations for aligning the working electrode in amperometric detection: (A) end-channel detection, (B) in-channel detection, (C) off-channel detection.

7.6.2 End-channel detection

End-channel detection is the mode most often used for amperometric detection. In this configuration the working electrode is positioned tens of micrometers from the end of the

separation channel. This distance allows sufficient decoupling of the separation voltage from the working electrode and detector. However, since the separation voltage is grounded within the detection reservoir, the remaining separation field causes potential shifts at the working electrode. Therefore, it is necessary to perform a hydrodynamic voltammogram for a given analyte using the exact separation conditions that will be used to determine the detection potential. Overall, end channel detection produces higher background currents and is less sensitive than the other detection modes. Separation efficiency is also decreased due to analyte diffusion that occurs in the area between the exit. It is also important not to place the working electrode too close to the end channel. Small fluctuation in the separation voltage can produce noise at the detector, resulting in higher LODs. Band broadening is also another major drawback to consider with end-channel detection [11-14,]. To overcome some of these disadvantages, Mathies and co-workers have developed a new end-channel detection scheme. Better LODs have been reported using this new scheme. The LODs for the new end channel detection range from low nanomolar (10-100 nM) to micromolar concentration [34].

7.6.3 In-channel detection

To eliminate some of the problems associated with end-channel detection like band broadening, the in-channel detection mode was developed. The working electrode is placed directly within the separation channel. The analyte migrates over the electrode while still confined to the channel, thus eliminating band-broadening. The working electrode can be placed in the separation channel due to a developed electrically isolated (floating) potentiostat. This method was employed by Wallingford and Ewing in their initial report on CEEC. This approach still involves a tedious set-up procedure prior to the CEEC experiment. However, once the electrode is successfully placed inside the capillary, the alignment is more or less fixed and the system markedly improves. The benefits of this configuration is lower LODs, a 4.6 fold decrease in plate height while lowering the peak skew by a factor of 1.3 compared with end-channel detection [13,14,35,36].

7.6.4 Off-channel detection

This mode is also known as detection using capillary fractures. Most CEEC applications to date utilize an off-column detector design. The decoupling of the CE and EC system is accomplished by making a small opening or fracture in the capillary wall before the exit window. This divides

the capillary into two sections. The section before the fracture is called the separation capillary and the part beyond it is known as the detection capillary. The electrode placement is similar to that of in-channel detection, but a decoupler is used to isolate the separation voltage from the amperometric detector. The decoupler effectively shunts the separation voltage to ground and an electrophoretic free region is created in which the analytes are pushed past the working electrode by the EOF generated prior to the decoupler [11,12]. Wallingford and Ewing [4] used a porous glass capillary as material for their conductive coating on top of the fracture site. Lately a number of alternative materials have been employed in place of the porous glass: Nafion tubing [37], Nafion films [38], Teflon tubing [39], and palladium tubing [40]. To improve shunting the Lunte groups have developed much longer cellulose acetate and Nafion decoupling systems [41,42]. In this manner it was possible to fabricate 2 mm long decoupling elements which did not degrade CE efficiency but were able to maintain low EC noise levels while shunting CE currents up to 30 μA [8,41,42]. Currently, Nafion appears to be the material of most frequent choice for decoupler use due to its ready availability and high conductivity [8].

7.7 Experimental

7.7.2 Capillary electrophoresis

All experiments were performed on a Waters Quanta 4000 capillary electrophoresis system capable of delivering 0-30 kV. Experiments were carried out using fused silica capillaries (Composite Metal Services Ltd., Worcester, UK) of 50 μm i.d and 65 cm long (50 cm effective length). Before use, the capillaries were washed with Milli-Q triple distilled water followed by 1 M NaOH and the separation buffer. The electrolyte and samples were sonicated and filtered through a 0.45 μm membrane filter prior to use. Data analysis was carried out with DAX 32 software (Eindhoven, Netherlands). All experiments were performed at 25°C. Between each injection the capillary was filled with the buffer solution by flushing the capillary for 5 min. The sample was introduced into the capillary by hydrodynamic injection for 5 seconds.

7.7.3 Amperometric detection

The AD cell (Figure 7.2) was a 40 x 40 x 20 mm cuvette with 4 small holes drilled through in the form of a cross hair. The holes were large enough to pass a gold (Au) micro-wire working electrode and a capillary through it. A silver micro wire was used as the reference electrode and

fitted into the third leg of the cross hair. As no commercial sources were available to supply the right size Au micro electrode, the working electrode was made in house by sealing a 60 μm diameter Au wire (Goodfellows Metals Cambridge, UK) in a 125 μm i.d fused silica capillary. The one end of the micro electrode was sealed using nail polish while the other end was filled with silver epoxy for contact with a copper wire. After drying for 15-18 hours, the Au micro electrode was activated by successive cyclic sweeps in a 0.1 M Fe_3CN_6 and 0.1M KCl solution between -400 mV and 400 mV (fig 7.4), testing its electrochemical activity. Before every CE run, the Au micro electrode was kept at -500 mV for 5 min to ensure that all deposited mercury and impurities were reduced and stripped from the Au micro electrode surface. Amperometric detection was performed at a constant potential with a with a BAS LC-4CE amperometric detector (West Layfayette, IN, USA).

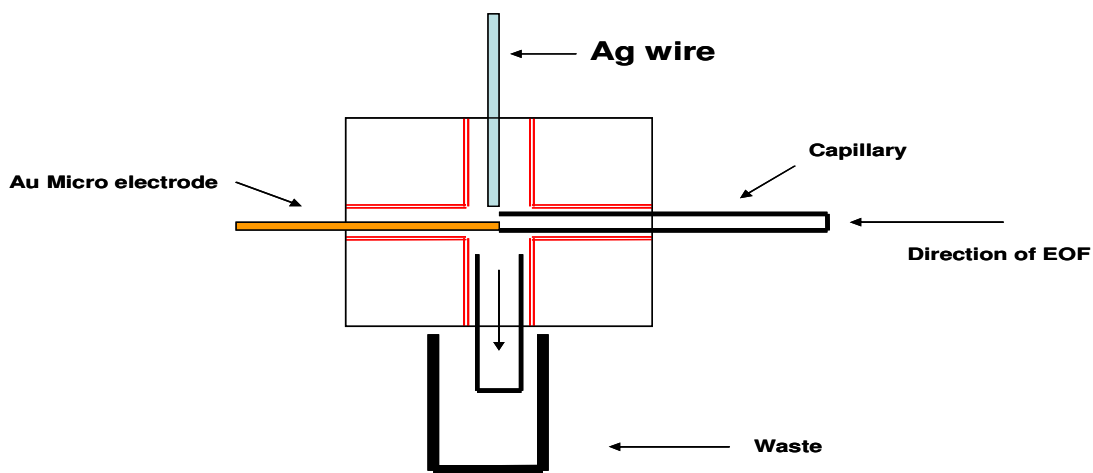


Fig.7.2 Schematic representation of the newly developed CEEC cross hair design



Fig. 7.3 Example of the gold micro electrode and the CEEC cross hair setup

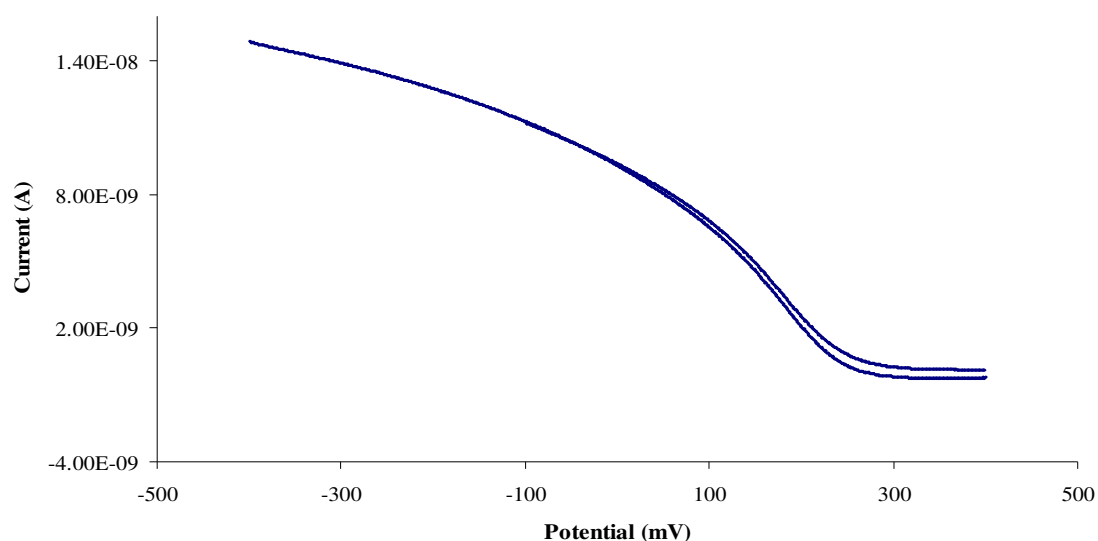


Figure 7.4 Cyclic voltammogram of a Au micro electrode in 0.1 M Fe_3CN_6 and 0.1M KCl solution

All the electrodes and capillaries were aligned under a (B# Zeiss KF2 Nikon) microscope. The Au micro electrode was set at a distance of 20 μm from the end of the capillary and kept in position with peak ferrules and screws modified to fit the EC cell. The cross hair design system was placed inside the CE Faraday cage and kept in position by using a plastic ruler and double sided tape as the support system (Fig 7.5). All AD of mercury complexes were performed at a controlled potential of 0.5 V vs. a Ag wire.

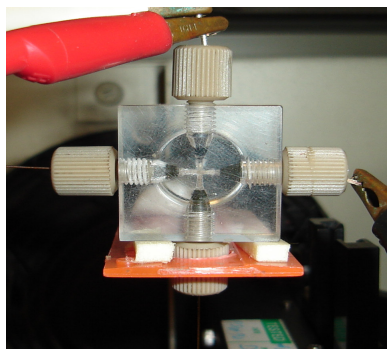


Fig. 7.5 CE-AD cross hair design for mercury speciation.

End column detection was employed by making use of the newly developed Au micro electrode cross hair construction. The following parameters were used during electrochemical detection of the respective mercury cysteine complexes.

Table 7.2. Parameters for CE-AD

Amperometric		CE	
Potential	0.5 V	Potential	25 kV
Filter	0.2 Hz	Injection time	5 sec
Range	5 μ A	Hydrodynamic injection	

7.8 Results and Discussion

To date, only one article was published dealing with the speciation of mercury by CE with amperometric detection [6]. In this report, Lai et al. used reductive voltammetry at a gold electrode for detection of mercury complexes. They were able to separate inorganic mercury, methyl and ethylmercury in a separation electrolyte composed of 0.1 M creatinine at pH 4.8 adjusted by acetic acid. The reductive mode in their work is not commonly used due to the problems with reduction of dissolved oxygen in aqueous solutions. Despite this setback the achieved LODs were excellent: 0.2 μ g/L for inorganic mercury and 3 μ g/L for methylmercury [10].

Chapter 7 – Results and Discussion III

In this study inorganic mercury and methylmercury were studied using the optimized conditions as described earlier for CE UV detection of mercury cysteine complexes. Figure 7.5 shows the separation of inorganic mercury cysteine complex. For CE-AD an oxidative mode was chosen making electrode cleaning easier when the negatively charged complex is formed on the surface of the electrode. The mercury complex can be clearly distinguished from the excess cysteine. The order of elution is the same in CE-AD as it was in UV detection under the same conditions. All components were separated in less than 11 minutes and very symmetrical peaks were observed. The migration time for Hg^{2+} increased by 4 min. This could be due to the fact that for CE-AD a different instrument was used with slightly different electrolyte conditions. The background noise was minimal in CE-AD therefore improving the detection limits for the mercury complexes. The separation was found to be reproducible ($n=3$) after electrode cleaning of 5 minutes.

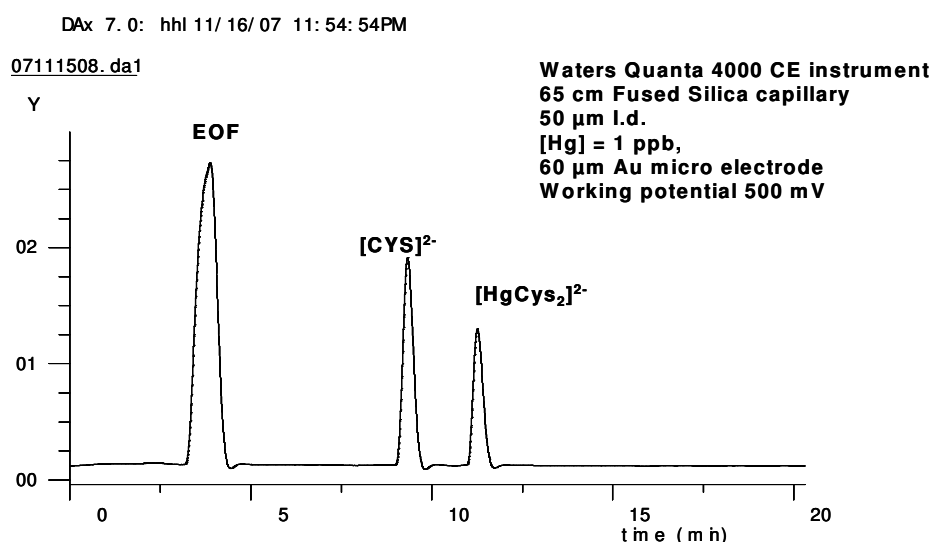


Fig. 7.6 Separation of $1.0 \mu\text{g/L}$ Hg^{2+} complexed with 33 mM cysteine: buffer 25 mM sodium borate, $\text{pH } 9.35$, Voltage = $+25 \text{ kV}$, CE-AD detection at 0.5 V .

The CE-AD system was calibrated with a series of Hg^{2+} standards up to $100 \mu\text{g/L}$. For high concentrations of mercury very broad peaks were observed making the separation of mercury from the excess cysteine very difficult due to overloading of the capillary. A linear range was observed for Hg^{2+} from 0.01 to $10 \mu\text{g/L}$. There were no visible signs of system performance degradation after several hours of CE-AD operation. The repeatability was determined by injecting the different standards mixtures three times into the CE instrument. Calibration graphs (concentration versus peak area) were constructed at seven concentration levels. Good linearity

Chapter 7 – Results and Discussion III

and reproducibility was observed during the experiments. The limit of detection (LOD) and limit of quantitation (LOQ) were calculated based on 3 and 10 times noise level, respectively. The limit of detection was determined with a signal to noise ratio of 3:1. Results for standard deviations (STD) and percentage relative standard deviations (%R.S.D) were calculated with Microsoft Excel for all CE-AD experiments. The LOD for Hg^{2+} was found to be 0.005 ± 0.002 $\mu\text{g/L}$. This performance is made possible by regular electrode cleaning of the micro electrode before analysis and also proper alignment of the Au micro electrode for end channel detection.

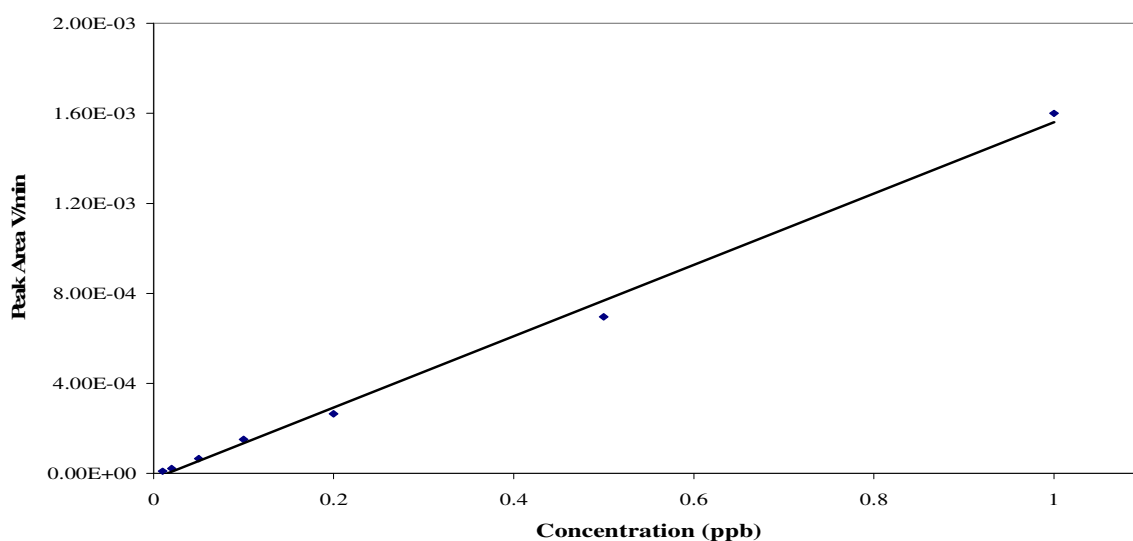


Fig.7.7. Calibration curve of Hg^{2+} with CE-AD

Table 7.3 Linear regression data of mercury cysteine complex

Range ($\mu\text{g/L}$)	Linear regression	Correlation coefficient	LOD ($\mu\text{g/L}$)	LOQ ($\mu\text{g/L}$)	% R.S.D
0.01 - 1	$0.0016x - 2E-05$	0.9958	0.005 ± 0.002	0.01	1.58

Methylmercury showed very complex but interesting electrochemical reactions when studied by CV. This complexity is due to the formation of the methylmercury radical species [43,44]. When a relatively high concentration of methylmercury was injected into the CE instrument and studied with CE-AD (Fig7.8), some new peaks appeared and can be contributed to the formation of different radical species of methylmercury.

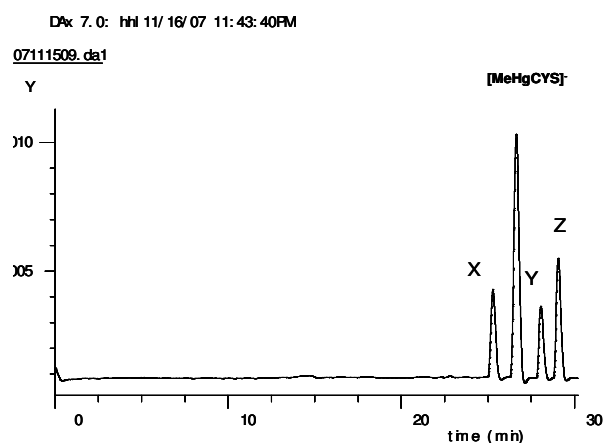


Fig. 7.8 Separation of 100 µg/L MeHg⁺ complexed with 33 mM cysteine: buffer 25 mM sodium borate, pH 9.35, Voltage = +25 kV, CE-AD detection at 0.5 V. (X, Y, Z are radical species which could not be identified)

These peaks were not detected when a UV detector was used. These new peaks were detected up to a concentration of 100 µg/L.

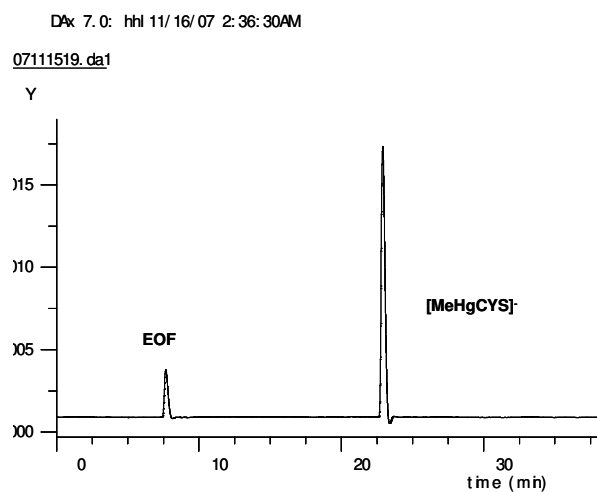


Fig. 7.9 Separation of 50 µg/L MeHg⁺ complexed with 33 mM cysteine: buffer 25 mM sodium borate, pH 9.35, Voltage = +25 kV, CE-AD detection at 0.5 V.

At lower concentrations, only one peak was found and can be assigned to the methylmercury cysteine complex. For the separation of methylmercury the increase in the retention time was very high compared to CE-UV analysis. The complex appeared after 20 minutes. The reason for

the increase in retention time is yet unknown but the long retention time was consistent throughout when methylmercury was studied. A linear range was observed for MeHg^+ from 0.5 to 50 $\mu\text{g/L}$. The LOD for MeHg^+ was found to be $0.40 \pm 0.05 \mu\text{g/L}$ and the LOQ was 1.0 $\mu\text{g/L}$ and were calculated based on 3 and 10 times noise level, respectively. The results obtained by CE-AD were found to be comparable and in good agreement with work done by Lai et al. where the LOD for MeHg^+ was 3.0 $\mu\text{g/L}$. [10].

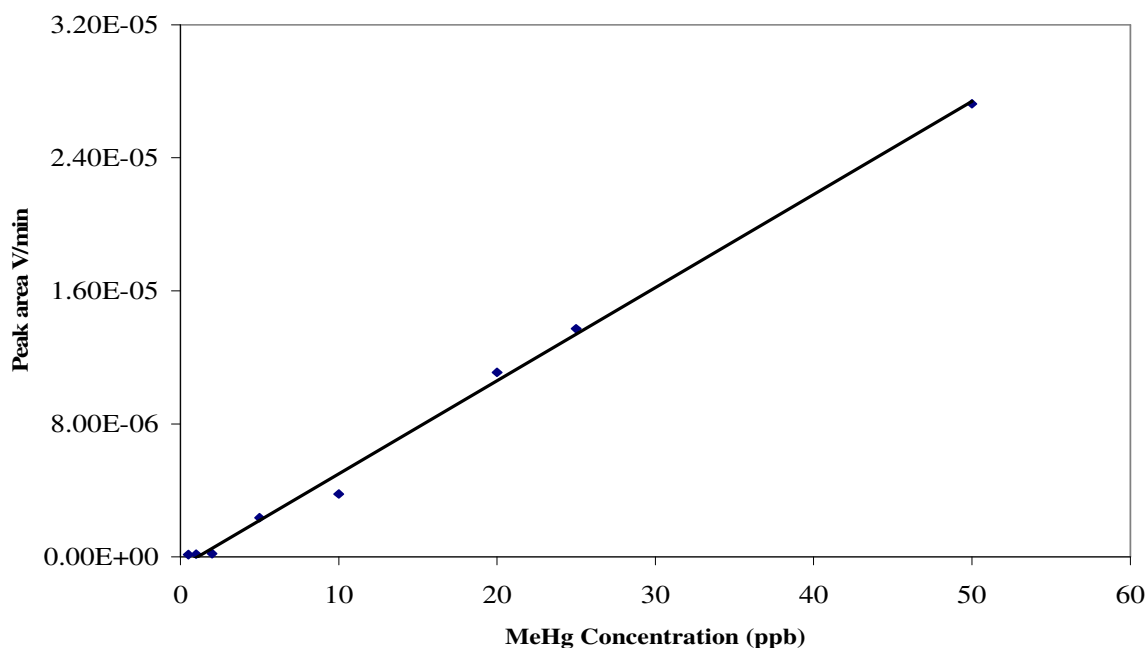


Fig. 7.10 Calibration curve of MeHg^+ with CE-AD

Table 7.4 Linear regression data of methylmercury cysteine complex

Range ($\mu\text{g/L}$)	Linear regression	Correlation coefficient	LOD ($\mu\text{g/L}$)	LOQ ($\mu\text{g/L}$)	% R.S.D
0.5 - 50	$6.6\text{E-}5x + 7\text{E-}07$	0.9838	0.40 ± 0.05	1.0	5.21

7.9. Comparison of CE -UV detection with CE-AD

From the experimental results (LOD's) it is clear that CE-AD is a much more sensitive and selective detection system than CE-UV detection. CE-AD shows great promise and with further test even lower detection limits is possible. In all compartments CE-AD is better suited than CE-

UV detection. Overall CE-AD is sensitive, selective, quick and cheap method for the determination of mercury complexes and suitable for environmental analysis.

7.10.1 Analysis of coal samples for mercury with CE-UV

The developed method was tested on coal samples (**C1632-C1644**) from different power station plants in South Africa. Before sampling, mercury certified reference standards (**SARM 18 & SARM 20**) were used to evaluate the CE method for mercury detection. This formed part of the validation process for this method. 8 g of **SARM 18** was placed in a quartz tube in a furnace.

The sample was purged with oxygen gas connected from the one side of the quartz tube while the other side was connected to 3 sample traps containing 200 ml of 1 M potassium chloride (KCl) in the first trap, the second one filled with 200 ml of mixture of 0.585 M nitric acid (HNO₃) and 30% of hydrogen peroxide (H₂O₂) and the last one filled with 200 ml of the mixture of 4% w/v of potassium permanganate (KMnO₄) and 10% w/v of sulphuric acid (H₂SO₄). The coal sample was heated for 1 hour at 790 °C. 1 ml of each of the traps were analyzed by capillary electrophoresis. This procedure is known as the Ontario Hydro Method and was used for all the coal samples analyzed with CE [45-53].

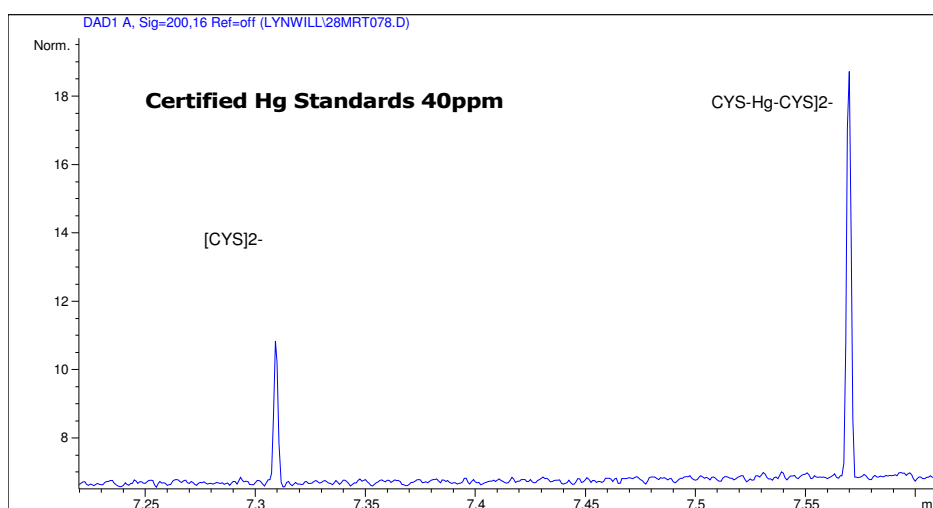


Fig. 7.11 Electropherogram of mercury certified reference standard (**SARM 20**): buffer 25mM sodium borate, pH 9.35, Voltage = +25 kV, UV = 200 nm

Most of the mercury in coal was oxidized to inorganic mercury (Hg²⁺) therefore, no organic mercury was detected. No Hg was detected in the HNO₃-H₂O₂ and the H₂SO₄-KMnO₄ traps. The

Chapter 7 – Results and Discussion III

results of the certified reference material, SARM 18 and SARM 20 are summarized in figures 7.11 and 7.12 and the concentrations of the reference materials are summarized in table 7.5 ($n = 3$).

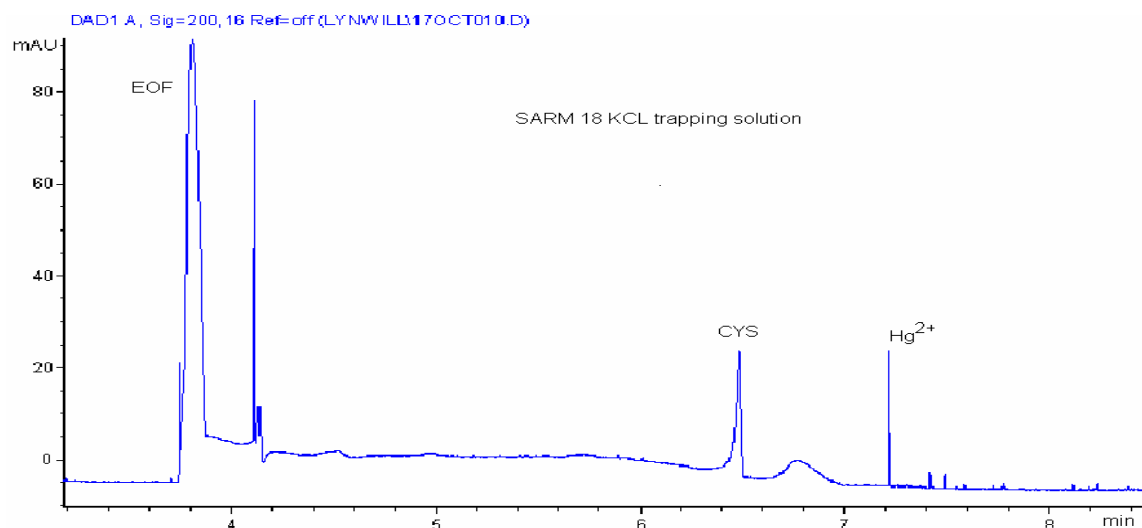


Fig. 7.12 Electropherogram of **SARM 18** complexed with cysteine: buffer 0.025 M sodium borate, pH 9.35, Voltage = +25 kV, UV = 200 nm.

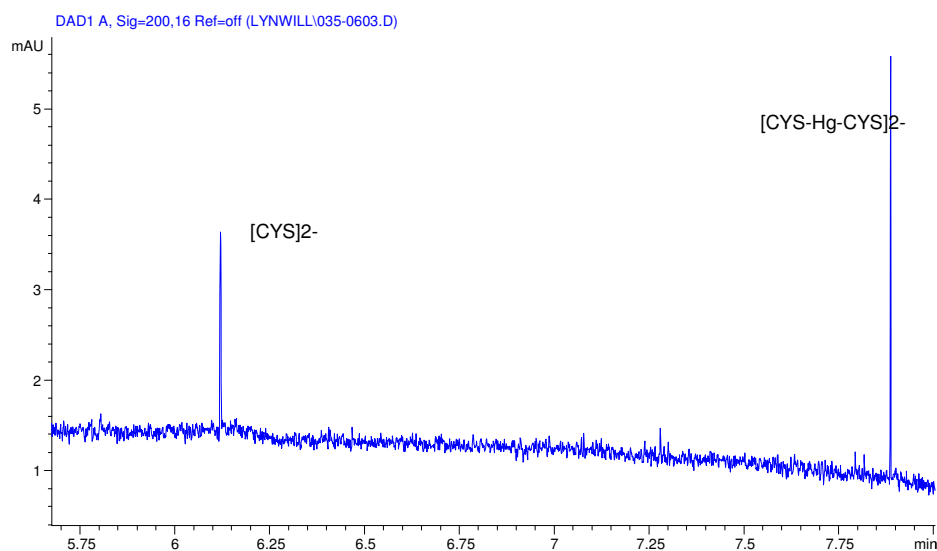


Fig. 7.13 Electropherogram of test sample **C1632** complexed with cysteine: buffer 0.025 M sodium borate, pH 9.35, Voltage = +25 kV, UV = 200 nm.

Table 7.5 Experimental data of coal samples for mercury determination with CE-UV

Name	Concentration of reference ($\mu\text{g/g}$)	Experimental data (mg/L) (n =3)	% R.S.D
SARM 18	25.0 \pm 0.55	23.26 \pm 2.18	7.18
SARM 20	40.0 \pm 0.98	38.95 \pm 1.03	4.03
C1632	unknown	5.25 \pm 1.87	6.07

7.10.2 Analysis of coal samples for mercury with CE-AD

The CE method for mercury cysteine separation was applied to the determination of Hg^{2+} in a coal sample. Certified reference material **SARM 20** was used and before CE analysis was treated with the Ontario Hydro Method as described earlier and diluted to a final concentration of 0.4 $\mu\text{g/L}$. [48-51]. The results obtained for Hg^{2+} was $0.39 \pm 0.072 \mu\text{g/L}$, with (n=3) and was comparable to the certified value of 0.4 $\mu\text{g/L}$. The results obtained indicate that the proposed method can be applied to the analysis of mercury in coal samples.

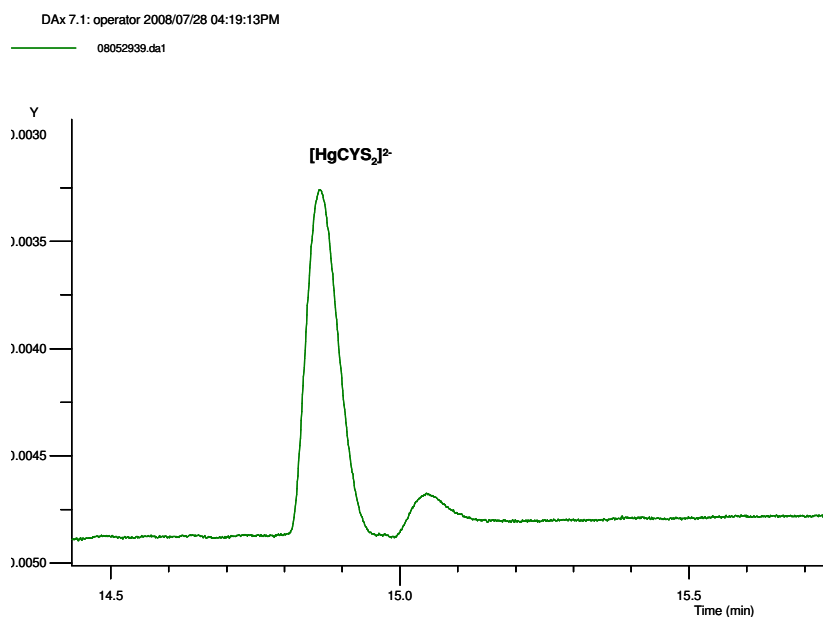


Fig.7.14. Electropherogram of mercury certified reference standard (**SARM 20**): buffer 0.025 M sodium borate, pH 9.35, Voltage = +25 kV, CE-AD detection at 0.5 V

7.11 Analysis of air samples for mercury

Sampling was done at the Cape Town Weather Station at Cape Point. Two adsorption tubes, Tennax and Tennax GR were used for sampling. Both tubes were preconditioned before sample taking. The tubes were washed with 2 ml methanol and activated at 300 °C for one hour. A pump (DG Brunner 190BG) coupled with a flow controller was used for air sample collection. The air was drawn through the Tennax and Tennax GR thermal absorption glass tubes for 12 hours at a flow rate of 2 L/min. To each tube 1 ml of methanol was added and kept on a shaker for one hour to extract the adsorbed compounds. After one hour methanol was collected in a sample vial and made up to a known volume and injected. A blank methanol sample was also prepared similar to the sample preparation. Only inorganic mercury was detected by the Tennax adsorption tube. The Tennax GR adsorption tube was not suited for mercury detection. In both applications inorganic mercury was detected. The peak was integrated and from the calibration curve the value was obtained. The peak area and peak height was taken into consideration for this value. A signal of 2.93 mAU for peak height corresponded to a concentration of $2.15 \pm 4.78 \mu\text{g Hg}^{2+}/\text{m}^3$ air. CE-UV is useful for the analyses of inorganic mercury but when more complex matrixes will be analysed, CE-UV will not be sufficient. With further development and testing CEEC might be able to overcome all the limitations associated with CE-UV for mercury speciation and detection.

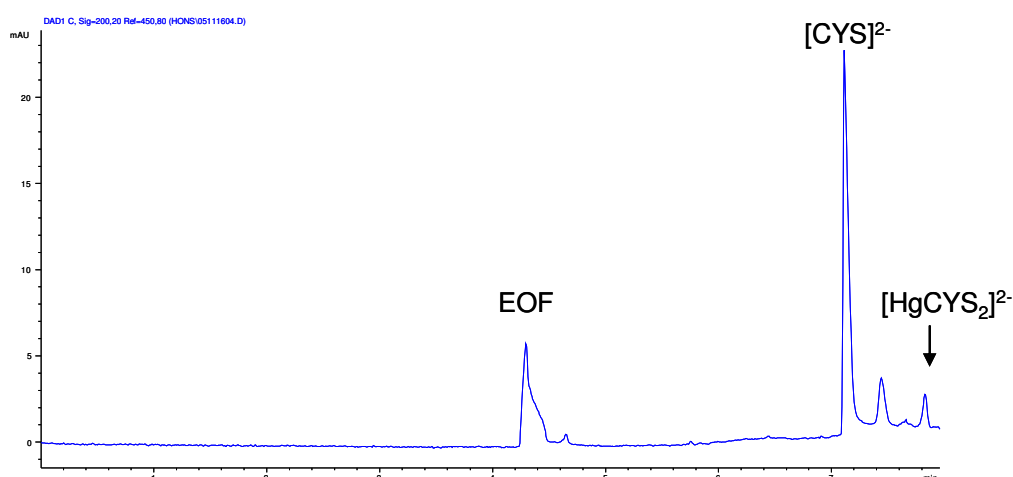


Fig.7.15. Electropherogram of Cape Point sampling results for airborne mercury with Tennax adsorption tubes, buffer 25 mM sodium borate, pH 9.35, Voltage = +25 kV, UV = 200 nm:

7.12 Conclusion

The resolution provided by CE separation in conjunction with amperometric detection at 0.5 V is useful for the speciation and determination of mercury complexes. Constant voltage amperometric detection is simple to implement, does not cost very much and provides very good sensitivity. The detection limits of 0.005 $\mu\text{g/L}$ for Hg^{2+} and 0.4 $\mu\text{g/L}$ for MeHg^+ are attractive for the monitoring of mercury in coal. The correct alignment and proper electrode cleaning is of utmost importance to achieve very low and accurate detection levels. Despite all these attractive features of CE-AD it is still not a popular detection mode. The preparation of the micro electrode takes time and there is a lot of skill involved when the electrodes alignment is performed. These few obstacles can however be overcome once you are familiar with the techniques of manufacturing and working with micro electrodes. When tested on real coal samples the CE-AD system performance was satisfactory. Comparing the LOD's of this study with work done by Lai et. al., which were 0.2 $\mu\text{g/L}$ for Hg^{2+} and 3.0 $\mu\text{g/L}$ for MeHg^+ , the LOD's achieved in this study are much lower and better suited for Hg detection. The CE-AD method is competitive with well established methods like cold vapor atomic absorption detection methods developed for mercury detection by the United States Environmental Protection Agency (U.S EPA Method 245.6) where the LOD for mercury in water is 0.2 $\mu\text{g/L}$ using permanganate oxidation and better than the LOD of 0.8-1.9 $\mu\text{g/L}$ achieved with HPLC with AD [10,54]. Overall CE-AD is a quick, inexpensive and sensitive detection mode for mercury and is definitely worth further exploration.

References:

1. A. Gaspar, C.S. Pager, *Microchemical Journal* 73, (2002) 53-58.
2. D. Goodall, D. Lloyd, S. Williams, *LC-GC* 8, (1990), 788-799.
3. C. Vogt, G.L. Klunder, *Frensenius Journal of Analytical Chemistry* 370, (2001), 316-331
4. R. Wallingford, AG. Ewing, *Analytical Chemistry* 59, (1987), 1762-1766.
5. R. Wallingford, AG. Ewing, *Analytical Chemistry* 60, (1988), 1972-1975
6. P. Kuban, P.C. Hauser, V. Kuban, *Electrophoresis* 28, (2007), 58-68.
7. A.R. Timerbaev, O.A. Shpigun, *Electrophoresis* 21, (2000), 4179-4191.
8. R. Ciucu, P. Baldwin, *Romanian Biotechnology Lett.*, 7, (2002) 959-974.
9. T. O'Shea, S. Lunte, *Current Separations*, 14, (1995), 18-22.
10. E. Dabek-Zlotorzynska, E.P.C. Lai, A.R. Timerbaev, *Anal. Chim. Acta* 359, (1998), 63-74.
11. R. Weinberger, *Practical Capillary Electrophoresis* 2nd Edition, Academic Press, NYC, (2000).
12. J.P. Landers, *Handbook of Capillary Electrophoresis* 2nd Ed, CRC Press, Boca Raton, Florida, (1997).
13. W.R. Vandaveer, D.J. Farmer, S.M. Lunte, *Electrophoresis* 25, (2004), 3528-3549.
14. W.R. Vandaveer. S.A. Pasas, R.S. Martin, S.M. Lunte, *Electrophoresis* 23, (2002), 3667-3677.
15. T. Kappes, P. Hauser, *Journal of Chromatography A* 834, (1999), 89-101.

16. M. Pumera, *Talanta* 74, (2007), 358-364.

17. P. Kubáň, V. Kubáň, *Electrophoresis* 27, (2006), 1368-1375.

18. P. Tůma, E. Samcová, K Andělová, *Journal of Chromatography B* 839, (2006), 12-18.

19. E. M. Abad-Villar, S.F. Etter, M.A. Thiel, P. C. Hauser, *Anal. Chim. Acta* 561, (2006), 133-137

20. P. Kubá, B. Karlberg, P. Kubá, V. Kubá, *Journal of Chromatography A* 964, (2002), 227-241.

21. T. Kappes, P.C. Hauser, *The Analyst* 124, (1999), 1035-1039.

22. J. Savory, M. Herman, *Annals of Clinical and Laboratory Science* 29, (2004), 212-222.

23. A. Durgbanshi, W. Kok, *Journal of Chromatography A* 798, (1998), 289-296.

24. F. Matysik, *Journal of Chromatography A* 802, (1998), 349-354.

25. N.A. Lachner, S.M. Lunte, R.S. Martin, *Anal. Chem.*, 76, (2004), 2482-2491.

26. D.M. Osborne, C.E. Lunte, *Anal. Chem.*, 75, (2004), 2710-2714.

27. J. Wang, M.P. Chantrathi, *Anal. Chem.*, 75, (2003), 525-529.

28. P.D. Voegel, W. Zhou, R.P. Baldwin, *Anal. Chem.*, 951, (1997), 957-964.

29. T. Kappes, P.C. Hauser, *Electroanalysis* 12, (2000), 165-170.

30. P.D. Voegel, R.P. Baldwin, *Electrophoresis* 19, (1998), 2226-2232.

31. L. Hau, S.N. Tan, *Anal. Chim. Acta* 403, (2000), 179-186.

32. M.L. Kovarik, N.J. Torrence, D.M. Spence, R.S. Martin, *The Analyst* 129, (2004), 400-405.
33. N.E. Herbert, B. Snyder, B. McCereery, W.G. Kuhr, S.A. Brazill, *Anal. Chem.*, 75, (2003), 4265-4271.
34. P. Ertl, C.A. Emrich, P. Singhal, R.A. Mathies, *Anal. Chem.*, 76, (2004), 3749-3755.
35. F. Bianchi, H. Lee, H.H. Girault, *J. Electroanal. Chem.*, 523, (2002), 40-48.
36. R.S. Martin, K.L. Ratzlaff, B.H. Huynh, S.M. Lunte, *Anal. Chem.*, 74, (2002), 1136-1143.
37. M. Zhong, S.M. Lunte, *Anal. Chem.*, 68, (1996), 2488-2493.
38. T.I. O'Shea, S.M. Lunte, W.R. LaCrouse, *Anal. Chem.*, 65, (1993), 948-951.
39. W. Lu, R.M. Cassidy, *Anal. Chem.*, 66, (1994), 200-204.
40. W.T. Kok, Y. Sahin, *Anal. Chem.*, 65, (1993), 2497-2501.
41. S. Park, S.M. Lunte, C.E. Lunte, *Anal. Chem.*, 67, (1995), 911-918.
42. S. Park, C.E. Lunte, *Anal. Chem.*, 67, (1995), 4366-4370.
43. R. Agraz, M.T. Sevilla, L. Hernandez, *Journal of Electroanalytical Chemistry* 390, (1995), 45-57.
44. R. Heaton, H. Laitinen, *Analytical Chemistry* 46, (1974) 547-553.
45. L.T. Jongwana, October Progress Report on Mercury in Coal, Stellenbosch 2007.
46. S. Lee, Y.C. Seo, J. Jung, J.H. Hong, J.W. Park, J.E. Hyun, T.G. Lee, *Science of the total environment* 325, (2002), 155-161.

47. R. Meij, L.H. Vredendregt, H. Winkel, *Journal of the Air and Waste Management Association* 52, (2002), 917-917.

48. P. Pui, P. Kuranchandani, “*Uncertainties in modeling long-range transport and fate of Hg emissions in North America*”, presented at EPRI Managing Hazardous Air Pollutants, 4th international conference, Washington DC, (1999).

49. U.S. EPA 1997, Mercury study report to congress, Volume VIII, EPA-452/R-97-010

50. US EPA 1999, “*Mercury information collection request (ICR)*”, Part 111

51. US EPA 2000a, “*Control of Hg emissions from coal fired electric utility boilers*”, EPA 600/R-01-109

52. D.L Laudal, T.D Brown, B.R. Nott, *Fuel Processing Technology* 65, (1999), 157-165.

53. M.H. Keating, “*Mercury study report to congress*,” (1997).

54. J. Scifres, M. Wasko, W. McDaniel, *Amer. Environ. Lab.*, 5, (1994), 34.

Chapter 8

Overall Conclusions and Recommendations

8.1 Overall Conclusions

The main objectives of this project were to develop a new and simple analytical technique to detect and speciate different mercury complexes with the use of CE-UV detection and CEEC. Speciation is vital for the understanding of the mercury cycle in the environment, its toxicity and the effect different mercury species have on human life and the chemical industry.

Chapter 1.

The importance of speciation and especially mercury speciation is outlined in this chapter. The main goals and motivation for the study is presented and also the proposed strategy for solving this problem is outlined.

Chapter 2.

A complete overview of mercury is given in this chapter. Focus is placed on all the major aspect of mercury like transformation in the environment, toxicology, mercury cycle, methods ect.

Chapter 3.

The different classical methods for detection and determination of mercury is looked at. Most of these classical methods can only give total mercury concentration. Methods that can speciate mercury are also discussed. The potential of using capillary zone electrophoresis for mercury speciation is outlined. Its rapid separation speed, high efficiency and very small sample requirement are some of its advantages and is therefore chosen as the analytical technique to speciate mercury.

Chapter 5

This chapter discusses extensively the obtained cyclic voltammograms of the different mercury complexes. The organomercury compounds all showed the same mechanism where a radical species is formed after the first oxidation step. From the result it can be concluded that to detect different mercury species with CEEC a potential of 0.5 V is needed and that the mercury dithizone sulfonate complex is more stable than the other ligands used in this study.

Chapter 6 & 7

In this chapter mercury cysteine and dithizone complexes are separated by CE. The LODs were lower for the mercury dithizone complexes. An electrochemical detector was developed to improve the detection limits. A gold micro electrode was developed for CE-AD. It can be concluded that the results for the gold micro electrode was better and improved the method since lower detection limits were obtained by CE-AD compared with UV detection.

8.2 Recommendations and future work

- Synthesis of new dithizone derivatives for mercury complexation
- Electrochemical and electrophoretic studies of the new mercury dithizone complexes
- Coating the gold micro electrodes with nano particles
- Apply the new developed method to environmental samples for mercury detection

8.3 Conference contributions

Posters and Talks

1. **L.G Martin, A.M Crouch**, Speciation and detection of mercury with Capillary Electrophoresis, *38th Convention of the South African Chemical Institute (SACI), 3-8 December 2006, Durban, South Africa.* (Poster)

2. **L.T. Jongwana, L.G Martin, A.M Crouch**, Mercury speciation in coal with Capillary Electrophoresis, *38th Convention of the South African Chemical Institute (SACI), 3-8 December 2006, Durban, South Africa.* (Poster)

3. **L.G Martin, A.M Crouch**, Electrochemistry and Electrophoresis of mercury cysteine and dithizone complexes, *Inorganic 2007, Club Mykonos, South Africa, 8-12 July 2007.* (Poster)

4. **L.G Martin, A.M Crouch**, Electrochemistry and Electrophoresis of mercury and methylmercury complexes, *SEANAC Conference: 15-18 July 2007, Gabarone Sun Hotel, Gabarone, Botswana, Chemistry for Health.* (Invited Talk)

5. **L.G Martin, L.T. Jongwana, A.M Crouch**, Post column electrochemical detection for mercury speciation analysis. *1st International Symposium on Electrochemistry, University of the Western Cape, Bellville, South Africa, 9 – 11 July 2008.* (Keynote Speaker)

6. **L.G Martin, L.T. Jongwana, A.M Crouch**, Mercury speciation using capillary electrophoresis with electrochemical detection, *16th International Symposium in Capillary Electromigration Techniques, Catania, Italy, 31 Aug- 3 Sept 2008* (Poster)